Latent disconnectome prediction of long-term cognitive symptoms in stroke.

Lia Talozzi[1,2], Stephanie J Forkel*[1,2,3], Valentina Pacella*[1,2], Victor Nozais[1,2], Maurizio Corbetta[4,5,6], Parashkev Nachev[7], Michel Thiebaut de Schotten[1,2].

[1] Groupe d'Imagerie Neurofonctionnelle, Institut des Maladies Neurodégénératives-UMR 5293, CNRS, CEA, University of Bordeaux, Bordeaux, France.
[2] Brain Connectivity and Behaviour Laboratory, Sorbonne Universities, Paris, France.
[3] Centre for Neuroimaging Sciences, Department of Neuroimaging, Institute of Psychiatry, Psychology and Neuroscience, King's College London, London, UK.
[4] Clinica Neurologica, Department of Neuroscience, University of Padova, Padova, Italy.
[5] Padova Neuroscience Center (PNC), University of Padova, Padova, Italy.
[6] Venetian Institute of Molecular Medicine, VIMM, Padova, Italy.
[7] Institute of Neurology, UCL, London, UK.

*Authors contributed equally

Contacts: liatalozzi@gmail.com, michel.thiebaut@gmail.com.

Abstract

Stroke significantly impacts quality of life. However, the long-term cognitive evolution in stroke is poorly predictable at the individual level. There is an urgent need for a better prediction of long-term symptoms based on acute clinical neuroimaging data. Previous works have demonstrated a relationship between the location of white matter disconnections and clinical symptoms. However, rendering the entire space of possible lesion-deficit associations optimally surveyable will allow for a systematic association between brain disconnections and cognitive-behavioural measures at the individual level. Here we exploit nonlinear dimensionality reduction to report the characteristics of disconnection patterns of more than 1000 stroke lesions in a two-dimensional summary morphospace. Acute disconnectomes drawn from an independent distribution were projected into the morphospace to predict neuropsychological scores 1 year after stroke. Linking the latent disonnectome morphospace to neuropsychological outcomes yields a comprehensive atlas of disconnectome-deficit relations across 86 neuropsychological scores. Out-of-sample prediction derived from this atlas achieved average accuracy over 80%. Our novel predictive framework is available as an interactive web application, the *disconnectome symptoms discoverer* (DSD), to provide the foundations for a new approach to modelling cognition in stroke.

Introduction

The fidelity of lesion-deficit models depends not only on the quality of the data but also on the underlying theoretical framework. Together they produced evidence of a relationship between the location of brain lesions and clinical symptoms such as visuospatial neglect (Karnath et al. 2001; Dorrichi et al. 2005; Verdon et al. 2010), aphasias (Bates et al. 1999; Caplan et al. 1996; Graff-Radford et al. 2014), apraxias (Goldenberg and Spatt 2009; Manuel et al. 2012) or motor anosognosia (Berti et al. 2005; Karnath et al. 2005) amongst others. Recently, the associations between anatomical white matter networks and clinical presentations revealed that there is no one-to-one relationship between structures and clinical presentation, as different lesions can cause the same functional impairments (Forkel et al 2021; Thiebaut de Schotten et al. 2020). One example would be that a stroke in the middle or posterior cerebral artery may lead to visuospatial neglect (Mort et al. 2003), just like different perisylvian white matter disconnections can lead to aphasia (Forkel et al. 2020). Hence, the current methodologies do not capture the potential overlap between brain signatures and clinical manifestations nor the distributed nature of their neural substrate, now familiar from network analyses of functional imaging data (Corbetta et al. 2015). Therefore, a comprehensive framework that would systematically associate brain disconnections with cognitive-behavioural assessments is needed for accurate precision medicine (Von Monakow 1914; Feeney & baron 1986; Carrera & Tononi 2014; Fornito et al. 2015; Fox 2018).

Modelling distributed relations is computationally expensive and requires large scale data. With advances in data modelling and the availability of databases, tackling the high complexity of clinical-anatomical relationships is now conceivable. Beneath the surface complexity there may lie a simpler order that can be described within a compacted representational space. As such, dimensionality reduction algorithms allow defining low-dimensional spaces that can embed multivariate data. In embedding spaces, also known as morphospaces (Galton 1907, Mitteroecker and Huttegger 2009), patients with similar features cluster together while diverging features are placed apart (Bonkhoff et al. 2021; Thiebaut de Schotten et al. 2020). Morphospaces render lesion-deficit relations more easily surveyable. Hence, specific brain features can define territories in a morphospace and help predict symptoms and brain pathologies, similar to typical machine learning approaches (Varoquaux & Thirion , 2014; Ruffle et al. 2021). AI has recently progressed in modelling the association of symptom severity with medical imaging modalities, e.g., reaching high accuracy and sensitivity in the

characterisation of tumour tissues (Ardilla et al. 2019). However, AI models need to be refined with a broader spectrum of clinically practical endpoints, including neuropsychological measures. The next challenge will be making AI patient-centric for a more effective deployment into the clinical routine and to efficiently benefit patients' quality of life (Oren 2020).

To drive the realisation of this challenge forward, we propose a modelling approach that employs a morphospace to predict neuropsychological assessments of one of the most common neurological disorders: stroke (Wafa et al. 2020). We first mapped the distribution of 1333 brain disconnectivity patterns in stroke — the disconnectome morphospace. A second dataset (N=119 stroke patients "training set") with rich neuropsychological measures 1-year after stroke was imported into this disconnectome morphospace. This second dataset enriched the morphospace with clinical symptoms obtained from 86 neuropsychological assessments. An out-of-sample "validation set" (N=20 strokes) with the same neuropsychological data served to assess prediction accuracy. This procedure, hereafter referred to as *disconnectome symptoms discoverer* (DSD), reliably predicted the performance of patients on 63 neuropsychological scores with an average accuracy > 80%. To make the DSD tool readily available to the clinical-academic community and facilitate its incorporation into the clinic, we provide an open-access web application (http://disconnectomestudio.bcblab.com), in which individual disconnectivity patterns can be uploaded to predict the expected 1-year neuropsychological scores. The web application will be interactively updated, thanks to future crowdsourcing, informing the DSD model with any newly available datasets.

Results

The disconnectome morphospace

The first dataset (N=1333 stroke lesions; Xu et al. 2018) was processed to obtain disconnectome maps. Disconnectome maps quantify the pattern of connections interrupted by each lesion based on the high-resolution tractography of a healthy population (Thiebaut de Schotten et al. 2020-2015; Vu et al. 2015). Subsequently, the Uniform Manifold Approximation and Projection (UMAP, McInnes & Healy 2018) method was used to embed disconnection complexity. A latent 2 dimensions configuration of the disconnectome maps was obtained. Figure 1 indicates that patients' disconnectome profiles distribute based on lesion location and commonly disconnected tracts. For instance, patients with major left or right hemisphere disconnections were embedded in the right and left half of the

morphospace, respectively. Similarly, patients with anterior or posterior disconnections were localised at the top and the bottom of the embedded space. Patients with a prominent disconnection of the inferior-fronto occipital fasciculus (IFOF) located at the bottom left and right extremities of the morphospace while corticospinal (CST) and arcuate (AF) disconnections were relatively more central. Hence the morphospace appropriately segregated the different profiles of disconnection of the classic tract (Rojkova et al. 2016; Catani & Thiebaut de Schotten 2012).

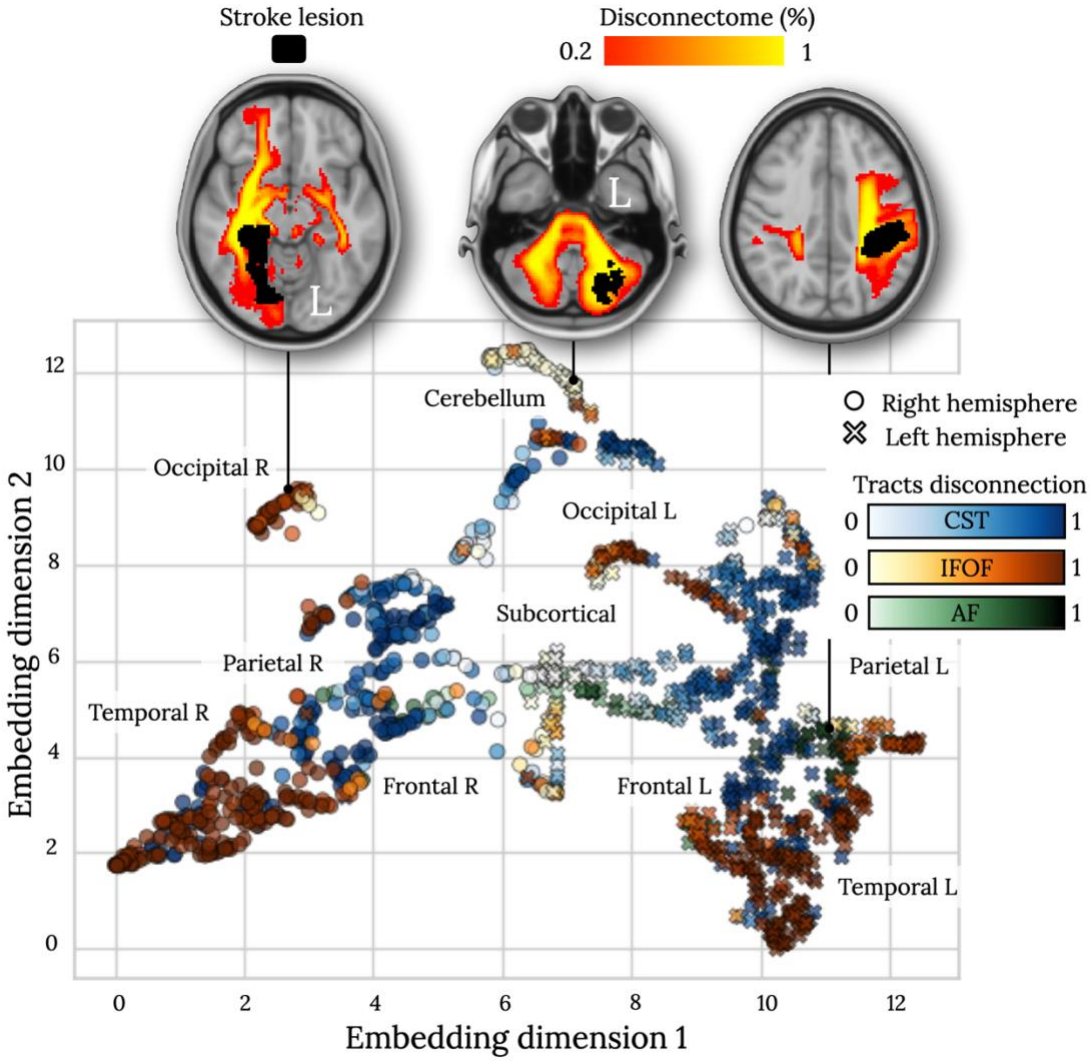

Figure 1. Disconnectome morphospace. Embedding of N=1333 stroke disconnectomes. (Top) three patients' disconnectomes, where a red-yellow colour map indicates the probability of disconnection. (Bottom) the disconnectome morphospace, where patients are marked with a circle ("o") or with a cross ("x") when their disconnection involves dominantly the right (R) or the left (L) hemisphere, respectively. Colours in the morphospace indicate the probability of disconnection of three white matter tracts: the cortico-spinal tract (CST), the arcuate fasciculus (AF), and the inferior-fronto occipital fasciculus (IFOF). Brain lobe annotations indicate the dominant location of each stroke lesion.

The composite morphospace

The extent to which the disconnectome morphospace can predict different neuropsychological performances is currently unknown. To answer this question, we took advantage of the second independent dataset of stroke patients (N=119) that was extensively explored with standard neuropsychological assessments (N=86). For each patient of the second dataset, disconnectome maps were calculated and imported into the disconnectome morphospace using the UMAP defined transformation. To tackle uncertainty, patient coordinates in the morphospace were spatially smoothed (see methods). In so doing, each patient's coordinates in the disconnectome morphospace were converted into probabilities of localisation. A Pearson correlation approach was then used to estimate the association between each morphospace coordinate and a neuropsychological performance (see Supplementary Materials for more details). Figure 2 indicates that a medium to large effect size association (all $|r| > 0.2$) existed between territories in the disconnectome morphospace and neuropsychological scores (Fig. 2). Importantly, for some scores, multiple clusters in the disconnectome morphospace, corresponding to different disconnection profiles, apparently led to the same neuropsychological impairment. This confirmed that no one-to-one relationship exists between lesion of structures and clinical disorders, and likewise, different locations of brain damage can lead to the same functional impairment. In order to avoid simple linear association between the morphospace coordinates magnitude and neuropsychological scores, patients' probabilities of localisation in clusters of significance were modelled by a principal component analysis (later referred to as spatial PCA). For each patient, the first three-component of the spatial PCA were entered into a multiple regression analysis to predict single-patient neuropsychological scores 1 year after symptom onset. The multiple regressions created equations modelling the relationship between each patient's potential localisation in the disconnectome morphospace (i.e., as defined by the three first components of the spatial PCA) and their neuropsychological scores. In so doing, we obtained a composite morphospace that takes advantage of the joint strengths of the two datasets. The composite morphospace accurately and reliably predicted 83 out of 86 neuropsychological scores with a small to large effect size (see Supplementary Table 3).

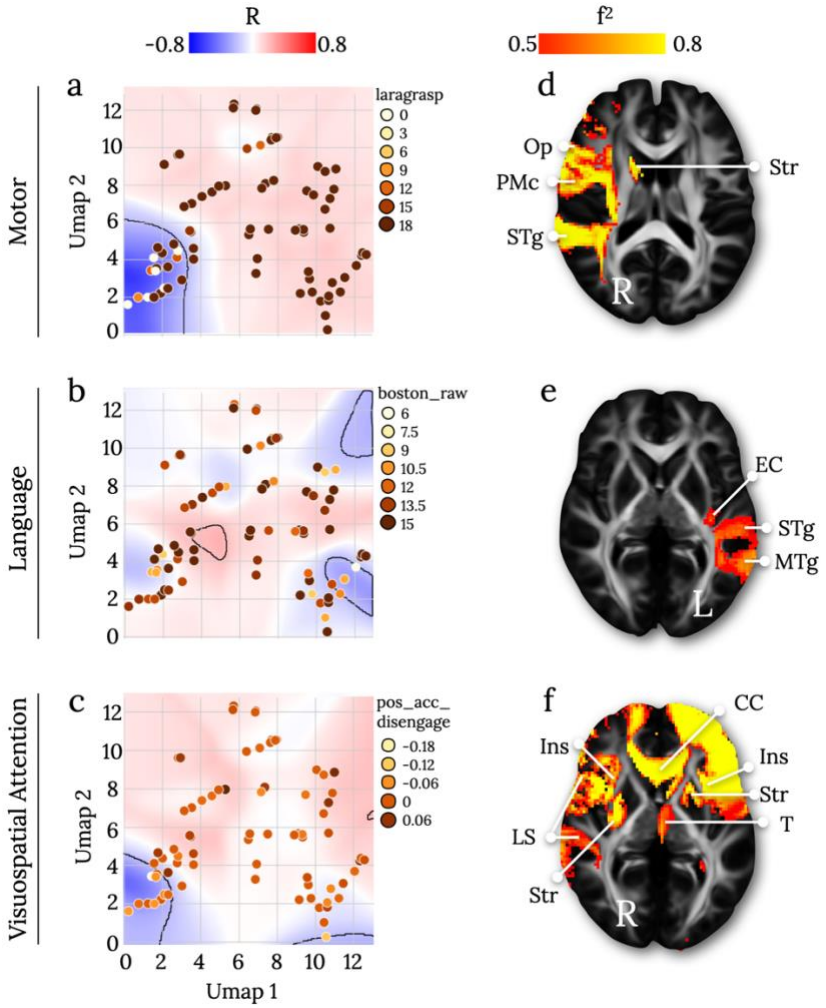

Figure. 2 Composite morphospace. The composite morphospace corresponds to the disconnectome morphospace statistically combined with individual neuropsychological scores, (a-c) are three examples of different neuropsychological score associations with morphospace territories presented together with (d-f) their prototypical disconnection profile. Blue-Red background colours in the morphospace correspond to Pearson correlation scores (R) with neuropsychological scores. Medium effect size territories ($|R > 0.2|$) are delineated in black. All neuropsychological assessments and maps are reported in the Supplementary Materials (Section B). f^2: effect size; laragrasp: left grasping Action Research Arm test test; boston_raw: Boston naming test; pos_acc_disengage: accuracy in the Posner orienting task; Op: Rolandic Operculum; PMc: Pre-Motor cortex; STg: superior temporal gyrus; EC: external capsule; MTg: middle temporal gyrus; Ins: insula; LS: arcuate long-segment; Str=Striatum; CC=corpus callosum; T=thalamus.

Disconnectome morphospace component mapping

In the next level, we brought the score prediction results back to the neuroimaging space to explore the neuroanatomical patterns leading to symptoms. The first dataset was split in half (2 X 666 disconnectomes maps) to assess reproducibility. Latent patterns of predicted neuropsychological performances were statistically associated with brain disconnections maps of the two halves of the first dataset using voxelwise linear regressions. In doing so we

obtained two sets of maps of brain disconnection for each neuropsychological score (see example in figure 2d-f and all maps together with their full discussion in Supplementary Material - Section C). We were able to produce a comprehensive atlas of the brain disconnections associated with neuropsychological test scores and the statistical comparison of the two sets of maps indicated a good level of reproducibility (Pearson R = 0.82). Figure 3 summarises the highest statistical associations spanning from a medium ($0.15 > f^2 > 0.35$; Figure 3a) to high effect size ($f^2 > 0.35$; Figure 3b). The highest effect sizes were located in the left hemisphere, particularly in the frontal lobe connections, indicating the strongest associations between these disconnections and neuropsychological scores. Some areas can also be associated with multiple different neuropsychological scores. To summarise this information, we calculated a versability map that indicates how many neuropsychological scores can be predicted with a large effect size per volume unit of white matter (Figure 3c). The versatility maps revealed a clear asymmetry between the left and the right hemispheres. This lower effect size and higher versatility in the right hemisphere suggests that more work is required to finely measure and dissociate right hemisphere functions in neuropsychology.

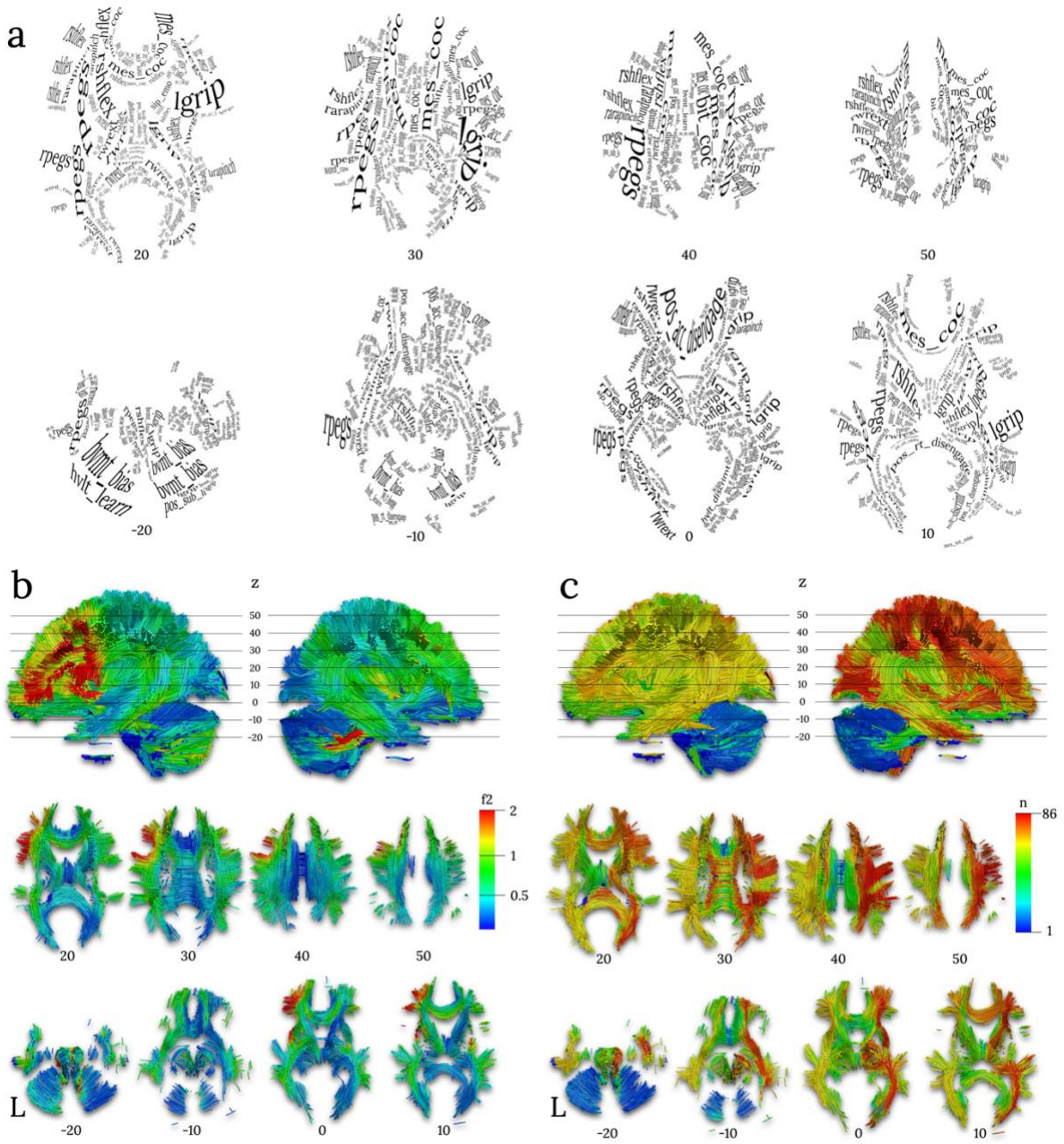

Figure 3. White matter neuropsychological atlas. (a) Summary maps of neuropsychological scores associated with white matter disconnections with the highest statistical level (see Supplementary Materials Section C for high-resolution images). **(b)** Effect size maps (f^2) for the most significant associations between disconnectome and neuropsychological performances. **(c)** Disconnectome versability maps indicating how many neuropsychological scores can be predicted for each voxel of white matter.

Accuracy in predicting neuropsychological score at 1-year after stroke

To assess the accuracy of the predictions, data derived from a third independent dataset (20 stroke patients withheld from the original dataset) were projected into the morphospace. From there, equations derived from the composite morphospace predicted individual neuropsychological scores. Prediction accuracy was assessed as the difference between the observed and predicted scores, normalized by the maximum score (Figure 4). The profile of neuropsychological scores for single patients was predicted with an average accuracy of 84.3 ± 5.6 % while each test was predicted individually with an average accuracy of 83.9 ± 7 %. Accuracy of continuous values was assessed in relation to the normalized prediction error. The prediction of two-thirds (N=65) of the tests was replicated in this third independent dataset with an accuracy >80% (Supplementary Table 4).

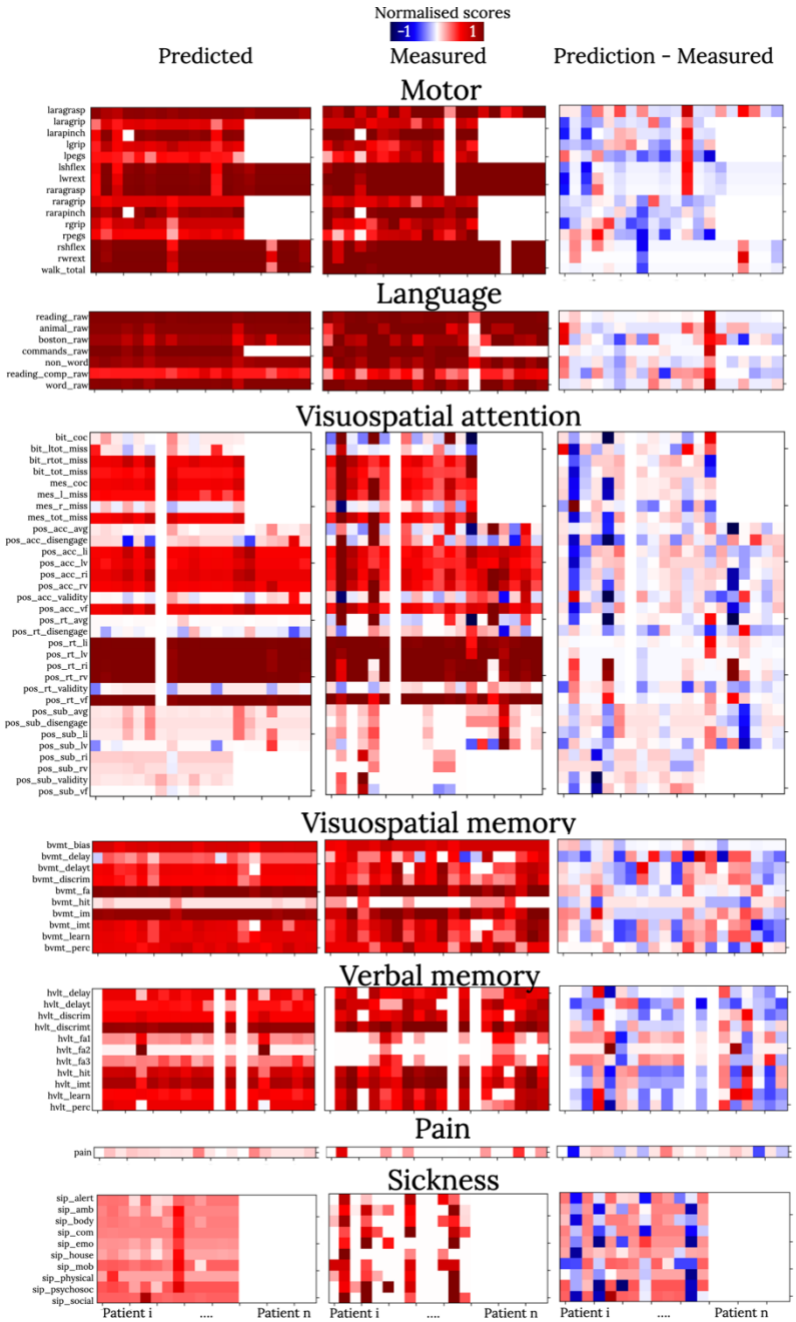

Figure 4 Accuracy of the neuropsychological scores. (left) Predicted neuropsychological scores, according to the composite disconnectome morphospace modelling. (center) Measured neuropsychological scores 1-year after the stroke onset. (right) Normalised error as the difference between predicted and measured scores. Rows correspond to single patients' neuropsychological profiles. Columns correspond to different neuropsychological scores. See the Supplementary Materials Figure 4 for the same figure derived from the training set.

Disconnection Symptoms Discovery web application

To make this resource and method available for the clinical-research community, we deployed an interactive web application platform called *Disconnectome Symptoms Discovery - DSD* (http://disconnectomestudio.bcblab.com). The DSD requires the input of brain lesions converted to disconnection maps and returns the expected 1-year neuropsychological scores for individual disconnectome maps (see the DSD user guide in the Supplementary Material Section E). The DSD tool prediction model relies on the databases presented in this study that can be updated on-demand with new neuropsychological assessments and patients' disconnectomes.

Discussion

Applying state-of-the-art data embedding methods we succeeded in combining complementary databases of stroke patients and produced an atlas of neuropsychological scores associated with brain disconnections. This atlas applied to an out-of-sample dataset accurately predicted 65 neuropsychological scores with an accuracy of over 80%. An openly available web application, the *disconnectome symptoms discoverer* (DSD) capitalises on our methods and provides new anatomical insights into cognitive symptoms for researchers and clinicians.

Similar patterns of stroke-induced white matter disconnections were distributed close by in the embedding space comparably to other research fields using UMAP methods (McInnes & Healy 2018), e.g., single-cell genetic transcriptomes (Cao et al. 2019, Packer et al. 2019). Therefore, the disconnectome morphospace acted as a reference to quickly import and summarize new stroke disconnections. Such embedded information allowed us to associate single-patient neuropsychological profiles at 1-year after a stroke with territories in the morphospace and profile of disconnection. By exploring white matter correlates systematically, we created a comprehensive atlas of the neuropsychological scores associated with brain disconnections. Classical functional associations were confirmed, e.g., in the lateralisation of motor functions, the left perisylvian language network, the fronto-parietal attentional networks, or the right insula for sickness sensations. In addition, new insights on functioning and disconnection were reported, e.g., the callosum connectivity related to visual neglect, the cerebellum hub for visuospatial memory, and the lingual gyrus for verbal memory (for individual results and discussion see Supplementary Material - Section C).

The atlas allowed for the evaluation of acute MRI scans to predict long-term stroke symptom severity. These results indicate the suitability of the disconnectome model in predicting a wide range of functional performances and addressing a complete personalised, individual patient profile. This information will be a valuable resource in clinical settings, for example for the planning of personalized therapeutic and rehabilitation strategies. This is a step forward in comparison to many stroke AI methods that have a purely diagnostic purpose (Sirat et at. 2020). Instead, the DSD model has a prognosis vocation based on cross-modal data (neuroimaging input - neuropsychological outcome prediction).

However, predictions were not equally accurate across functions (see Supplementary Table 4). Three factors might explain this difference. First, some neuropsychological scores are more reliable than others in assessing performances (Calamia et al. 2013). Second, plasticity and interindividual variability might interact with recovery (Forkel et al. 2014, Umarova et al. 2016, Forkel et al 2020). Third, the disconnectome model may not capture all the variance of brain injuries. Indeed, hypoperfusion (Hillis et al. 2001) and hypometabolism (Jha et al. 2020) factors as well as acute imaging changes such as pseudonormalization (Forkel et al., 2018) are not included.

Besides these limitations, the *disconnectome symptoms discoverer* (DSD) web application is a free and user-friendly web browser tool that only requires an internet connection. Instant software access and automatic updates make the word-wide-web the ideal media for clinical translations. The application of the DSD results can help personalized prognosis. Further, while our predictions were validated in an out-of-sample dataset, the DSD web application allows for a wider validation with crowdsourcing usage, through new dataset implementation. Hence, the DSD aims to benefit the researchers' understanding of brain functioning and the patient's treatments alike.

Methods

Bash and Python programming languages have been used for automatizing all the processing steps summarized in Supplementary Materials figure 1.

Stroke lesions. Lesion data were derived from three different centres. Dataset 1: (N=1333 strokes) MRI scans were acquired at University College London Hospitals (Xu et al. 2018). Patient demographics were an average age of 64±16 years [age range: 18-97 years] and 56% were men. Dataset 2 and dataset 3 were recruited at

the School of Medicine of the Washington University in St. Louis and included both MRI and neuropsychological assessments (Corbetta et al. 2015). For dataset 2 (N=119 strokes), the patient average age was 54±11 years [age range: 19-83 years] and 46% women. The average education level was 13±2.5 years, and 91% were right-handed participants. For dataset 3 (N=20 strokes), the average age was 58±12 years [age range: 34-95 years], with 40% men; average education level was 14±2.6 years, and 85% were right-handed. Patient demographics and imaging acquisition parameters are reported in the Supplementary Materials Section A and lesion distributions across the three databases in the Supplementary Material Figure 2.

Neuropsychological scores. Neuropsychological scores were available for datasets 2 and 3. The details of each neuropsychological evaluation (grading, test battery, administration) are reported in the Supplementary Materials Section C. In brief, motor abilities (Section C.1) were assessed for upper limb hand grasping, gripping, pinching, grip strength, peg replacement, motion shoulder flexion, wrist extension, and lower limb walking. Language abilities (Section C.2) were assessed using picture naming, non-word repetition, commands, sentence reading, sentence comprehension, and semantic fluency. Visuospatial abilities (Section C.3) were tested for using discrimination accuracy, reaction time, subbing, behavioural inattention, and unstructured symbol cancellation. Visuospatial memory (Section C.4) was evaluated using abstract figures retrieval scores and verbal memory (Section C.5) for listed word recognition scores. A pain scale during the MRI scanning was recorded (Section C.6) and a stroke sickness questionnaire administrating, investigating physical and psychosocial daily sickness (Section C.7).

Disconnectome. The probability of white matter disconnections caused by the stroke event was quantified accounting for controls' connectivity where the lesion occurred. Stroke lesions were manually delineated in T1-weighted MRI scans and subsequently normalized to the MNI space (2 mm resolution). The BCBtoolkit "normalization tool" was used with the enantiomorphic normalization option (http://toolkit.bcblab.com; Nachev et al. 2008). From the Human Connectome Project (HCP), 7T MRI diffusion-weighted scans were processed for N=163 healthy participants, 45% males (imaging parameter specifications are reported in Supplementary Materials Section A). For the healthy participants, whole-brain tractography was reconstructed using the same procedure reported in Thiebaut de Schotten M et al. (2020). Then, disconnectome profiles were processed with the BCBtoolkit (Foulon et al., 2018). HCP tractography was filtered considering

only streamlines passing through each stroke lesion. The filter tractography was binarized and averaged across the HCP participants. As a result, for each stroke patient a map of probability, ranging from 0 to 1, was obtained to quantify lesion disconnections.

Spatial embedding. Dimensionality reduction of patients' disconnectome was obtained using the UMAP method (McInnes & Healy 2018). A non-linear embedding method that distributes data variability along major axes. Dataset 1 3-dimensional disconnectome maps were vectorised and imported as features of the embedding methods. As UMAP parameters, an approximation of 15 neighbours and a minimum 0.1 Euclidean distance was set to obtain a two-dimensional embedding of dataset 1. A space locally connected as Riemannian manifold that we addressed in the paper as disconnectome morphospace. The UMAP embedding transformation was stored as a Python object, using the Pickle library, to apply the same low-dimensional transformation further when new patients are imported into the model. Subsequently, to have positive coordinates with a zero origin, the maximum negative dataset 1 umap values were added to shift the coordinate scale.

Relationship to neuropsychological scores. Statistical correlations between patient localisation in the disconnectome morphospace and neuropsychological scores were conducted. Before the multiple regression formula, UMAP coordinates were converted into a 2D nifti image (260x260 matrix, 0.05 mm pixel size), and a Gaussian kernel spatial smoothing of 1 mm was applied (using FSL libraries https://fsl.fmrib.ox.ac.uk/fsl/fslwiki/). This step was conducted to take into account the uncertainty of UMAP coordinates and obtaining a spatial distribution of patient localisation in the disconnectome morphospace. Pixel-wise Pearson correlations between the patient probability of localisation and neuropsychological scores were conducted with iterative loops in Python (python numpy.corrcoef). Medium effect size correlation results only were considered informative ($R > |0.2|$). Subsequently, since multiple clusters of voxels survived the threshold, a principal component analysis has been run to compress the patient coordinate distribution variability (later referred to as spatial PCA). Three main principal components have been considered (Python sklearn.decomposition.PCA). Subsequently, patients' principal components have been entered, as dependent variables, in the multiple regression model (Python sklearn.linear_model.LinearRegression) to predict neuropsychological scores:

$$score_{predicted\ at\ 1\ year} = c + \sum_{i=1}^{3} w_i\, PCA_{patient\ score} \quad (1.1)$$

Where c is the intercept of the linear regression model, w_i are the model weights, and $PCA_{patient\ score}$ the model variables obtained as the inner product between the patient distribution of localisation and PCA components.
The multiple regression formula was trained with dataset 2 disconnectomes and validated using the independent dataset 3 cohort.
Accuracy of prediction was assessed by normalising the prediction error ($score_{measured} - score_{predicted}$) to the maximum score obtained in the neuropsychological evaluation:

$$score_{accuracy} = 1 - \frac{|score_{measured} - score_{predicted}|}{max(score_{measured})} \quad (1.2)$$

White matter atlas of neuropsychological components. In order to create a white matter atlas of the evaluated neuropsychological assessments, white matter disconnectomes (dataset 1) were correlated with patients' PCA scores (dataset 2). The former disconnectome data were used in defining the UMAP space, whereas the latter PCA scores as variables of the multiple regression model to predict long term neuropsychological symptoms. Using *randomise* (FSL libraries) a generalized voxel-based linear regression model was run, with disconnectome maps as independent variables and PCA scores as dependent variables. To address the result of replicability this procedure was repeated twice, splitting the dataset 1 into two halves of n=666 subjects each.
The *randomise* T-maps obtained were used to calculate the correspondent effect size maps (f^2, python code reported in http://www.bcblab.com/BCB/Coding/Coding.html). For each neuropsychological score three principal component scores were evaluated and the maximum effect size across the components was considered. Subsequently, the highest effect size across neuropsychological assessments was reported in the white matter atlas summary map (FSL libraries *find_the_biggest* function). The replicability of the neuropsychology white matter atlas was quantified by means of Pearson correlations between the two summary maps.

DSD web application development. The DSD web application was built using the Django framework (https://www.djangoproject.com). This web framework allows database manipulation and is Python-based. The DSD frontend was created with standard Javascript and css templates; whereas the backend is hosted in a DigitalOcean webserver (https://www.digitalocean.com).

Visualization.
A visualisation of the results was performed using Trackvis (http://trackvis.org), FSLeyes for imaging data, and Python matplotlib and seaborn libraries for scatter plots and matrices.

References

1. Ardila D, Kiraly AP, Bharadwaj S, Choi B, Reicher JJ, Peng L, Tse D, Etemadi M, Ye W, Corrado G, Naidich DP, Shetty S. End-to-end lung cancer screening with three-dimensional deep learning on low-dose chest computed tomography. Nat Med. 2019 Jun;25(6):954-961. doi: 10.1038/s41591-019-0447-x. Epub 2019 May 20. Erratum in: Nat Med. 2019 Aug;25(8):1319. PMID: 31110349.
2. Bates E. Language and the infant brain. J Commun Disord. 1999 Jul-Aug;32(4):195-205. doi: 10.1016/s0021-9924(99)00015-5. PMID: 10466093.
3. Berti A, Bottini G, Gandola M, Pia L, Smania N, Stracciari A, Castiglioni I, Vallar G, Paulesu E. Shared cortical anatomy for motor awareness and motor control. Science. 2005 Jul 15;309(5733):488-91. doi: 10.1126/science.1110625. PMID: 16020740.
4. Calamia M, Markon K, Tranel D. The robust reliability of neuropsychological measures: meta-analyses of test-retest correlations. Clin Neuropsychol. 2013;27(7):1077-105. doi: 10.1080/13854046.2013.809795. Epub 2013 Jun 25. PMID: 24016131.
5. Cao J, Spielmann M, Qiu X, Huang X, Ibrahim DM, Hill AJ, Zhang F, Mundlos S, Christiansen L, Steemers FJ, Trapnell C, Shendure J. The single-cell transcriptional landscape of mammalian organogenesis. Nature. 2019 Feb;566(7745):496-502. doi: 10.1038/s41586-019-0969-x. Epub 2019 Feb 20. PMID: 30787437; PMCID: PMC6434952.
6. Caplan D, Hildebrandt N, Makris N. Location of lesions in stroke patients with deficits in syntactic processing in sentence comprehension. Brain. 1996 Jun;119 (Pt 3):933-49. doi: 10.1093/brain/119.3.933. PMID: 8673503.
7. Caramazza A. On drawing inferences about the structure of normal cognitive systems from the analysis of patterns of impaired performance: the case for single-patient studies. Brain Cogn. 1986 Jan;5(1):41-66. doi: 10.1016/0278-2626(86)90061-8. PMID: 3954906.
8. Carrera E, Tononi G. Diaschisis: past, present, future. Brain. 2014 Sep;137(Pt 9):2408-22. doi: 10.1093/brain/awu101. Epub 2014 May 28. PMID: 24871646.
9. Corbetta M, Ramsey L, Callejas A, Baldassarre A, Hacker CD, Siegel JS, Astafiev SV, Rengachary J, Zinn K, Lang CE, Connor LT, Fucetola R, Strube M, Carter AR, Shulman GL. Common behavioral clusters and subcortical anatomy in stroke. Neuron. 2015 Mar 4;85(5):927-41. doi: 10.1016/j.neuron.2015.02.027. PMID: 25741721; PMCID: PMC4646844.
10. Doricchi F, Tomaiuolo F. The anatomy of neglect without hemianopia: a key role for parietal-frontal disconnection? Neuroreport. 2003 Dec 2;14(17):2239-43. doi: 10.1097/00001756-200312020-00021. Erratum in: Neuroreport. 2004 Jan 19;15(1):217. PMID: 14625455.
11. F. Galton. Classifications of portraits. Nature, 76, pages 617–618 (1907).
12. Feeney DM, Baron JC. Diaschisis. Stroke. 1986 Sep-Oct;17(5):817-30. doi: 10.1161/01.str.17.5.817. PMID: 3532434.
13. Forkel SJ, Rogalski E, Drossinos Sancho N, D'Anna L, Luque Laguna P, Sridhar J, Dell'Acqua F, Weintraub S, Thompson C, Mesulam MM, Catani M. Anatomical evidence of an indirect pathway for word repetition. Neurology. 2020 Feb 11;94(6):e594-e606. doi:

10.1212/WNL.0000000000008746. Epub 2020 Jan 29. PMID: 31996450; PMCID: PMC7136066.
14. Forkel SJ, Rogalski E, Drossinos Sancho N, D'Anna L, Luque Laguna P, Sridhar J, Dell'Acqua F, Weintraub S, Thompson C, Mesulam MM, Catani M. Anatomical evidence of an indirect pathway for word repetition. Neurology. 2020 Feb 11;94(6):e594-e606. doi: 10.1212/WNL.0000000000008746. Epub 2020 Jan 29. PMID: 31996450; PMCID: PMC7136066.
15. Forkel SJ, Thiebaut de Schotten M, Dell'Acqua F, Kalra L, Murphy DG, Williams SC, Catani M. Anatomical predictors of aphasia recovery: a tractography study of bilateral perisylvian language networks. Brain. 2014 Jul;137(Pt 7):2027-39. doi: 10.1093/brain/awu113. PMID: 24951631.
16. Fornito A, Zalesky A, Breakspear M. The connectomics of brain disorders. Nat Rev Neurosci. 2015 Mar;16(3):159-72. doi: 10.1038/nrn3901. PMID: 25697159.
17. Foulon C, Cerliani L, Kinkingnéhun S, Levy R, Rosso C, Urbanski M, Volle E, Thiebaut de Schotten M. Advanced lesion symptom mapping analyses and implementation as BCBtoolkit. Gigascience. 2018 Mar 1;7(3):1-17. doi: 10.1093/gigascience/giy004. PMID: 29432527; PMCID: PMC5863218.
18. Fox MD. Mapping Symptoms to Brain Networks with the Human Connectome. N Engl J Med. 2018 Dec 6;379(23):2237-2245. doi: 10.1056/NEJMra1706158. PMID: 30575457.
19. Goldenberg G, Spatt J. The neural basis of tool use. Brain. 2009 Jun;132(Pt 6):1645-55. doi: 10.1093/brain/awp080. Epub 2009 Apr 7. PMID: 19351777.
20. Graff-Radford J, Jones DT, Strand EA, Rabinstein AA, Duffy JR, Josephs KA. The neuroanatomy of pure apraxia of speech in stroke. Brain Lang. 2014 Feb;129:43-6. doi: 10.1016/j.bandl.2014.01.004. Epub 2014 Feb 18. PMID: 24556336; PMCID: PMC4004427.
21. Hanna Damasio and Antonio R. Damasio. “Lesion analysis in neuropsychology”. New York: Oxford University Press, 1989.
22. Hillis AE, Wityk RJ, Tuffiash E, Beauchamp NJ, Jacobs MA, Barker PB, Selnes OA. Hypoperfusion of Wernicke's area predicts severity of semantic deficit in acute stroke. Ann Neurol. 2001 Nov;50(5):561-6. doi: 10.1002/ana.1265. PMID: 11706960.
23. Jha A, Teotonio R, Smith AL, Bomanji J, Dickson J, Diehl B, Duncan JS, Nachev P. Metabolic lesion-deficit mapping of human cognition. Brain. 2020 Mar 1;143(3):877-890. doi: 10.1093/brain/awaa032. PMID: 32203579; PMCID: PMC7089650.
24. Karnath HO, Baier B, Nägele T. Awareness of the functioning of one's own limbs mediated by the insular cortex? J Neurosci. 2005 Aug 3;25(31):7134-8. doi: 10.1523/JNEUROSCI.1590-05.2005. PMID: 16079395; PMCID: PMC6725240.
25. Karnath HO, Ferber S, Himmelbach M. Spatial awareness is a function of the temporal not the posterior parietal lobe. Nature. 2001 Jun 21;411(6840):950-3. doi: 10.1038/35082075. PMID: 11418859.
26. Manuel AL, Radman N, Mesot D, Chouiter L, Clarke S, Annoni JM, Spierer L. Inter- and intrahemispheric dissociations in ideomotor apraxia: a large-scale lesion-symptom mapping study in subacute brain-damaged patients. Cereb Cortex. 2013 Dec;23(12):2781-9. doi: 10.1093/cercor/bhs280. Epub 2012 Sep 17. PMID: 22989580.
27. McInnes, L., Healy, J., & Melville, J. (2018). Umap: Uniform manifold approximation and projection for dimension reduction. arXiv preprint arXiv:1802.03426.
28. Mitteroecker P. and Huttegger S.. The Concept of Morphospaces in Evolutionary and Developmental Biology: Mathematics and Metaphors. March 2009 Biological Theory 4(1):54-67. doi: 10.1162/biot.2009.4.1.54

29. Mort DJ, Malhotra P, Mannan SK, Rorden C, Pambakian A, Kennard C, Husain M. The anatomy of visual neglect. Brain. 2003 Sep;126(Pt 9):1986-97. doi: 10.1093/brain/awg200. Epub 2003 Jun 23. PMID: 12821519.
30. Nachev P, Coulthard E, Jäger HR, Kennard C, Husain M. Enantiomorphic normalization of focally lesioned brains. Neuroimage. 2008 Feb 1;39(3):1215-26. doi: 10.1016/j.neuroimage.2007.10.002. Epub 2007 Oct 12. PMID: 18023365; PMCID: PMC2658465.
31. Oren O, Gersh BJ, Bhatt DL. Artificial intelligence in medical imaging: switching from radiographic pathological data to clinically meaningful endpoints. Lancet Digit Health. 2020 Sep;2(9):e486-e488. doi: 10.1016/S2589-7500(20)30160-6. PMID: 33328116.
32. Pacella V, Foulon C, Jenkinson PM, Scandola M, Bertagnoli S, Avesani R, Fotopoulou A, Moro V, Thiebaut de Schotten M. Anosognosia for hemiplegia as a tripartite disconnection syndrome. Elife. 2019 Aug 6;8:e46075. doi: 10.7554/eLife.46075. PMID: 31383259; PMCID: PMC6684265.
33. Packer JS, Zhu Q, Huynh C, Sivaramakrishnan P, Preston E, Dueck H, Stefanik D, Tan K, Trapnell C, Kim J, Waterston RH, Murray JI. A lineage-resolved molecular atlas of C. elegansembryogenesis at single-cell resolution. Science. 2019 Sep 20;365(6459):eaax1971. doi: 10.1126/science.aax1971. Epub 2019 Sep 5. PMID: 31488706; PMCID: PMC7428862.
34. Sirsat MS, Fermé E, Câmara J. Machine Learning for Brain Stroke: A Review. J Stroke Cerebrovasc Dis. 2020 Oct;29(10):105162. doi: 10.1016/j.jstrokecerebrovasdis.2020.105162. Epub 2020 Jul 28. PMID: 32912543.
35. Thiebaut de Schotten M, Foulon C, Nachev P. Brain disconnections link structural connectivity with function and behaviour. Nat Commun. 2020 Oct 9;11(1):5094. doi: 10.1038/s41467-020-18920-9. PMID: 33037225; PMCID: PMC7547734.
36. Thiebaut de Schotten M, Tomaiuolo F, Aiello M, Merola S, Silvetti M, Lecce F, Bartolomeo P, Doricchi F. Damage to white matter pathways in subacute and chronic spatial neglect: a group study and 2 single-case studies with complete virtual "in vivo" tractography dissection. Cereb Cortex. 2014 Mar;24(3):691-706. doi: 10.1093/cercor/bhs351. Epub 2012 Nov 15. PMID: 23162045.
37. Umarova RM, Nitschke K, Kaller CP, Klöppel S, Beume L, Mader I, Martin M, Hennig J, Weiller C. Predictors and signatures of recovery from neglect in acute stroke. Ann Neurol. 2016 Apr;79(4):673-86. doi: 10.1002/ana.24614. Epub 2016 Mar 15. PMID: 26873402.
38. Varoquaux G, Thirion B. How machine learning is shaping cognitive neuroimaging. Gigascience. 2014 Nov 17;3:28. doi: 10.1186/2047-217X-3-28. PMID: 25405022; PMCID: PMC4234525.
39. Verdon V, Schwartz S, Lovblad KO, Hauert CA, Vuilleumier P. Neuroanatomy of hemispatial neglect and its functional components: a study using voxel-based lesion-symptom mapping. Brain. 2010 Mar;133(Pt 3):880-94. doi: 10.1093/brain/awp305. Epub 2009 Dec 22. PMID: 20028714.
40. Von Monakow C., Die Localization im Grosshirn und der Abbau der Funktion durch korticale Herde, 1914Wiesbaden, GermanyJF Bergmann.
41. Wafa HA, Wolfe CDA, Emmett E, Roth GA, Johnson CO, Wang Y. Burden of Stroke in Europe: Thirty-Year Projections of Incidence, Prevalence, Deaths, and Disability-Adjusted Life Years. Stroke. 2020 Aug;51(8):2418-2427. doi: 10.1161/STROKEAHA.120.029606. Epub 2020 Jul 10. PMID: 32646325; PMCID: PMC7382540.

42. White matter variability, cognition, and disorders: a systematic review. (MedRxiv 2021). Forkel J.S., Friedrich P, Thiebaut de Schotten M, Howells H. doi: https://doi.org/10.1101/2020.04.22.20075127
43. Xu T, Rolf Jäger H, Husain M, Rees G, Nachev P. High-dimensional therapeutic inference in the focally damaged human brain. Brain. 2018 Jan 1;141(1):48-54. doi: 10.1093/brain/awx288. PMID: 29149245; PMCID: PMC5837627.
44. Yarkoni T, Poldrack RA, Nichols TE, Van Essen DC, Wager TD. Large-scale automated synthesis of human functional neuroimaging data. Nat Methods. 2011 Jun 26;8(8):665-70. doi: 10.1038/nmeth.1635. PMID: 21706013; PMCID: PMC3146590.

Supplementary Materials

TABLE OF CONTENTS

A. Imaging acquisition parameters

Dataset 1. MRI was acquired at the University College London Hospitals in London, on GE Signa, Philips Achieva and Ingenia, Siemens Avanto, Skyra and Verio with either 1.5 T or 3 T. The MRI protocol was harmonized and standardized between the different scanners used in the clinical routine, including DWI with null b-value and b-value=1000 s/mm2 and T2-weighted images. The MRI sequence choice was given to better segment acute stroke lesions. For further details see (Xu et al. 2018).

Dataset 2 and 3. MRI was acquired at the School of Medicine of the Washington University in St. Louis, on a Siemens 3T Tim-Trio scanner. The MRI acquisition protocol included: 1) structural imaging MP-RAGE T1-weighted, sagittal acquisition with repetition time = 1950 ms, echo time = 2.26 ms, flip angle = 9 deg, voxel size = 1.0 x 1.0 x 1.0 mm, slice thickness = 1.00 mm. 2) a transverse turbo spin-echo T2-weighted image with repetition time = 2500 ms, echo time = 435 ms, voxel-size = 1.0 x 1.0 x 1.0 mm, slice thickness = 1.00 mm. 3) a sagittal FLAIR (fluid attenuated inversion recovery) with repetition time = 7500 ms, echo time = 326 ms, voxel-size = 1.5 x 1.5 x 1.5 mm, slice thickness = 1.50 mm. Lesion segmentation was conducted considering these three sequence metacontrast data in acute stroke. For further details see Corbetta et al. (2015).

	Dataset 1	**Dataset 2**	**Dataset 3**
N. of stroke patients	1333	119	20
Males/Females	748/585	65/54	12/8
Age	64±16 [18-97]	54±11 [19-83]	58±12 [34-95]
Education	N.A.	13.2±2.5 [5-20]	13.7±2.6 [9-19]
Handedness Right/Left	N.A.	109/10	17/3
Recruitment site	University College London Hospitals, London (UK).	School of Medicine of the Washington University, St. Louis (USA).	School of Medicine of the Washington University, St. Louis (USA).

Supplementary Table 1. Patient demographics. N.A.= Not Available.

B. Neuropsychological scores prediction mode

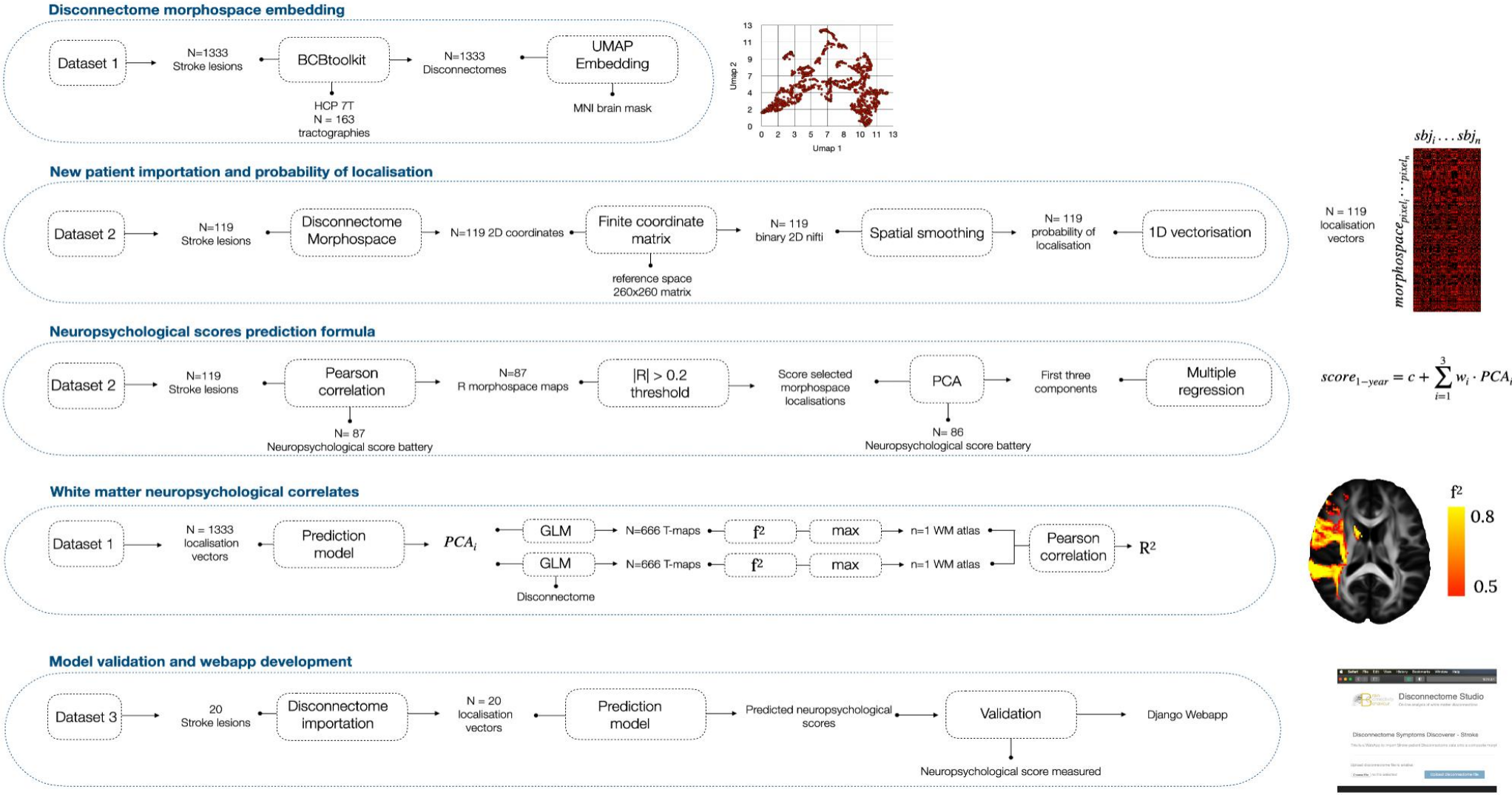

Supplementary figure 1: graphical summary of neuroimaging and statistical model workflow.

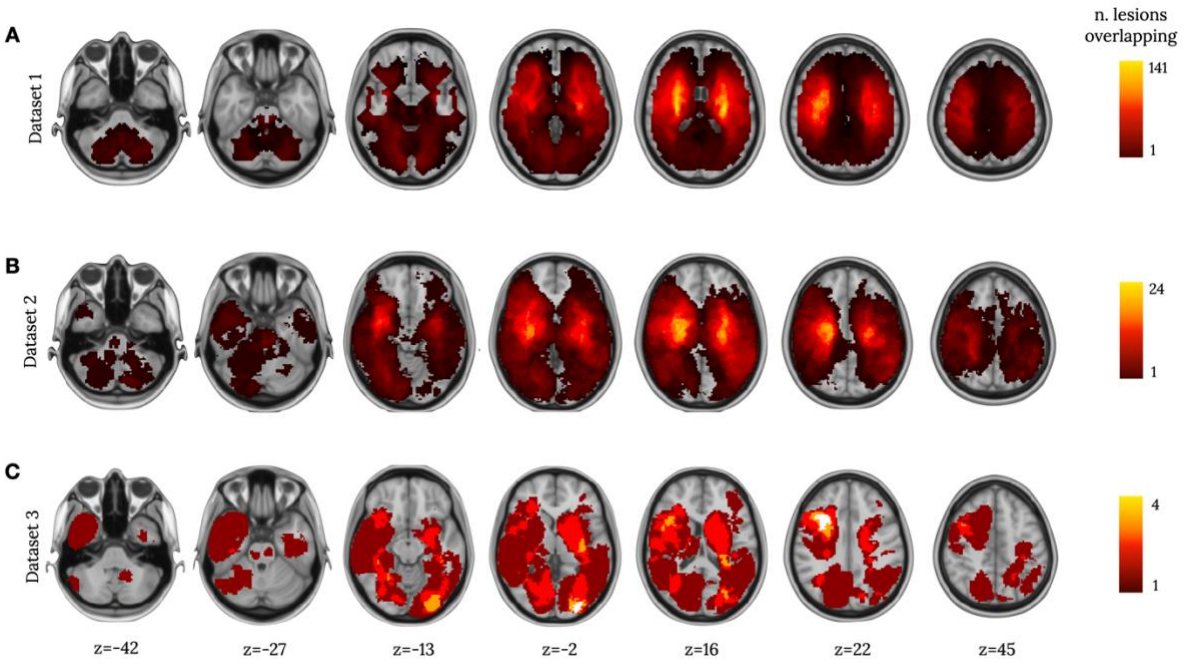

Supplementary figure 2: Lesion group variability maps for dataset 1 (panel A), dataset 2 (panel B), and dataset 3 (panel C). Colormaps show the number of lesions overlapping. Inferior-superior z-coordinates are reported according to the MNI atlas reference.

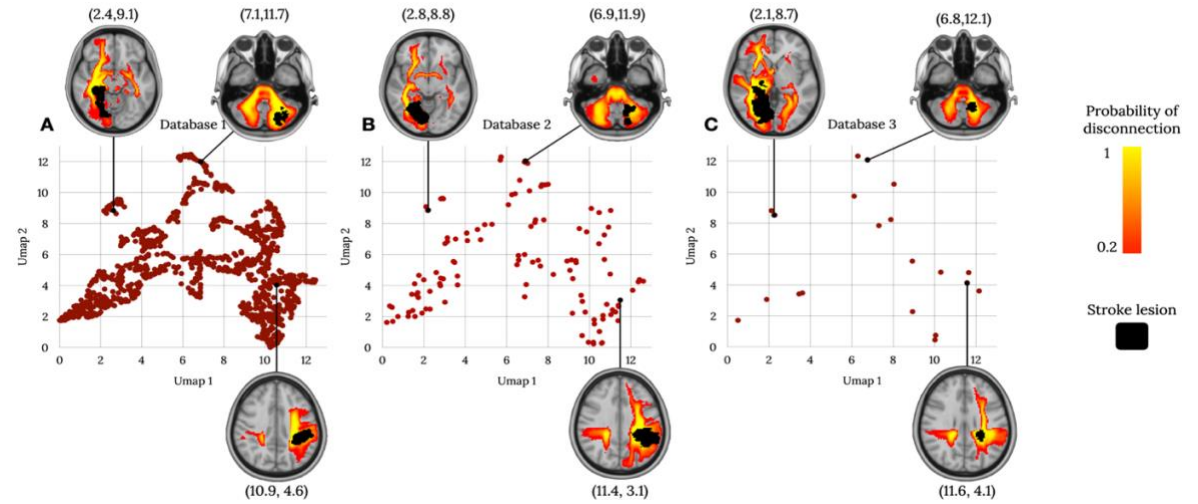

Supplementary figure 3: disconnectome morphospace patient projections for dataset 1 (panel A), dataset 2 (panel B), and dataset 3 (panel C).

Domain	Acronym	Neuropsychological score (test battery)
Motor	laragrasp	Left hand grasp (ARAT)
	laragrip	Left hand grip (ARAT)
	larapinch	Left hand pinch (ARAT)
	lgrip	Left hand grip strength
	lpegs	Left hand peg replacement
	lshflex	Left shoulder flexion (AROM)
	lwrext	Left wrist extension (AROM)
	raragrasp	Right hand grasp (ARAT)
	raragrip	Right hand grip (ARAT)
	rarapinch	Right hand pinch (ARAT)
	rgrip	Right hand grip strength
	rpegs	Right hand peg replacement
	rshflex	Right shoulder flexion (AROM)
	rwrext	Right wrist extension (AROM)
	walk_total	Walking combined score
Language	reading_raw	Sentence reading (BDAE)
	animal_raw	Animal name fluency (SVFT)
	boston_raw	Picture naming (BDAE)
	commands_raw	Performing listen commands (BDAE)
	nonword	Nonword repetition (BDAE)
	reading_comp_raw	Comprehension of read sentence (BDAE)
	word_raw	Comprehension of listen word (BDAE)
Visuospatial attention	bit_coc	Center of cancellation (BIT)
	bit_ltot_miss	Left misses (BIT)
	bit_rtot_miss	Right misses (BIT)
	bit_tot_miss	Total misses (BIT)
	mes_coc	Center of cancellation (Mes-USCT)
	mes_l_miss	Left misses (Mes-USCT)
	mes_r_miss	Right misses (Mes-USCT)
	mes_tot_miss	Total misses (Mes-USCT)
	pos_acc_avg	Accuracy average (Posner)
	pos_acc_disengage	Accuracy disengagement (Posner)
	pos_acc_li	Accuracy left invalid (Posner)
	pos_acc_lv	Accuracy left valid (Posner)
	pos_acc_ri	Accuracy right invalid (Posner)
	pos_acc_rv	Accuracy right valid (Posner)

	pos_acc_validity	Accuracy validity (Posner)
	pos_acc_vf	Accuracy visual effect (Posner)
	pos_rt_avg	Reaction time average (Posner)
	pos_rt_disengage	Reaction time disengagement (Posner)
	pos_rt_li	Reaction time left invalid (Posner)
	pos_rt_lv	Reaction time left valid (Posner)
	pos_rt_ri	Reaction time right invalid (Posner)
	pos_rt_rv	Reaction time right valid (Posner)
	pos_rt_validity	Reaction time validity (Posner)
	pos_rt_vf	Reaction time visual effect (Posner)
	pos_sub_avg	Subbing average (Posner)
	pos_sub_disengage	Subbing disengagement (Posner)
	pos_sub_li	Subbing left invalid (Posner)
	pos_sub_lv	Subbing left valid (Posner)
	pos_sub_ri	Subbing right invalid (Posner)
	pos_sub_rv	Subbing right valid (Posner)
	pos_sub_validity	Subbing validity (Posner)
	pos_sub_vf	Subbing visual effect (Posner)
Visuospatial memory	bvmt_bias	Figure bias (BVMT)
	bvmt_delay	Figure delayed recall (BVMT)
	bvmt_delayt	Figure delayed recall t-score (BVMT)
	bvmt_discrim	Figure recognition discrimination (BVMT)
	bvmt_fa	Figure false alarm (BVMT)
	bvmt_hit	Figure recognition hit (BVMT)
	bvmt_im	Figure immediate recall (BVMT)
	bvmt_imt	Figure immediate recall t-score (BVMT)
	bvmt_learn	Figure learning (BVMT)
	bvmt_perc	Figure percent retained (BVMT)
Verbal memory	hvlt_delay	Word recall (HVLT)
	hvlt_delayt	Word recall t-score (HVLT)
	hvlt_discrim	Word recognition (HVLT)
	hvlt_discrimt	Word recognition t-score (HVLT)
	hvlt_fa1	Word recognition related false alarms (HVLT)
	hvlt_fa2	Word recognition unrelated false alarms (HVLT)
	hvlt_fa3	Word recognition false positive (HVLT)
	hvlt_hit	Word recognition hits (HVLT)
	hvlt_imt	Word immediate recall t-score (HVLT)

	hvlt_learn	Word learning (HVLT)
	hvlt_perc	Word recall retained (HVLT)
Pain	pain	Pain
Sickness	sip_alert	Alertness behaviour (SA-SIP)
	sip_amb	Ambulation (SA-SIP)
	sip_body	Body care and movement (SA-SIP)
	sip_com	Communication (SA-SIP)
	sip_emo	Emotional behavior (SA-SIP)
	sip_house	Household (SA-SIP)
	sip_mob	Mobility (SA-SIP)
	sip_physical	Psychosocial (SA-SIP)
	sip_psychosoc	Physical function (SA-SIP)
	sip_social	Social (SA-SIP)

Supplementary Table 2. Neuropsychological score abbreviations. Among the adopted examination tests: ARAT=Action Reaction Arm total test, AROM= Active Range Of Motion, BDAE=Boston Diagnostic Aphasia Examination, SVFT= Standard Verbal Fluency Test, BIT= Behavioural Inattention Test, Mes-USCT=Mesulam Unstructured Symbol Cancellation Test, BVMT=Brief Visuospatial Memory Test-revised, HVLT= the Hopkins Verbal Learning Test-revised, SA-SIP=Stroke-Adapted Sickness Impact Profile.

Neuropsychological scores		**PCA variance explain (%)**			**Multiple regression model**		
Domain	**Acronym**	**PCA 1**	**PCA 2**	**PCA 3**	**ES**	**p-value**	**FDR**
Motor	laragrasp	47	25	14	0.78	2.01E-09	5.75E-08
	laragrip	51	22	12	0.39	1.50E-05	1.43E-04
	larapinch	46	25	13	0.89	3.03E-10	1.30E-08
	lgrip	32	19	16	0.33	1.84E-04	1.05E-03
	lpegs	39	26	9	0.70	5.10E-08	1.10E-06
	lshflex	35	27	10	0.54	2.00E-06	3.44E-05
	lwrext	47	29	8	0.24	2.05E-03	5.04E-03
	raragrasp	47	29	12	0.37	2.70E-05	2.32E-04
	raragrip	46	30	12	0.44	5.00E-06	7.17E-05
	rarapinch	42	29	13	0.40	1.40E-05	1.43E-04
	rgrip	36	28	13	0.16	1.68E-02	2.12E-02
	rpegs	37	17	13	0.26	1.25E-03	3.83E-03
	rshflex	49	27	11	0.38	5.00E-05	3.73E-04
	rwrext	52	27	11	0.17	1.09E-02	1.56E-02
	walk_total	69	21	6	0.13	2.18E-03	5.04E-03
Language	reading_raw	65	21	9	0.21	3.04E-03	6.23E-03

	animal_raw	50	21	12	0.20	3.20E-03	6.41E-03
	boston_raw	69	12	10	0.13	2.64E-02	3.11E-02
	commands_raw	56	32	7	0.37	7.20E-05	4.73E-04
	nonword	67	13	7	0.28	4.01E-04	1.82E-03
	reading_comp_raw	61	27	8	0.12	4.31E-02	4.79E-02
	word_raw	48	28	9	0.19	4.58E-03	8.10E-03
Visuospatial attention	bit_coc	85	9	3	0.19	7.81E-03	1.27E-02
	bit_ltot_miss	73	17	6	0.30	4.46E-04	1.92E-03
	bit_rtot_miss	75	16	3	0.31	3.45E-04	1.71E-03
	bit_tot_miss*	85	8	4	0.35	2.24E-01*	2.27E-01*
	mes_coc	64	15	9	0.24	1.05E-03	3.48E-03
	mes_l_miss	69	14	10	0.22	2.27E-03	5.04E-03
	mes_r_miss	56	29	9	0.15	1.39E-02	1.86E-02
	mes_tot_miss	45	32	16	0.22	2.28E-03	5.04E-03
	pos_acc_avg	45	34	12	0.24	1.67E-03	4.62E-03
	pos_acc_disengage	48	24	12	0.28	4.92E-04	2.01E-03
	pos_acc_li*	57	21	14	0.11	6.30E-02*	6.77E-02*
	pos_acc_lv	53	20	15	0.44	1.00E-05	1.23E-04
	pos_acc_ri	57	25	9	0.24	1.56E-03	4.47E-03
	pos_acc_rv	58	21	8	0.32	3.57E-04	1.71E-03
	pos_acc_validity	46	18	9	0.15	1.85E-02	2.28E-02
	pos_acc_vf	54	19	14	0.16	1.32E-02	1.81E-02
	pos_rt_avg	59	16	13	0.15	1.81E-02	2.26E-02
	pos_rt_disengage	48	25	8	0.23	1.75E-03	4.70E-03
	pos_rt_li	60	17	9	0.15	1.64E-02	2.10E-02
	pos_rt_lv	56	22	12	0.18	8.48E-03	1.31E-02
	pos_rt_ri	39	26	14	0.17	1.07E-02	1.56E-02
	pos_rt_rv	59	17	9	0.29	3.57E-04	1.71E-03
	pos_rt_validity	48	18	16	0.22	2.41E-03	5.05E-03
	pos_rt_vf	43	24	10	0.25	1.04E-03	3.48E-03
	pos_sub_avg	70	14	6	0.21	6.03E-03	9.98E-03
	pos_sub_disengage	53	25	7	0.23	3.98E-03	7.45E-03
	pos_sub_li*	50	32	10	0.11	7.62E-02*	7.89E-02*
	pos_sub_lv	61	15	13	0.21	5.50E-03	9.46E-03
	pos_sub_ri	74	13	8	0.18	1.30E-02	1.81E-02

	pos_sub_rv	62	12	10	0.17	1.49E-02	1.94E-02
	pos_sub_validity	54	27	6	0.22	4.62E-03	8.10E-03
	pos_sub_vf	39	33	7	0.25	2.05E-03	5.04E-03
Visuospatial memory	bvmt_bias	32	18	14	0.33	7.70E-05	4.73E-04
	bvmt_delay	54	20	14	0.12	3.68E-02	4.22E-02
	bvmt_delayt	46	21	12	0.25	6.87E-04	2.57E-03
	bvmt_discrim	53	26	11	0.13	2.69E-02	3.13E-02
	bvmt_fa	49	24	18	0.13	2.39E-02	2.90E-02
	bvmt_hit	53	32	5	0.24	9.60E-04	3.44E-03
	bvmt_im	58	16	12	0.16	1.00E-02	1.48E-02
	bvmt_imt	53	23	10	0.18	5.94E-03	9.98E-03
	bvmt_learn*	91	5	4	0.09*	9.59E-02*	9.81E-02*
	bvmt_perc	49	26	8	0.26	5.65E-04	2.21E-03
Verbal memory	hvlt_delay	86	10	2	0.13	2.60E-02	3.10E-02
	hvlt_delayt	67	20	7	0.11	4.34E-02	4.79E-02
	hvlt_discrim	54	18	13	0.19	4.32E-03	7.90E-03
	hvlt_discrimt	41	24	14	0.20	3.51E-03	6.71E-03
	hvlt_fa1	44	30	10	0.15	1.42E-02	1.87E-02
	hvlt_fa2	73	16	10	2.07	5.61E-18	4.82E-16
	hvlt_fa3	43	27	13	0.20	3.49E-03	6.71E-03
	hvlt_hit*	73	10	7	0.10*	7.24E-02*	7.60E-02*
	hvlt_imt*	82	17	1	0.05*	3.06E-01*	3.06E-01*
	hvlt_learn	80	10	4	0.11	4.46E-02	4.86E-02
	hvlt_perc	43	34	17	0.21	2.35E-03	5.05E-03
Pain	pain	43	24	17	0.42	5.20E-05	3.73E-04
Sickness	sip_alert*	50	26	9	0.11	6.92E-02*	7.35E-02*
	sip_amb	51	25	8	0.18	8.24E-03	1.31E-02
	sip_body	53	24	10	0.24	1.93E-03	5.03E-03
	sip_com	57	13	12	0.18	8.54E-03	1.31E-02
	sip_emo	44	23	12	0.26	1.13E-03	3.61E-03
	sip_house	47	35	9	0.13	4.18E-02	4.73E-02
	sip_mob	60	17	7	0.23	2.29E-03	5.04E-03
	sip_physical	53	17	12	0.17	1.19E-02	1.68E-02
	sip_psychosoc	44	27	9	0.25	1.49E-03	4.42E-03
	sip_social	40	27	13	0.18	9.48E-03	1.43E-02

Supplementary Table 3: Neuropsychological scores are grouped according to functional domains, and the relative acronyms are reported. The percentage of variance explained

in each principal component is reported, evaluating the association between neuropsychological score measured and probability of localisation in the disconnectome morphospace. The reported effect size (ES) describes the correlation strength obtained in the multiple regression model with PCAs as independent variables and neuropsychological scores as dependent variables (large ES above 0.5, medium above 0.3 and small above 0.1). The corresponding multiple regression model p-values uncorrected and corrected for false discovery rate (FDR) are reported. Asterixis indicate scores with small effect size and/or p-value<0.05.

Neuropsychological scores		**Training**		**Validation**	
Domain	Acronym	N patients	Accuracy (%)	N patients	Accuracy (%)
	laragrasp	79	90.0	20	95.6
	laragrip	79	90.1	20	93.6
	larapinch	78	88.2	20	91.3
	lgrip	73	81.4	14	78.2
	lpegs	73	85.8	14	82.8
	lshflex	71	86.2	13	89.2
	lwrext	73	83.0	14	89.1
	raragrasp	79	90.5	20	90.4
	raragrip	79	90.8	20	90.3
	rarapinch	79	87.8	20	89.6
	rgrip	73	82.6	14	75.9
	rpegs	73	84.0	14	83.6
	rshflex	73	89.5	13	83.6
	rwrext	73	86.0	14	86.2
Motor	walk_total	79	84.5	20	82.2
	reading_raw	77	92.5	20	89.5
	animal_raw	79	88.4	20	83.0
	boston_raw	79	89.8	20	91.2
	commands_raw	73	96.7	14	92.2
	nonword	77	84.9	20	81.0
	reading_comp_raw	77	89.8	20	85.7
Language	word_raw	79	97.6	20	94.8
	bit_coc	72	89.6	13	86.2
	bit_ltot_miss	72	88.1	13	86.3
	bit_rtot_miss	72	87.7	13	91.1
	bit_tot_miss	72	86.0	13	88.1
	mes_coc	78	90.6	20	86.0
Visuospatial attention	mes_l_miss	78	91.6	20	88.5

	mes_r_miss	78	91.5	20	89.5
	mes_tot_miss	78	92.6	20	90.4
	pos_acc_avg	75	97.3	19	91.0
	pos_acc_disengage	75	88.8	19	86.7
	pos_acc_li	75	95.9	19	84.9
	pos_acc_lv	75	97.4	19	86.1
	pos_acc_ri	75	95.8	19	95.4
	pos_acc_rv	75	97.4	19	94.9
	pos_acc_validity	75	83.4	19	84.9
	pos_acc_vf	75	97.4	19	83.5
	pos_rt_avg	75	92.6	19	85.5
	pos_rt_disengage	75	87.6	19	80.2
	pos_rt_li	75	94.8	19	86.9
	pos_rt_lv	75	95.1	19	87.0
	pos_rt_ri	75	92.7	19	88.8
	pos_rt_rv	75	90.6	19	85.7
	pos_rt_validity	75	86.2	19	77.7
	pos_rt_vf	75	96.2	19	87.5
	pos_sub_avg	69	92.4	13	83.6
	pos_sub_disengage	69	81.8	13	78.7
	pos_sub_li	69	93.0	13	85.7
	pos_sub_lv	69	94.3	13	83.9
	pos_sub_ri	69	91.1	13	85.6
	pos_sub_rv	69	92.6	13	86.0
	pos_sub_validity	69	80.6	13	78.0
	pos_sub_vf	69	96.2	13	83.1
Visuospatial memory	bvmt_bias	79	90.1	20	87.7
	bvmt_delay	79	76.8	20	79.2
	bvmt_delayt	79	78.1	19	78.2
	bvmt_discrim	79	86.7	20	83.5
	bvmt_fa	79	89.0	20	89.6
	bvmt_hit	79	94.1	20	90.3
	bvmt_im	79	78.6	20	83.9
	bvmt_imt	79	79.3	19	82.0
	bvmt_learn	79	78.5	20	70.4
	bvmt_perc	79	93.0	20	94.8
Verbal memory	hvlt_delay	78	78.2	17	75.0
	hvlt_delayt	79	75.5	17	76.1

	hvlt_discrim	78	87.4	17	80.9
	hvlt_discrimt	79	80.1	17	73.0
	hvlt_fa1	78	82.1	17	81.2
	hvlt_fa2	78	95.5	17	84.2
	hvlt_fa3	78	82.4	17	81.1
	hvlt_hit	78	92.4	17	88.6
	hvlt_imt	79	84.0	17	81.9
	hvlt_learn	78	77.1	17	75.6
	hvlt_perc	78	85.8	17	85.6
Pain	pain	68	86.1	17	87.3
	sip_alert	73	69.4	13	60.8
	sip_amb	73	72.0	13	61.1
	sip_body	73	75.8	13	80.3
	sip_com	73	72.0	13	73.3
	sip_emo	73	78.3	13	79.7
	sip_house	73	72.1	13	66.7
	sip_mob	73	75.6	13	73.3
	sip_physical	73	80.2	13	79.0
	sip_psychosoc	73	79.9	13	74.2
Sickness	sip_social	73	77.9	13	76.5

Supplementary Table 4: The accuracy of prediction of each neuropsychological score is reported, using the multiple regression model defined in the disconnectome morphospace. Neuropsychological scores are grouped according to functional domains. Next to the accuracy of prediction, the number of patients included to inform the regression model (training phase, dataset 2), and to test it (validation phase, dataset 3).

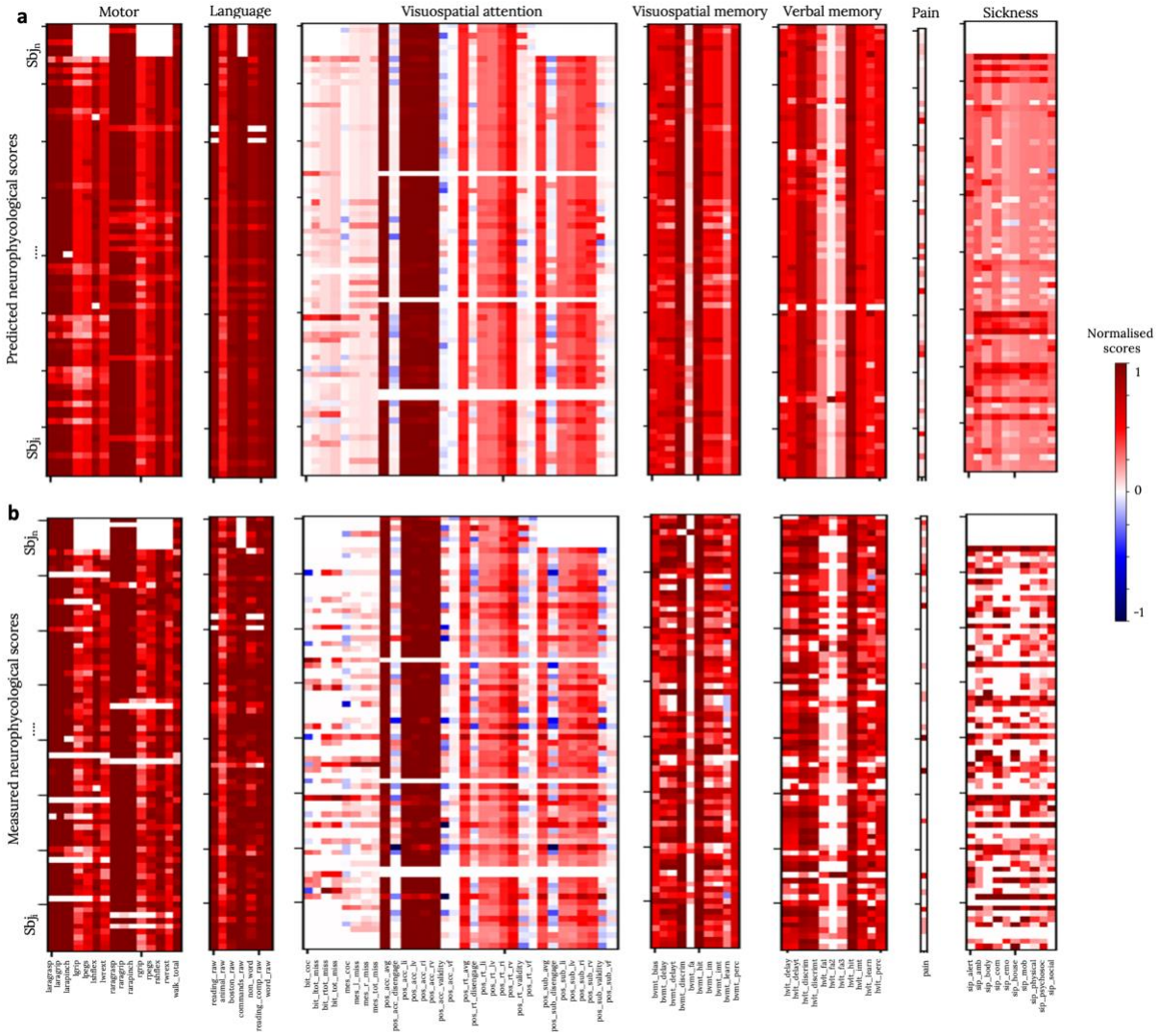

Supplementary Figure 4. Validation of the neuropsychological score prediction. Rows indicate different subjects (derived from validation phase, dataset 3) and columns correspond to neuropsychological tests, grouped according to domains Upper panel (a) corresponds to the predicted neuropsychological scores by the disconnectome morphospace prediction model. Lower panel (b) indicates measured scores during patients' neuropsychological evaluation at 1-year after the stroke onset.

C. Neuropsychological disconnectome map

C.1 Motor functions

The tests assessing the patients' upper limbs motor functions investigate the general movement abilities of the hand via the Action Research Arm test (Addis et al. ; Lyle 1981), the grip strength (Demeurisse et al. 1980), the dexterity via the 9-Hole Peg test (Oxford Grice et al. 2003), the shoulder flexion and wrist extension (Dreeben-Irimia 2008). The motor abilities of the lower limbs have been examined via the *combined walking index*.

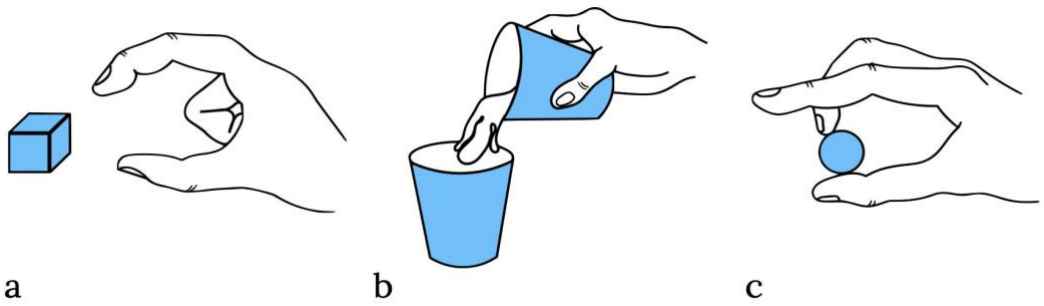

Supplementary Figure 5. Examples of the *Action Research Arm* subtests. a) First item of the grasp subtest. b) First item of the grip subtest. c) First item of the pitch subtest.

Action Research Arm - ARA test

The ARA test (Lyle 1981) assesses the ability to perform purposeful movements with the upper limb extremities. Specifically, it tests the ability to grasp, grip and pinch objects of different weights and shapes, and perform gross movements with the limb.
The ARA has four subtests of 19 items in total. Each item is rated on a four-point scale (0-3); higher scores indicate better performance. As the test aims to speed up the examination time, the score of 'three' on the first item of each subtest credits the patients with a score of 'three' in all the remaining items without completing the subtest. If the patients score less than 'three' in the first item, item two (the easiest item) is assessed. The score of 'zero' in item two credits the patients with the 'zero' score in the other items of the subtest, as it is unlikely for the patients to accomplish the remaining tasks. If the patients score less than 'three' on item one and more than 'zero' on item two, all the remaining items are administered (Lyle 1981). In clinical practice, the ARA is assessed on the impaired and unimpaired limbs, separately (Lyle 1981). For this study, only the scores of the impaired limb have been taken into account. Furthermore, only the grasp, grip, and pitch subtests have been considered in this study.
Grasp subtest. The grasp subtest is divided into six items. The patients are required to grasp different objects placed on a tray such as four wooden blocks of various sizes, one ball, and one sharpening stone. The first item is grasping the 10 cm block (Supplementary Figure 5a), whilst the second and easiest item is the grasping of the 2.5 cm block. The total subscore of the grasp subtest ranges from 0 to 18.
Grip subtest. Six tools are presented in the grip subtest, such as two plastic tumblers, two metal tubes of different diameters, a washer, and a bolt. In four items, patients are asked to i) pour water glass to glass (first item; Supplementary Figure 5b), ii) grip the 2.5 cm diameter tube (second and easiest item), iii) grip the 1 cm diameter tube, iv) grip the washer over the bolt. The total score of the four items ranges between 0 to 12.
Pitch subtest. During the six items of the pitch subtest, patients are required to bear balls of different sizes and one marble using different fingers. For instance, the first item requires bearing a 6 mm ball between the third finger and the thumb (Supplementary Figure 5c). In the second and easiest item, the patients pitch a marble with the first finger and the thumb. The total score of the six items ranges between 0 to 18.

Grip strength

The Jamar Dynamometer grip strength assessment investigated patients' grip strength (Supplementary Figure 6). The American Society of Hand Therapists' procedure (Fess and Moran 1981) requires patients to sit on a chair with their back straight and their feet flat on the floor. The examined arm is placed with the elbow flexed at 90°, the fingers flexed as needed for a maximal contraction over the Dynamometer handle, while the forearm and wrist were kept in a neutral position. The patients are asked to take a breath while exerting the maximum grip effort for three consecutive trials. The strength score is recorded in kilograms and the total score is calculated as mean kg over the three trials (Fess and Moran 1981).

Supplementary Figure 6.
Example of the *grip strength task*.

Dexterity

The hand's ability to coordinate the fingers' movement during objects manipulation in a timely way is defined as manual dexterity (Backman et al. 1992). The patients' dexterity has been measured via the 9-Hole Peg test (i.e. 9HPT, Kellor et al. 1971). The test setting includes a one-piece board with a concave folded dish containing nine pegs next to a 9-holes matrix for the pegs (Supplementary Figure 7). Patients sit on a height-custom chair with the tabletop at midchest level. The task instructions require patients to place and remove the nine pegs one at a time and in random order as quickly as possible (Mathiowetz et al. 1985; Oxford Grice et al. 2003). The final score is the time in seconds elapsed from when the patients touch the first peg until the last peg is placed back into the dish.

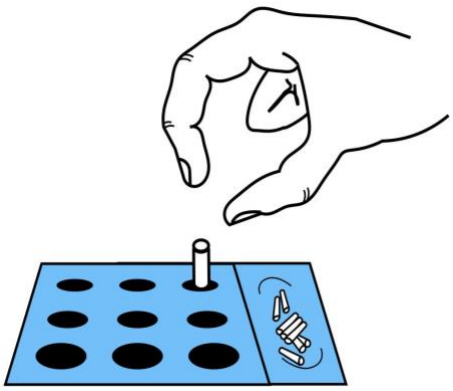

Supplementary Figure 7.
Example of the *9-Hole Peg* test.

Shoulder flexion and Wrist extension

The shoulder flexion and wrist extension assessments (Dreeben-Irimia 2008) investigate patients' movement range of the upper limb and extremity using a goniometer. The main muscles involved in the shoulder flexion are the anterior deltoid and coracobrachialis. During the examination for shoulder flexion, patients are asked to raise their arm against gravity as high as they can, while sitting on the chair. The wrist extension requires mainly the activation of the extensor carpi radialis longus, extensor carpi radialis brevis, and extensor carpi ulnaris (Dreeben-Irimia 2008). The patients sit with their arms on the table in a resting position and with palms down. They are asked to bend back their wrist against gravity. The movement amplitude in the two tasks is recorded as angle grades of the goniometer aligned to the shoulder and wrist respectively (Supplementary Figure 8).

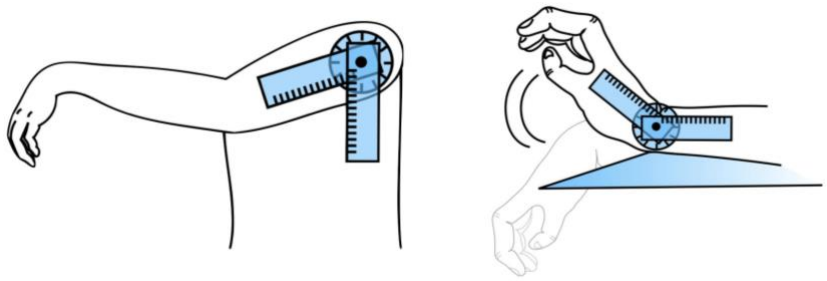

a b

Supplementary Figure 8. Example of the a) *shoulder flexion* and b) *wrist extension* tasks.

Combined walking index

To assess patients' lower limbs ability a combined walking index has been computed (Corbetta et al. 2015). The walking index combines the scores of the 10-meters walking test (i.e. 10MWT, Wade et al. 1987; Supplementary Figure 9a) and the Functional Independence Measure (i.e. FIM, Keith et al. 1987; Supplementary Figure 9b) to capture the variability of maximally and minimally impaired patients. The 10MWT requires patients to walk unassisted if safely able to do so for a distance of 10 meters. The time required to complete the task is recorded in seconds to compute the gait speed (meters/second). Patients unable to safely execute the task have been assessed via the walking item of the FIM. Each patient is assigned with a final, combined 1-9 score which describes on the same scale the performances of maximally and minimally impaired patients. describes the abilities of maximally impaired patients, assessed via the FIM, scores 8 and 9 assigned to each patient Specifically, the scores 1 to 6 correspond to the ranking of patients' walking ability assigned by the therapist according to the FIM (Supplementary Figure 9b): i) the score of one indicates total assistance required, ii) the score of two is assigned when maximal assistance is required, iii) the score of three denotes moderate assistance required, iv) the score of 4 is assigned when minimal contact assistance is needed, v) the score of 5 indicates standby assistance, vi) the score of 6 is assigned when use of assistive device. Scores from 7 to 9 are assigned to independent walking patients who are assessed via the 10MWT: i) the score of seven is assigned at a speed of <0.4 meters/second, ii) the score of 8 indicates a speed of 0.4 to 0.8 meters/second, iii) the score of 9 indicates a speed greater than 0.8 meters/second.

a

Item: Locomotion - Walk	
Score	Level of Functioning
1	Total assist
2	Maximal assist
3	Moderate assist
4	Minimal assist
5	Supervision
6	Modified independency

b

Supplementary Figure 9. Example of the a) the *10-meters walking test* and b) the walking ability ranking of the *Functional Independence Measure*.

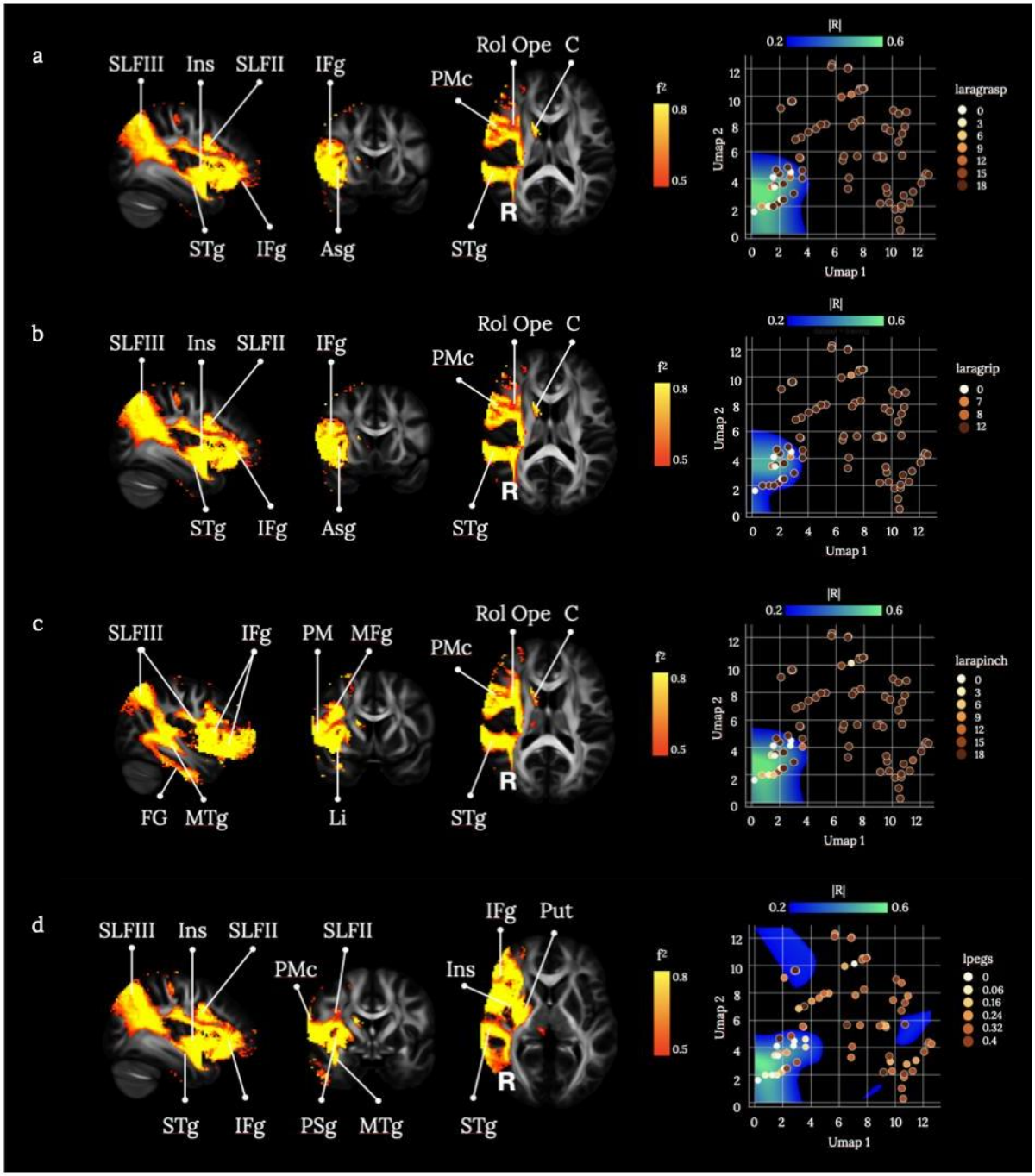

Supplementary Figure 10: Brain disconnections and Umap risk territories contributing significantly to the three subtests (grasp, grip, pitch) of the left hand *Action Research Arm* (ARA), and the 9-Hole Pegs (9HP) tests. *(a) Grasp subtest of the* ARA (laragrasp), (b) *Grip subtest of the* ARA (laragrip), (c) *Pitch subtest of the* ARA (larapitch)), (d) *9HP test* (lpegs). ASg: anterior short gyrus of the insula; C: caudate; FG: fusiform gyrus; IFg: inferior frontal gyrus; Ins: insula; Li: limen insular; Mfg: middle frontal gyrus; MTg: middle temporal gyrus; Put: putamen; PMc: premotor cortex; PSg: posterior short gyrus of the insula; Rol Ope: rolandic operculum; SLFII: second branch of the superior longitudinal fasciculus; SLFIII: third branch of the superior longitudinal fasciculus. Maps are freely available at https://neurovault.org/collections/11260/.

The disconnection in the right hemisphere of frontoparietal structures, the caudate, the post central gyrus, and the insular and temporal cortices cluster in correspondence to low scores in the three subtests (grasp, grip, pitch) of the left hand ARA, and the 9HP test.

Studies on healthy and clinical populations showed that the movement execution of the left upper limb is subserved mainly by structures of the right hemisphere (Nowak et al. 2003; Begliomini et al. 2015) and damage to the connections between motor areas and the spinal cord play a key role in motor impairment after stroke. Nevertheless, our findings reveal that the prediction of the patients' left upper limb motor abilities is given by the disconnection of structures deputed to higher cognitive functions.

The results of this study confirms that the integrity of the right fronto-parietal network seems to be crucial to execute fine contralesional-hand movements and its disconnection predicts the patients' motor abilities after stroke. Previous studies reported the contribution of right frontoparietal structures in the execution of fine left-hand movements such as grasping and gripping (Begliomini et al. 2015; Davare et al. 2007) and clinical evidence showed that the lesion to frontal and parietal structures impairs the execution of fine hand actions (Nowak et al. 2003)bb. The right fronto-parietal network subserves monitoring and attentional processes during the movement execution (Begliomini et al. 2015; Budisavljevic et al. 2017; Howells et al. 2018). In particular, it has been proposed that parietal and inferior frontal structures contribute to generating and maintaining the prediction of the motor outcome, and the updating of sensory expectations regarding the movement is prevented after their damage (Desmurget and Sirigu 2009). In addition, the lesion to the parietal cortex was found to prevent the voluntary initiation of the movement (i.e. anarchic hand, Sirigu et al. 2004).

The damage to frontal-parietal structures and the insular cortex and their association to poor motor performance suggest that bodily-related processes might play a role in motor outcome after stroke (Berti et al. 2005; Karnath et al. 2005; Baier and Karnath 2008; Pacella et al. 2019; Jenkinson et al. 2020). For instance, studies on awareness disorders specific for motor upper limb paralysis suggest that fronto-parietal-insular attentional networks may prevent the updating of the information about patients' current motor abilities (Pacella et al. 2019; Besharati et al. 2014). Moreover, the lack of sense of ownership of one's own upper limb can occur after the disconnection of fronto-parietal-insular network (Gandola et al. 2012; Invernizzi et al. 2013; Moro et al. 2021). These pathologies represent a burden on the success of patients' motor rehabilitation (Jenkinson et al. 2011; Romano and Maravita 2019).

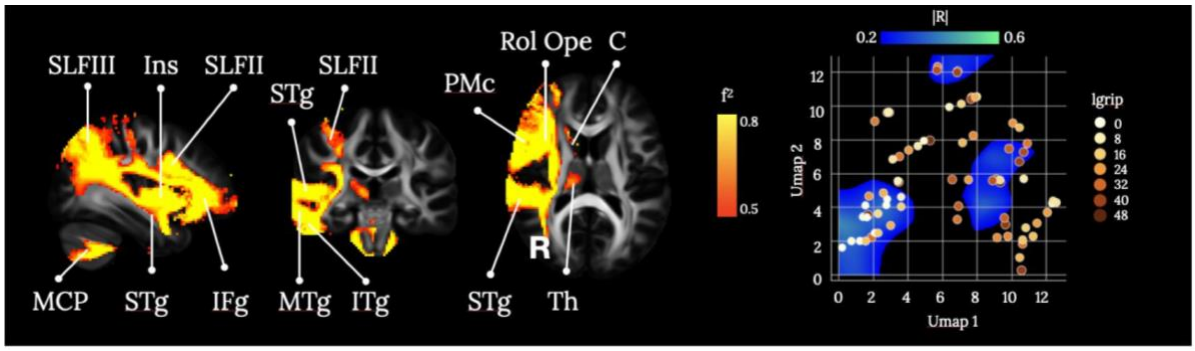

Supplementary Figure 11: Brain disconnections and Umap risk territories contributing significantly to the left hand *grip strength* (lgrip) assessment. C: caudate; IFg: inferior frontal gyrus; Ins: insula; ITg: inferior temporal gyrus; Li: limen insular; MCP: middle cerebellar peduncles; MTg: middle temporal gyrus; PMc: premotor cortex; Rol Ope: rolandic operculum; SLFII: second branch of the superior longitudinal fasciculus; SLFIII:

third branch of the superior longitudinal fasciculus; STg: superior temporal gyrus; Th: thalamus. Maps are freely available at https://neurovault.org/collections/11260/ .

The disconnection of the cortico-pontine-cerebellar loop together with fronto-parietal disconnection observed in prediction of the grip strength assessment scores confirm the participation of the cerebellum in specific components of the movement (Jenmalm et al. 2006) and the prediction and updating stages of the action (Miall et al. 2007; Tomatsu et al. 2016). For instance, the joint activity of the fronts-parietal network and the cerebellum is correlated to the calibration of the movement and force exerted according to different object weights (Schmitz et al. 2005; Jenmalm et al. 2006). This is in line with studies on patients with cerebellar damage, who show inaccurate grip force adjustments during object manipulation (Nowak et al. 2003) and impaired on-line correction of the movement (Desmurget and Grafton 2000).

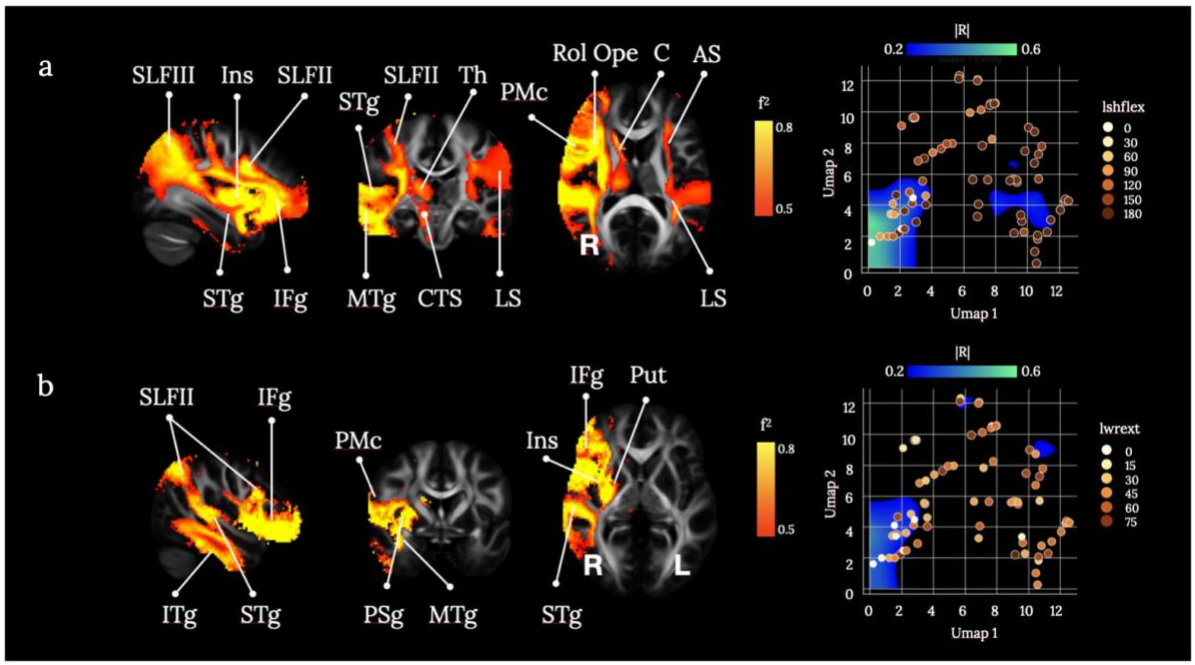

Supplementary Figure 12: Brain disconnections and Umap risk territories contributing significantly to the *(a) left shoulder flexion* (lshflex), and (b) *left wrist extension* (lwrex). AS: anterior segment of the arcuate fasciculus; C: caudate; CTS: cortico-spinal-tract; IFg: inferior frontal gyrus; Ins: insula; ITg: inferior temporal gyrus; LS: long segment of the arcuate fasciculus; MTg: middle temporal gyrus; PMc: premotor cortex; PSg: posterior short gyrus of the insula; Put: putamen; Rol Ope: rolandic operculum; SLFII: second branch of the superior longitudinal fasciculus; SLFIII: third branch of the superior longitudinal fasciculus; STg: superior temporal gyrus. Maps are freely available at https://neurovault.org/collections/11260/ .

The disconnection of fronto-parietal and temporal-parietal structures predicting low scores in wrist flexion and shoulder extension assessments is in line with the results of this study and previous findings on the right hemisphere role in sensorimotor stabilisation during motor execution (Mani et al. 2013; Mutha et al. 2012). However, the activation of left hemisphere structures damaged during shoulder flexion confirms the hypothesis of a degree of hemispheric specialisation in motor dynamics (Mutha et al.

2012; Serrien et al. 2006). Although contralesional motor deficits are more prominent after stroke, the impairment of the ipsilesional limb has been observed (Schaefer et al. 2009a). Differences in the extent of the ipsilesional deficits suggest that the left hemisphere supports multi-joint coordination and its damage prevents the accurate limb trajectory during a reaching movement (Schaefer et al. 2009b). Thus, the pivotal role of the shoulder in the multi-joint coordination for the upper limb motor performance (Galloway and Koshland 2002; Liu et al. 2013) is confirmed by the presence of ipsilesional disconnection only in the prediction of left shoulder extension deficits, compared to the other left limb assessments.

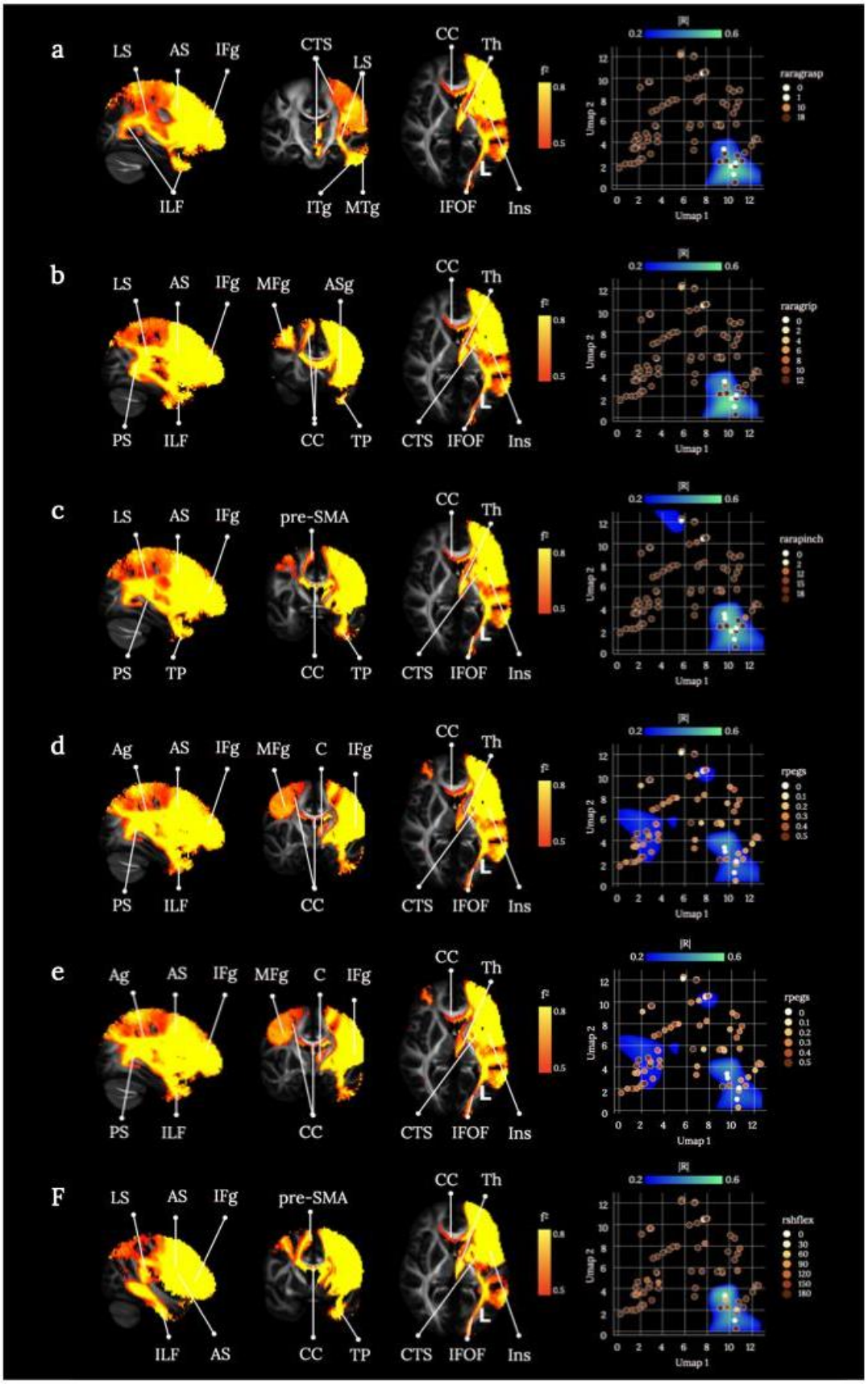

Supplementary Figure 13: Brain disconnections and Umap risk territories contributing significantly to the three subtests (grasp, grip, pitch) of the right hand *Action Research Arm* (ARA), the 9-Hole Pegs (9HP) test, and the right *shoulder flexion* and *wrist extension*. (*a*) *Grasp subtest of the* ARA (raragrasp), (b) *Grip subtest of the* ARA (raragrip), (c) *Pitch subtest of the* ARA (rarapitch)), (d) *9HP test* (rpegs), (e) *left shoulder flexion* (lshflex), and (f)

left wrist extension (lwrex). Ag: angular gyrus; ASg: anterior short gyrus of the insula; AS: anterior segment of the arcuate fasciculus; C: caudate; CC: corpus callosum; CTS: cortico-spinal-tract; IFg: inferior frontal gyrus; ILF: inferior longitudinal fasciculus; IFOF: inferior fronto-occipital fasciculus; Ins: insula; ITg: inferior temporal gyrus; LS: long segment of the arcuate fasciculus; MFg: middle frontal gyrus; pre_SMA: pre-supplementary motor area; PS: posterior segment of the arcuate fasciculus; Th: thalamus; TP: temporal pole. Maps are freely available at https://neurovault.org/collections/11260/ .

An extensive disconnection of the left hemisphere clusters in correspondence to low scores for the right hand in the three subtests (grasp, grip, pitch) of the ARA, 9HP test, the arm flexion and wrist extension tasks. The disconnection involved in the left hemisphere the cortico-spinal tract, postcentral gyrus, fronto-parietal, temporo-occipital and occipito-frontal connections and the interruption of frontal interhemispheric connections in correspondence to the motor section of the corpus callosum. Our results confirm that the disconnection of the corticospinal tract is associated with the motor outcome after brain damage. Previous studies demonstrated that the integrity of the cortico-spinal tract is a reliable predictor of the patients' motor abilities up to one year after the stroke (Stinear et al. 2007) In particular, integrity of the cortico-spinal tract has been associated with the hand dexterity performance (Schaechter et al. 2009) and hand strength (Borich et al. 2012; Qiu et al. 2011) stroke patients. Furthermore, previous studies showed that the severity of motor impairment is predicted by the integrity of the corpus callosum connection of the primary motor areas (Li et al. 2015; Stewart et al. 2017), and reduced interhemispheric resting-state connectivity between motor structures has been associated to motor impairment (Carter et al. 2010). In addition, studies on acallosal patients showed that the lack of callosal connection affects the grip formation in reach-to-grasp movements (Jakobson et al. 1994). These previous findings are in line with our results suggesting that a callosal disconnection of motor and sensory cortices predicts the movements abilities of stroke patients.

The prediction of low scores in ASA, 9-HP, and shoulder flexion and wrist extension via the disconnection of fronto-parietal and temporo-occipital structures, and the insula indicate that motor outcome after left hemisphere stroke is not related only to sensorimotor functions. In fact, movement impairment after left hemisphere stroke can manifest as the inability to perform voluntary, skilled movements such as tool use and gesture imitation (i.e. limb apraxia, De Renzi et al. 1982). Limb apraxia has been associated usually with an extensive network of structures within the left hemisphere (but see Barbieri and De Renzi 1988; Scandola et al. 2021; Vanbellingen et al. 2010`). The damage of left fronto-parietal structures is associated with kinematic deficits during object-related gesture movements (Buxbaum et al. 2014; Goldenberg and Spatt 2009; Tarhan et al. 2015) and non-object related imitation gestures (Pazzaglia et al. 2008; Weiss et al. 2016). Some studies have explored the neural structures related to specific errors performed by apraxic patients during movement (e.g. spatio-temporal and action-content errors) and revealed the involvement of the temporal lobe, the temporo-occipital cortex, and the insula (Hoeren et al. 2014; Scandola et al. 2021; Tarhan et al. 2015).

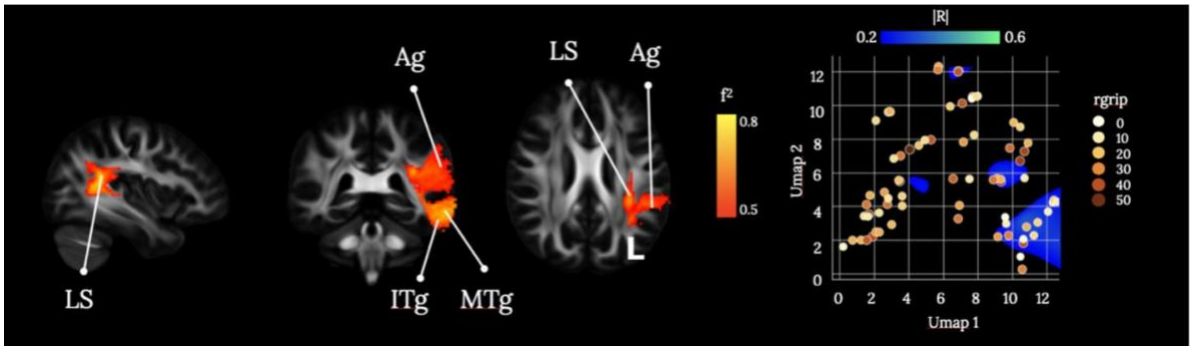

Supplementary Figure 14: Brain disconnections and Umap risk territories contributing significantly to the right hand *grip strength* (rgrip) assessment. Ag: angular gyrus; ITg: inferior temporal gyrus; LS: long segment of the arcuate fasciculus; MTg: middle temporal gyrus. Maps are freely available at https://neurovault.org/collections/11260/ .

The low scores of grip strength assessment are predicted by the solely disconnection of the angular gyrus from the temporal cortex via the damage of the long segment of the arcuate Fasciculus. These results are in contrast with other findings that correlate grip strength assessed via the dynamometer with portico-spinal tract integrity (Borich et al. 2012; Greene et al. 2019; Qiu et al. 2011). However, our results partially overlap the recent findings of Garcea and colleagues (2020), who report the association of reduced right-hand grip strength with lesion to the inferior parietal, middle and superior temporal cortices. Interestingly, our findings suggest that grip strength ability of the right hand may rely on the left hemisphere ventro-dorsal stream conveying information on object-related actions (Binkofski and Buxbaum 2013).

C.2 Language functions

Language was assessed using the 1-min animal verbal fluency test and the Boston Diagnostic Aphasia Examination (BDAE). Familiarity with the Boston school classification of aphasias is necessary to interpret the BDAE (e.g. Benson 1979), and other non-western assessment batteries have since been put forward (e.g. Ivanova et al. 2021).

Verbal fluency tests, like the semantic fluency test, rely on the retrieval of specific information from memory and to verbally produce a list of words. Two types of restrictions are commonly applied: phonological (e.g., letter fluency) and semantic (e.g. animals) clustering. The outcome measure is the speed and ease of production and the final number of words generated in a given time (e.g., 1 min). This group of tests is sometimes considered as speech/language assessments and sometimes as executive functioning tests (Whiteside et al. 2016). This is a sensitive clinical test as brain lesions can alter the speed and ease of verbal production in patients. Acquired aphasia after brain lesions or subsequent to neurodegeneration is commonly associated with greatly reduced verbal productivity Baldo et al., 2001; Baldo et al., 2006; Henry & Crawford, 2004; Marczinski & Kertesz, 2006; Catani et al., 2013. Particularly left frontal lobe lesions have been linked to reduced verbal fluency, especially if the lesion encompasses 'Broca's area' in the inferior frontal gyrus (Baldo et al. 2001). Recently, the frontal aslant tract (FAT) came into focus as a relevant pathway for verbal fluency (Catani et al. 2013). The FAT

connects the inferior frontal gyrus to the supplementary motor region and lateral superior frontal gyrus. The role of these cortical and white matter structures for fluency was further evaluated in awake surgical settings where direct cortical stimulation induced temporary interruptions to these networks (Kemerdere et al. 2016). However, the FAT is also involved in non-speech and language functions (Forkel et al. 2021). Education, sex, and age have been shown to impact the quantity and diversity of animal recollection and the raw scores are therefore usually corrected (e.g. Tombaugh et al. 1999).

Supplementary Figure 15: Example of a time-limited (1min) animal verbal fluency task.

Boston Naming test (BNT, *short version*). The BNT is a popular test of visual confrontation naming, where the patient is shown line drawings of objects with increasing difficulty, ranging from high-frequency (e.g. toothbrush) to low-frequency words (e.g. protractor) (Kaplan et al. 1983). Patients are asked to name the objects within 20 seconds, afterwards a phonemic or semantic cue can be given by the examiner. A shortened version was developed that includes only 15 items which was adopted in the most recent version of the BDAE-3 (Mack et al. 1992; Goodglass et al. 2000) and other test batteries (e.g. CERAD, https://www.memoryclinic.ch/fileadmin/user_upload/Memory_Clinic/CERAD-Plus/CERAD-Plus_Testheft.pdf) and is available in multiple languages. The scoring considers the total number of correct responses, cued responses, and an error code or paraphasia type analysis can also be conducted. Due to the limited original normative data, many other normative data had been provided over the years and also showed an interaction of sex, education, socioeconomic background, and age (e.g. for the short version see \ (Lansing et al. 1999; Villardita et al. 1985; Nicholas et al. 1989). The maximum score for the short version is 15, the scale can be interpreted as the higher the better. The items (and their semantic cues) of the short form include:

1. House (home, a kind of building)
2. Comb (used for fixing hair)
3. Toothbrush (used in the mouth)
4. Octopus (an ocean animal)
5. Bench (used for sitting)

6. Volcano (a kind of mountain)
7. Canoe (used in water)
8. Beaver (an animal)
9. Cactus (saguara, something that grows)
10. Hammock (you lie on it)
11. Stethoscope (used by doctors and nurses)
12. Unicorn (mythical animal)
13. Tripod (photographers or surveyors use it)
14. Sphinx (it's found in Egypt)
15. Palette (artists use it)

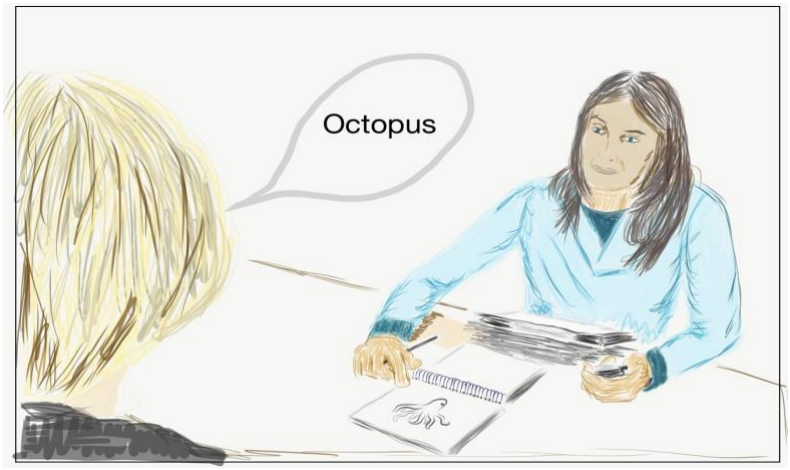

Supplementary figure 16. Example of the administration of the Boston Naming Test (BNT).

Boston Diagnostic Aphasia Examination (BDAE) is a neuropsychological assessment battery that samples from a range of language components for diagnostic and treatment purposes. The BDEA was originally developed and validated by Goodglass & Kaplan in 1983 (Goodglass and Kaplan 1983) and has since been through several iterations with the latest version also offering a shortened version (e.g. Goodglass et al. 2000). The BDAE is a systematic and comprehensive assessment comprising 34 subtests, which can take up to four hours. Patients are asked to answer a semi structured interview and engage in free conversation. Each subtest is scored for correct responses and converted into percentiles. Normative data is available for all subtests. In this study the following subtests were used: *Oral reading of sentences* (reading_raw), *comprehension* (reading_comp_raw), *word comprehension* (word_raw), *Boston picture naming* (boston_raw), *commands* (commands_raw). An additional non-word reading (nonword) test was conducted. Each subtest will be discussed below.

Oral reading of sentences. The read-out-loud sentence reading subtest requires the patient to read ten sentences. The whole sentences must be read without errors to be scored as pass (score of 1) otherwise they are scored as fail (score of 0). The maximum score of the standard form is 10 (short form: 5), and the scale can be interpreted as the higher the better.

1. Summertime.
2. A good beach day.
3. Jim and Mary pack a picnic lunch.
4. They load the car with beach chairs and towels.
5. Off they go with all their equipment.
6. After driving for forty-five minutes, they arrive at the seashore.
7. They decide to go swimming because the water is warm and calm.
8. When they emerge from the water they are famished.
9. That is when they realize they forgot to load their picnic lunch.
10. Luckily, they discover a refreshment stand with a variety of snacks to choose from.

Comprehension of oral reading of sentences. The patients are asked to read each of the comprehension statements aloud and answer by choosing the correct multiple-choice option out of four options. These questions relate to the scenario described in the oral reading of sentences test of the BDAE (see above). The examiner can point to the options on the first run and can ask the patient to select the best completing phrase. The examiner ought not to read the items aloud. The maximum score of the standard form is 5 (short form: 3), and the scale can be interpreted as the higher the better.

1. The weather was …. cool/sunny/crisp/rainy
2. Mary and Jim rode in a …..train/boat/car/plane
3. The trip took about…half a day/five minutes/45 minutes/two hours
4. The water was… rough/warm/ chilly/crowded
5. They forgot to bring a …. towel/umbrella/lunch/swimsuit

Word comprehension. The single word comprehension test belongs to the auditory comprehension assessment of the BDAE and is a basic word discremination task where stimulus items on the patient's body and in the examination booklet need to be pointed at after a verbal prompt from the examiner. The stimuli are grouped by body parts, colours, letters, and numbers. If the correct answer is offered within 5 sec the score is 1 point, if the answer takes longer it is 0.5 point, and 0 for erroneous answers. The maximum score of the standard form is 37 (short form: 16), and the scale can be interpreted as the higher the better.

"Show me your….."

1. Shoulder
2. Cheek
3. Ear
4. Nose
5. Knee

Using the booklet with the picture material the patient is again prompted to point to the following items:

1	Bear	17	J

2	Peanut	18	4
3	Shirt	19	13
4	Bus	20	5
5	Saw	21	20
6	Ant	22	257
7	Tulip	23	Telephone
8	Blue	24	Deer
9	Brown	25	Hamburger
10	Pink	26	Cap
11	Green	27	Wagon
12	Purple	28	Screw
13	T	29	Swan
14	N	30	Spider
15	G	31	Iris
16	K		

Commands. The patient is asked to carry out 1-5 step commands that vary in length and complexity. A point is given for every target element (underlined) that is performed. The command can be repeated in full if requested. The maximum score is 15 (short form: 10), and the scale can be interpreted as the higher the better. Additional items needed for this test are a pencil, a watch, and a card.

1. Make a fist.
2. Point to the ceiling, then to the floor.
3. Put the pencil on top of the card, then put it back.
4. Put the watch on the other side of the pencil and turn over the card.
5. Tap each shoulder twice with two fingers, keeping your eyes shut.

Nonword reading. In this study, we used an experimental measure where the patient was asked to pronounce non-meaningful syllables. Four-letter non words (e.g. NORD) were presented to the patients who were asked to read them aloud. The maximum score for this test is 20, and the scale can be interpreted as the higher the better.

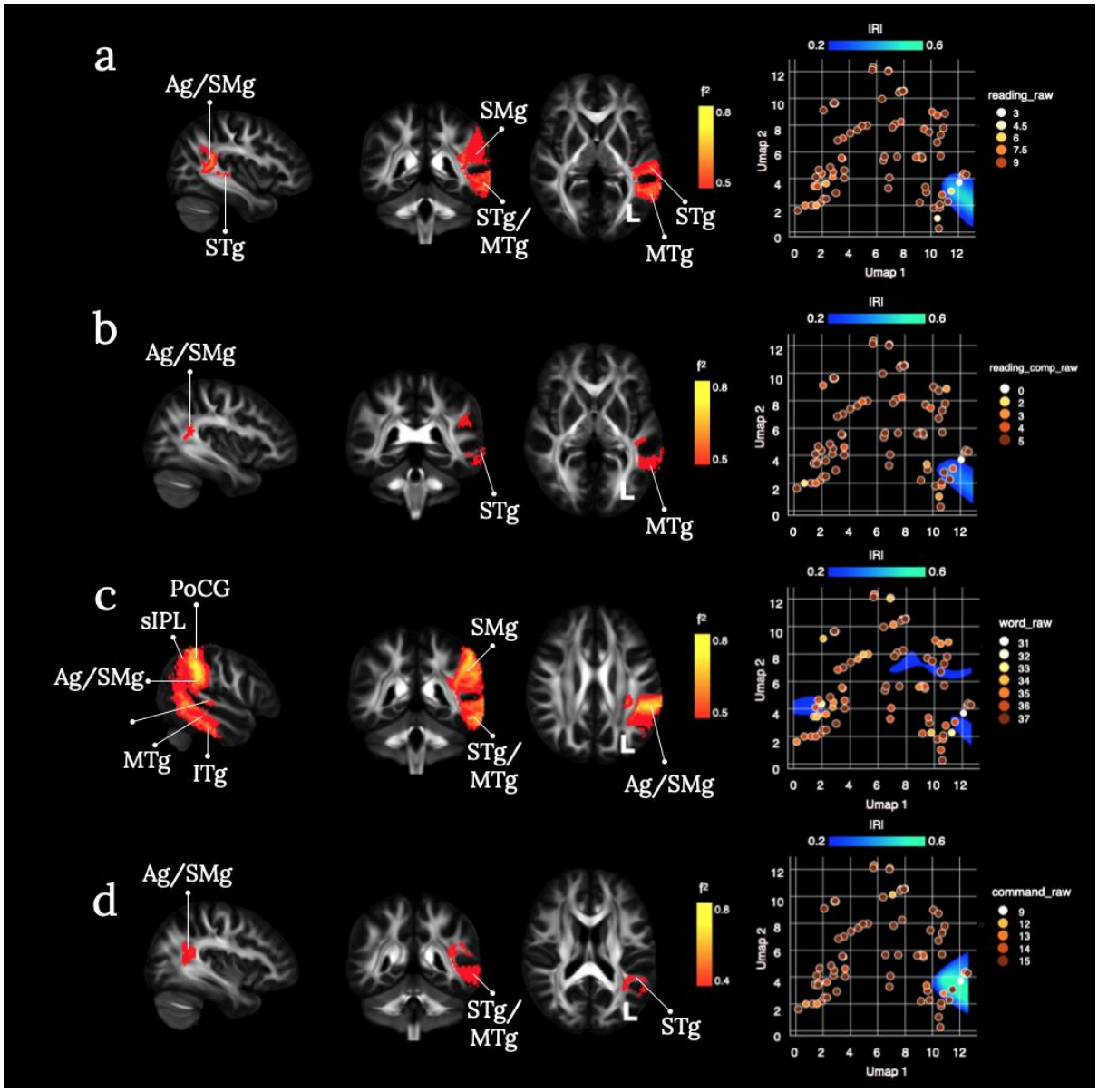

Supplementary Figure 17: Brain disconnections and Umap risk territories contributing significantly to the *Boston Diagnostic Aphasia Examination* (BDAE). (*a*) *Oral reading of sentences* (reading_raw), (b) *comprehension* (reading_comp_raw), (c) *word comprehension* (word_raw), (d) Commands from the BDAE (command_raw). Ag: angular gyrus; ASg: anterior short gyrus of the insula; MSg: middle short gyrus of the insula; IFg: inferior frontal gyrus; STg: superior temporal gyrus; MTg: middle temporal gyrus; Put: putamen; IC: internal capsule; SMg: supramarginal gyrus; PoCG: postcentral gyrus; sIPL: superior parietal lobe; alg: anterior long insular gyrus; ec/ecx: external/extreme capsule; li: limen insular; porb: posterior orbital cortex; ins: insular cortex. Maps are freely available at https://neurovault.org/collections/11260/ .

Profiles of disconnections predict individual deficits on the *Boston Diagnostic Aphasia Examination* (BDAE) subscales for reading aloud (reading_raw), reading comprehension of sentences (reading_comp_raw) and single word comprehension (word_raw), and impairments when following commands (command_raw).

Reading sentences aloud and sentence comprehension clustered in comparable areas in the Umap morphospace with medium effect size. These clusters corresponded to a significant disconnection of the left temporo-parietal network between the superior and middle temporal gyri and the inferior parietal lobe (e.g., angular and supramarginal gyrus). This temporo-parietal network has been shown to predict reading performance and the functional specialisation of the visual word form area (Thiebaut de Schotten et al. 2014a). This network was already postulated as relevant for reading as early as 1891, when one of Dejerine's case studies presented with pure alexia (reading impairment) and subsequent agraphia (writing impairment) (Dejerine 1891). Lesions associated with alexia are often ascribed to the posterior inferior temporal cortex in the left hemisphere (Epelbaum et al. 2008; Gaillard et al. 2006). In recent lesion studies using voxel-based lesion symptom mapping in chronic stroke patients the same network emerged as relevant for sentence-level reading that was uniquely associated with the superior and middle temporal gyri as well as the supramarginal gyrus (Baldo et al. 2018). As such, critical aspects of sentence reading may rely on the ventral visual stream for the identification of familiar words and the integration into a wider language network through parieto-temporal connections, such as the posterior segment of the arcuate fasciculus.

Auditory word comprehension requires the transformation of auditory signals into abstract concepts. As such the adjacent cortex to the primary auditory cortex embedded in the left and right superior temporal gyrus has been consistently shown to be relevant for comprehension in the aphasia stroke literature (Naeser et al. 1987; Crinion and Price 2005; Gajardo-Vidal et al. 2018; Robson et al. 2014; Kreisler et al. 2000; Bates et al. 2003; Damasio 1992). Recently, other temporal regions have also been implicated such as the temporal pole (Mesulam et al. 2015). Converging evidence from different lines of clinical research suggest that the inferior and middle temporal gyri are associated with word comprehension deficits as the integration of auditory and conceptual processing is interrupted (Bonilha et al. 2017). Additional semantic processing is likely to recruit more anterior temporal regions (Mesulam et al. 2015). Akin to sentence-level comprehension, single words comprehension is also associated with the left supramarginal gyrus (Baldo et al. 2018). Using fMRI in healthy adult readers, the sensitivity of this network was disentangled whereby the parieto-temporal cortex responded to phonology and the VWFA in the occipital-temporal cortex to orthography (Glezer et al. 2016). Current models suggest a delicate temporo-parietal and frontal network to be involved in single word comprehension that links lexical concepts (anterior temporal) lemma and lexical-syntactic information (posterior temporal), phoneme-to-motor transfer (parietal-frontal), top-down and executive modulation (frontal) (e.g. Hagoort 2019).

Following commands are significantly impaired with disconnections between the inferior parietal lobe and superior and middle temporal gyri. The cluster in the UMAP morphospace is comparable to sentence reading and comprehension. Identifying a similar network is to be expected as speech comprehension can be assessed using 1-2-3-stage commands {Price, 2010 #139;Wilson, 2018 #140;Price et al., 2010;Kertesz, 2006 #141}.

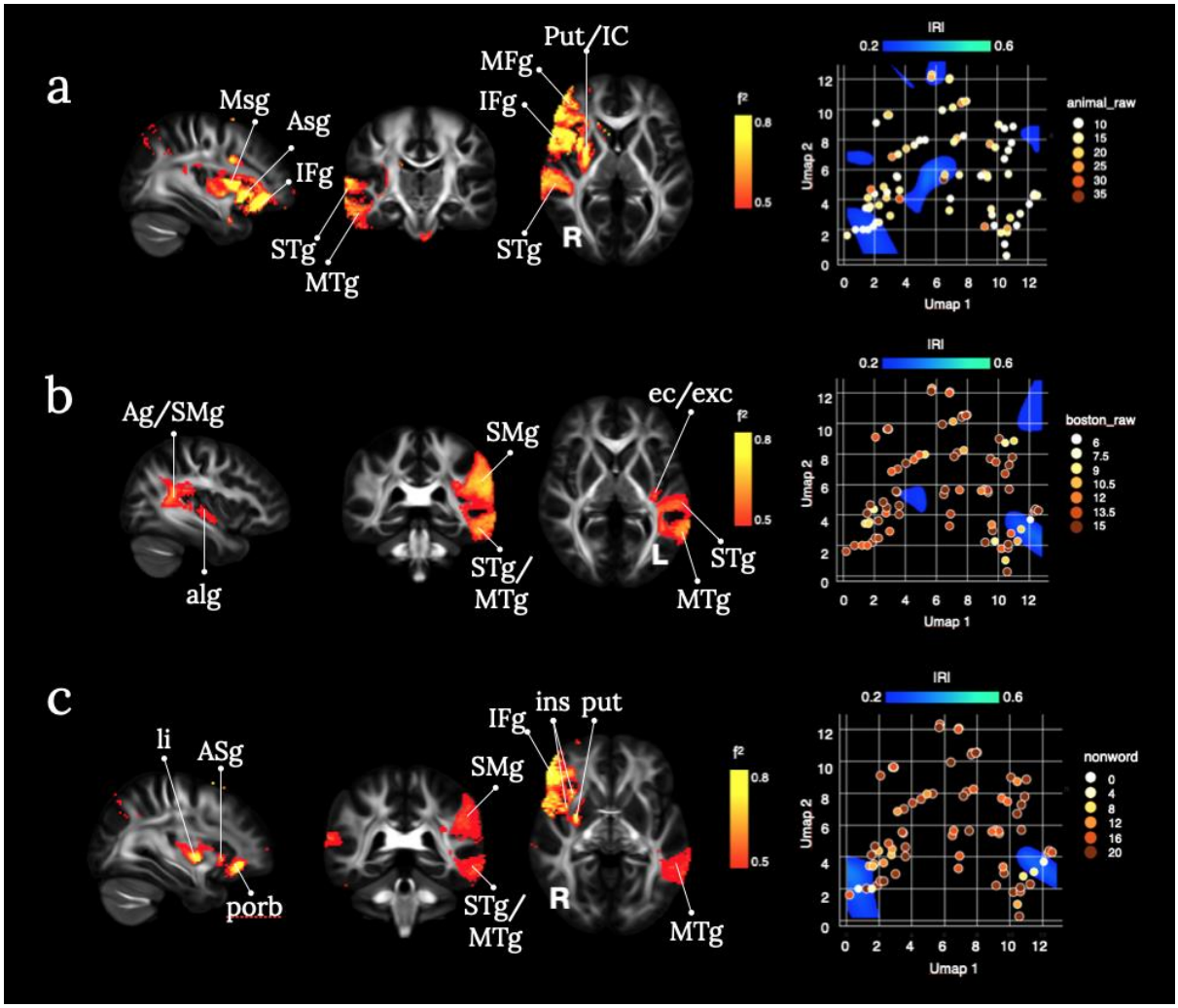

Supplementary Figure 18: Brain disconnections and Umap risk territories contributing significantly to semantic fluency (animals), the *Boston Naming Test* (BNT), and non-word reading. (*a*) 1-min animal fluency (animal_raw), (b) Boston Naming Test (boston_raw), and (c) non-word reading (nonword). Ag: angular gyrus; ASg: anterior short gyrus of the insula; MSg: middle short gyrus of the insula; IFg: inferior frontal gyrus; STg: superior temporal gyrus; MTg: middle temporal gyrus; Put: putamen; IC: internal capsule; SMg: supramarginal gyrus; PoCG: postcentral gyrus; sIPL: superior parietal lobe; alg: anterior long insular gyrus; ec/ecx: external/extreme capsule; li: limen insular; porb: posterior orbital cortex; ins: insular cortex. Maps are freely available at https://neurovault.org/collections/11260/ .

Reduced semantic fluency is associated with lesions to the left inferior frontal gyrus and insula, left medial temporal regions and the right inferior frontal gyrus and periventricular frontal white matter (Biesbroek et al. 2016). Disconnection patterns of the right middle and superior temporal gyri, right inferior frontal gyrus insular cortex (anterior and middle short gyri), and the right putamen/internal capsule predicted semantic fluency patterns.

BNT naming score impairments were predicted by disconnections of a temporal-parietal-insular network including the left hemisphere middle and superior temporal gyri, the inferior parietal lobe (angular and supramarginal gyrus), and the anterior long

insular gyrus and external/extreme capsule. Patients with persistent naming deficits were shown to have disruptions to this network whereby lesions in the posterior superior temporal and inferior parietal cortex caused semantic paraphasias while lesions to the insula and putamen caused phonological paraphasias (Knopman et al. 1984). More recent studies also highlighted that lesions to the angular gyrus cause paraphasia that are unrelated to the BNT target item (e.g. not semantic or phonological paraphasia) (Meier et al. 2020). In an attempt to isolate lexical-semantic retrieval from visual recognition and motor speech elements involved in this picture naming task, Baldo et al. (2013) identified the crucial role of the left mid-posterior middle temporal gyrus for naming errors on the BNT.

Nonword reading performance hinges on disconnections of the right hemisphere temporal-parietal-frontal network as well as the insula putamen. Previous research has highlighted this network as well where lesions to the middle and inferior frontal gyrus (pars opercularis and triangularis), insular cortex, central and parietal opercular cortex, and anterior middle temporal gyrus in addition to the precentral gyrus predicted reading deficits (Woollams et al. 2018; Cloutman et al. 2011). While these areas are most commonly reported for the left hemisphere, studies of right hemisphere patients have identified the same network albeit the flavour of linguistic errors when reading nonwords may be different (Buiatti et al. 2012).

C.3 Visuospatial attention

Visuospatial attention has been assessed along several dimensions, including visual search (i.e., cancellations tasks) and reaction time.

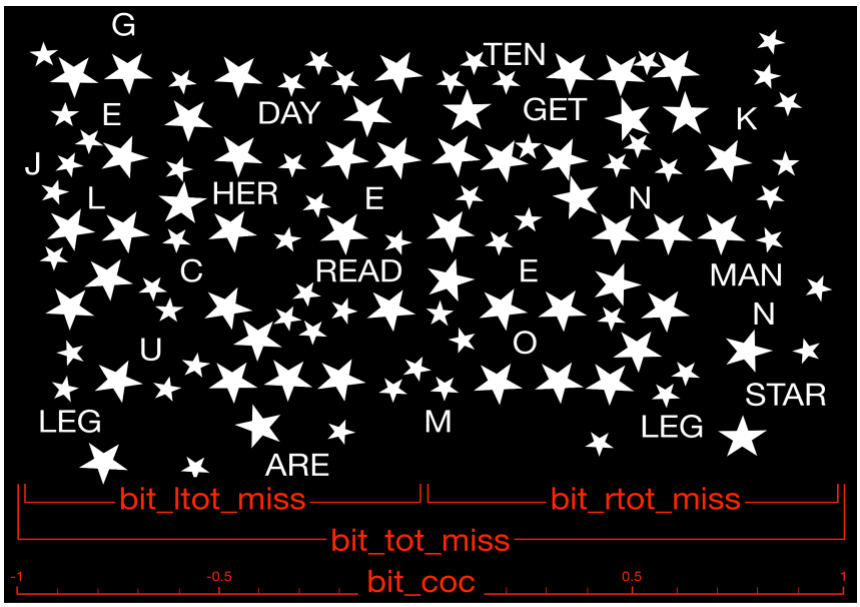

Supplementary Figure 19: Example of the *Star cancellation test* modified from (Wilson et al. 1987). bit_tot_miss: total missed stars; bit_ltot_miss: stars missed on the left; bit_rtot_miss: stars missed on the right; bit_coc: 'centre of mass' of the total cancellation.

Star cancellation is a paper and pencil visual search test originally proposed in and part of the Behavioral Inattention Test (Wilson et al. 1987). The patient has to circle all stars printed on a large A4 piece of paper. Stars are mixed with letters and words that the patient should not circle, as shown in an example of the star cancellation test in Supplementary Figure 19 derived from the original.
Total misses (bit_tot_miss), total left misses (bit_ltot_miss), and total right misses (bit_rtot_miss) scores can be derived from this test, with excellent reliability (i.e. test-retest, Bailey et al. 2004). *Star cancellation* also has a high sensibility and specificity for unilateral spatial neglect (Jehkonen et al. 1998). Additionally, the centre of cancellation (bit_coc) corresponding to the 'centre of mass' of the cancellation can also be calculated (Rorden and Karnath 2010).

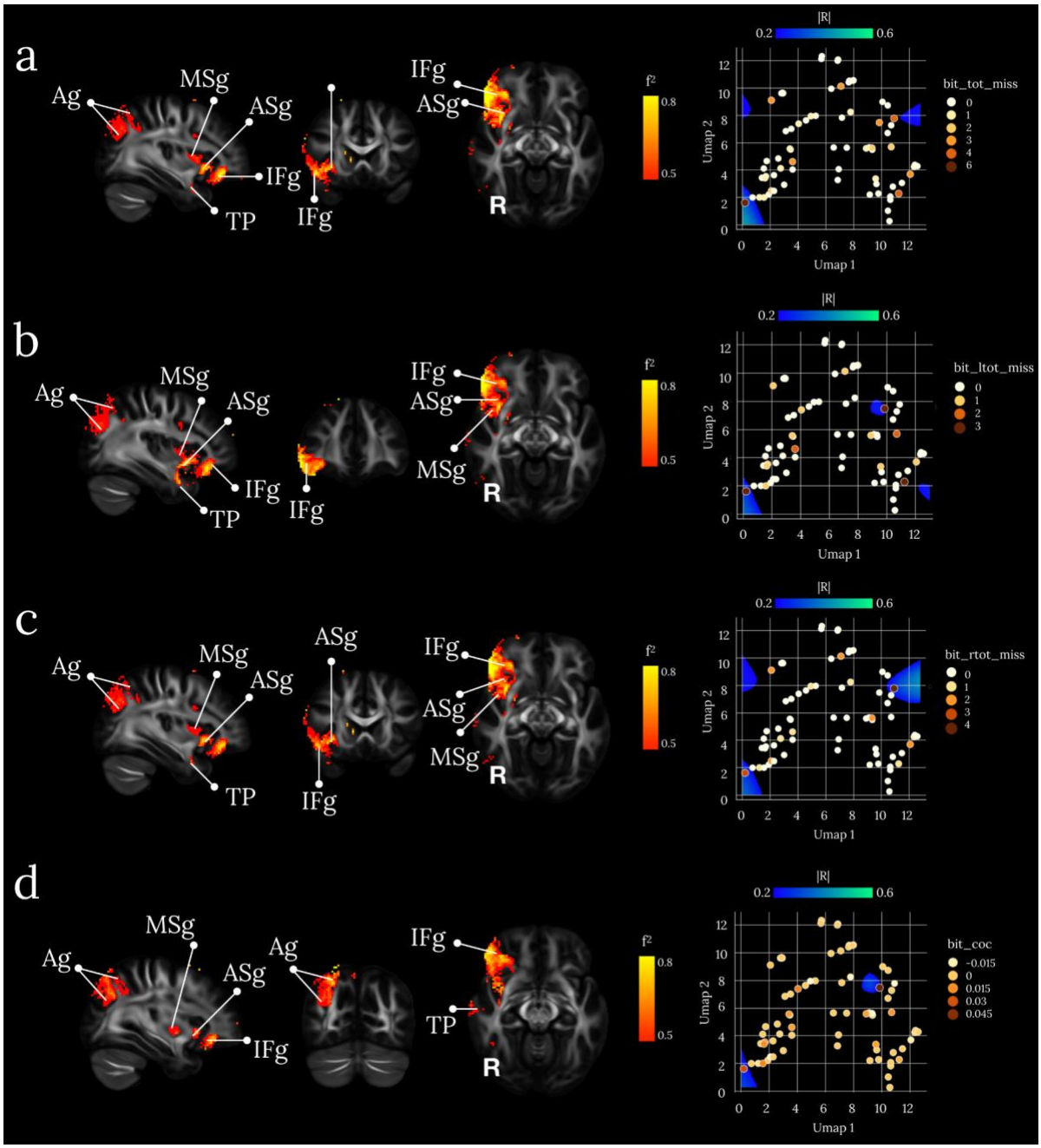

Supplementary Figure 20: brain disconnections and Umap risk territories contributing significantly to the *Star cancellation test*. (*a*) Total misses (bit_tot_miss), (b) total left misses (bit_ltot_miss), (c) total right misses (bit_rtot_miss) scores and (d) the centre of

cancellation (bit_coc). Ag: angular gyrus; ASg: anterior short gyrus of the insula; MSg: middle short gyrus of the insula; IFg: inferior frontal gyrus; TP: temporal pole. Maps are freely available at https://neurovault.org/collections/11260/ .

Profiles of disconnections predicting individual total misses (bit_tot_miss), total left misses (bit_ltot_miss), total right misses (bit_rtot_miss) and the centre of cancellation (bit_coc) clustered together in comparable areas in the Umap morphospace with medium to large effect size. These clusters correspond either to a significant disconnection the right inferior frontal gyrus from the anterior and middle short gyri of the insula via fronto-insular tracts (Catani et al. 2012; Rojkova et al. 2016) and the temporal pole via the uncinate fasciculus (Catani and Thiebaut de Schotten 2012). Local disconnection of the angular gyrus (Catani et al. 2017) was also significant. The role of the inferior frontal gyrus in cancellations tasks such as the *Star cancellation* has been widely documented in the context of unilateral visual neglect (Corbetta et al. 2005; He et al. 2007; Heilman and Valenstein 1998) and discussed with regards to its contribution to visual search in the presence of distractors (Husain and Kennard 1997). The insula has also been reported as a critical area leading to unilateral visual neglect (Manes et al. 1999) due to its contribution to the integration between extrapersonnal stimuli and internal milieu and is typically unactivated when attention lapses (Kranczioch et al. 2005; Weissman et al. 2006). Additionally, lesions to the temporal pole have been significantly associated with a significant drop in cancellation task performance (Karnath et al. 2001; Karnath et al. 2011) because of its contribution to the visual ventral stream and the conscious identification of the target amongst distractors. Finally, the angular gyrus, when damaged, have also been reported as critical to the performance in cancellation tasks (Mort et al. 2003) due to its role in spatial attention (Husain and Rorden 2003).
The disruption of the circuitry constituted by the frontoinsular tracts, the uncinate and local parietal connections elegantly reconcile these four theories explaining the pathophysiological mechanisms related to cancellation tasks performance and unilateral visual neglect.

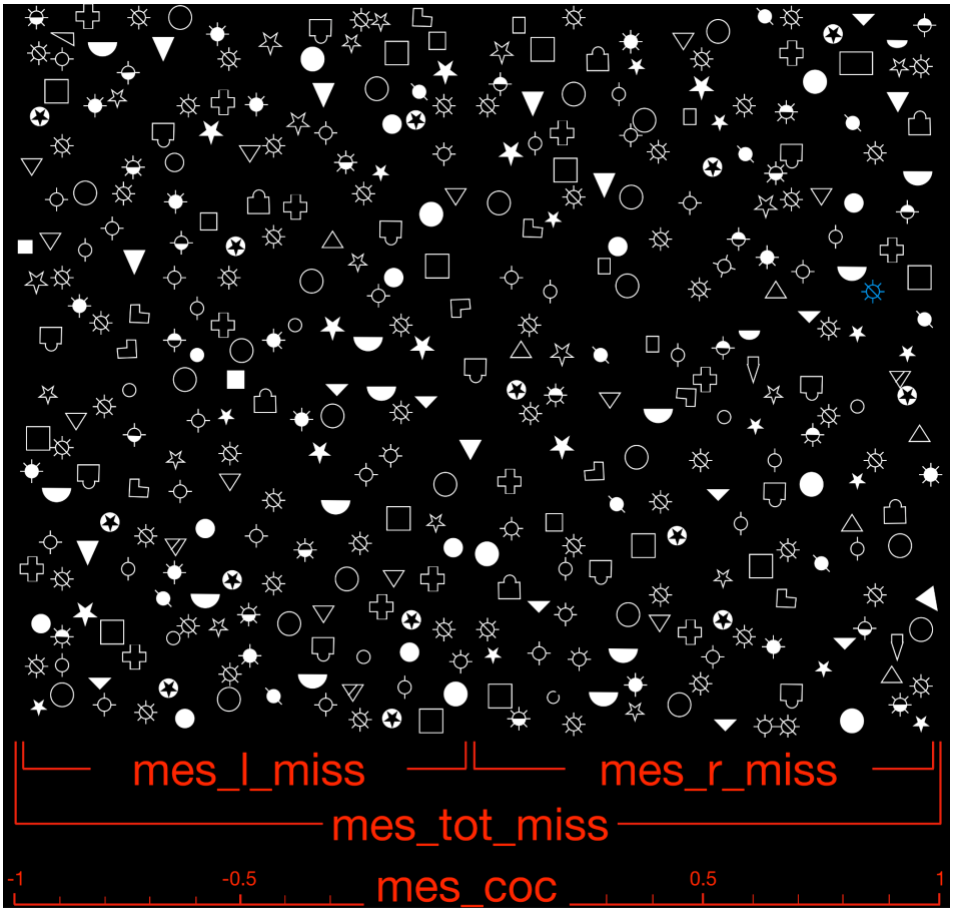

Supplementary Figure 21: Example of the *Mesulam Unstructured Symbol Cancellation Test* modified from (Mesulam 1985). The item in blue is an example of the target to be cancelled by the patients. mes_tot_miss: total missed stars; mes_ltot_miss: stars missed on the left; mes_rtot_miss: stars missed on the right; mes_coc: 'centre of mass' of the total cancellation.

Mesulam Unstructured Symbol Cancellation Test is a paper and pencil visual search test. Patients are asked to bar the full cancel suns (as the one coloured in blue in supplementary figure 21 derived from Mesulam 1985) amongst distrators. Compared to *the star cancellation task*, the higher number of distractors and the use of feature conjunctions (Treisman and Gelade 1980) in the *Mesulam Unstructured Symbol Cancellation Test* makes it a more challenging task to achieve in the clinic.
Four metrics can be derived from the *Mesulam Unstructured Symbol Cancellation Test:* Total misses (mes_tot_miss), total left misses (mes_l_miss), total right misses (mes_r_miss), and centre of cancellation (mes_coc) corresponding to the 'centre of mass' of the cancellation (Rorden and Karnath 2010).

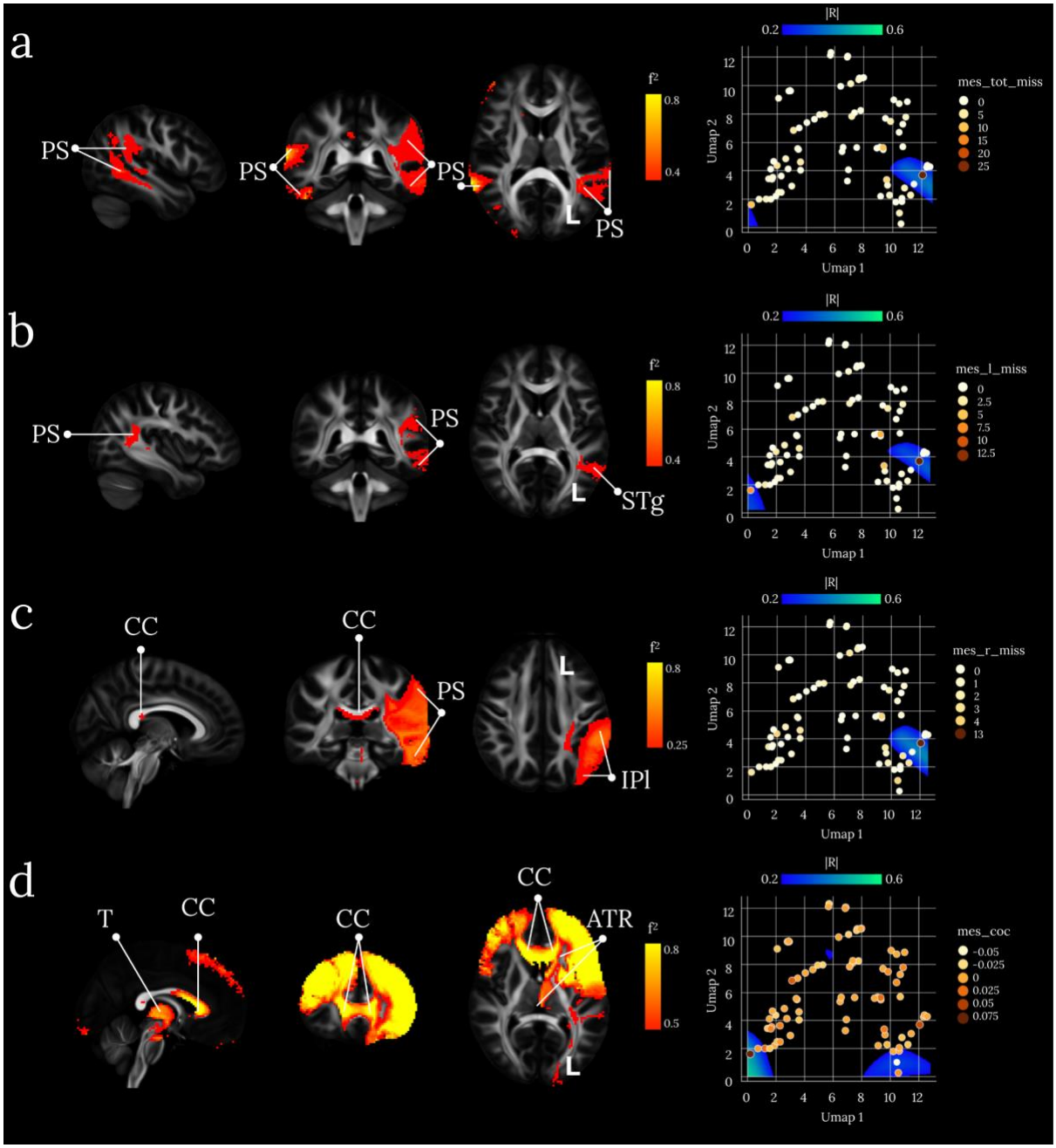

Supplementary Figure 22: brain disconnections and Umap risk territories contributing significantly to the *Mesulam Unstructured Symbol Cancellation Test*. (*a*) Total misses (mes_tot_miss), (b) total left misses (mes_l_miss), (c) total right misses (mes_r_miss) scores and (d) centre of cancellation (mes_coc). ATR: anterior thalamic radiations; CC: corpus callosum; PS: posterior segment of the arcuate fasciculus; T: Thalamus. Maps are freely available at https://neurovault.org/collections/11260/ .

The profiles of disconnections associated with the number of targets missed, whether on the left, right or in total, clustered together in comparable areas in the Umap morphospace with medium to large effect size. These profiles mostly involved the temporoparietal circuits bilaterally (posterior segment of the arcuate fasciculus) and their interhemispheric callosal connections. Of interest, the disconnection of the left hemisphere for left and right misses was more prominent statistically than the right hemisphere. In contrast, the centre of mass of the task was also well predicted but by different risk territories in the UMAP morphospace, also characterised by

interhemispheric connections, but this time in the frontal lobe. A diencephalic disconnection via the anterior thalamic radiations was also significant.

The temporo-parietal disconnection fits with previous theories suggesting that visual awareness deficits would be related to a disconnection between the visual ventral stream and the global workspace (Dalla Barba et al. 2018). Such disconnection would prevent preprocessed visual information (i.e. the visual ventral stream, Ungerleider and Mishkin 1982; Kravitz et al. 2011) to access conscious manipulation (i.e. the global workspace; (Baars 2002; Dehaene and Changeux 2011; Parlatini et al. 2017) indispensable to compare each target mentally to the model during the complex visual search as the *Mesulam Unstructured Symbol Cancellation Test.*

On the other hand, the callosal disconnection fits with Norman Geschwind original theory (1965) suggesting neglected items result from the disconnection of right hemisphere-based knowledge from the left hemisphere. In so doing, the absence of mental verbalisation of right hemisphere-based visual knowledge would prevent their conscious representation (Bartolomeo et al. 2007) and lead to targets' omissions. Of note, the integrity of the corpus callosum also contributes significantly to the recovery of visuospatial neglect (Lunven et al. 2015) and might therefore have contributed to the visual search scores of the chronic patients reported in our study.

Finally, lesions to the thalamus have also been documented to contribute to visual search deficits and hemispatial visual neglect through an interruption of the cortico-subcortical loops critical to the proper function of the cortex (Watson and Heilman 1979; Cambier et al. 1980; Watson et al. 1981; Graff-Radford et al. 1985; Hirose et al. 1985; Bogousslavsky et al. 1986; Vallar and Perani 1986; Waxman et al. 1986; Rafal and Posner 1987; Kumral et al. 1995; Chung et al. 1996; Leibovitch et al. 1998; Karussis et al. 2000; Karnath et al. 2002; De Witte et al. 2008). Hence, through the capture of high dimensional interactions, our method revealed the poly-origin mechanisms leading to a decreased performance at the *Mesulam Unstructured Symbol Cancellation Test* in patients and reconciled the inter- with interhemispheric theories of hemispatial neglect.

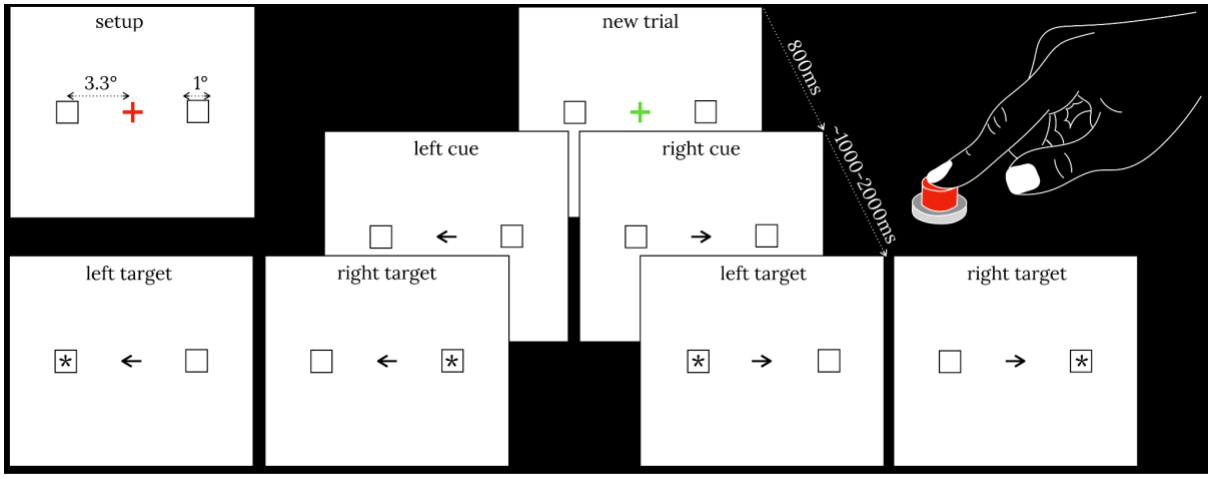

Supplementary Figure 23: Example of the *The Posner orienting task* modified from (Posner 1984). The arrow (i.e. the cue) is presented for 2360ms. The asterisk (i.e. the target) is presented for 300ms.

The Posner orienting task is a detection paradigm initially designed by Posner (1984). The paradigm is computerised and consists of two square frames (1° size) placed on the left and the right of a central fixation (at 3.3° of eccentricity). Trials start when the central fixation turns from red to green. After 800ms, an arrow points left or right. 1000 to 2000ms later, an asterisk appears in one of the two square frames, 75% of the time at the location indicated by the cue (valid trials). In the other 25% the asterisk appears in the opposite location (invalid trials). Patients are required to press a button when an asterisk appears on the screen with their ipsilesional hand. A pause of 2360 ms separates each trial. Each patient performed 120 trials divided into one practice block and two test blocks.

Twenty-four metrics can be derived from *the Posner orienting task* and can be divided into four categories.
Accuracy metrics corresponds the percentage of target missed in average (pos_acc_avg), left (pos_acc_lv) and right (pos_acc_rv) valid trials and in left (pos_acc_li) and right (pos_acc_ri) valid trials.
The effect of validity in accuracy (pos_acc_validity) can subsequently be assessed by subtracting the percentage of target missed in valid conditions (i.e. pos_acc_lv and pos_acc_rv) from invalid conditions (i.e. pos_acc_li and pos_acc_ri) divided by 2.
The effect of disengagement in accuracy (pos_acc_disengage) can also be assessed by subtracting the percentage of target missed in valid trials from invalid trials for left (pos_acc_lv - pos_acc_li) and the right (pos_acc_rv - pos_acc_ri) asterisks separately. The result of the right subtraction is further subtracted from the left and divided by 2 to obtain the accuracy's disengagement effect.
Reaction time metrics correspond to the time in milliseconds between the asterisk and pressing of the button in average (pos_rt_avg), left (pos_rt_lv), and right (pos_rt_rv) valid trials and in left (pos_rt_li) and right (pos_rt_ri) invalid trials.
As for accuracy metrics, the effect of validity in reaction time (pos_rt_validity) can subsequently be assessed by subtracting the average reaction time for valid conditions (i.e. pos_rt_lv and pos_rt_rv) from the average reaction time for invalid conditions (i.e. pos_rt_li and pos_rt_ri) divided by 2.
Similarly, the effect of disengagement in reaction time (pos_rt_disengage) can also be assessed by subtracting the average reaction time for valid trials from the average reaction time for invalid trials for left (pos_acc_lv - pos_acc_li) and the right (pos_acc_rv - pos_acc_ri) asterisks separately. The result of the right subtraction is further subtracted from the left and divided by 2 to obtain the reaction time's disengagement effect.
Subbing metrics are a statistical refinement of the reaction times metrics presented above. For these metrics, two standard deviations above or under the average reaction time are discarded from the analysis for precision leading to corresponding new metrics for average (pos_suv_avg), left (pos_sub_lv), and right (pos_sub_rv) valid trials, left (pos_sub_li) and right (pos_sub_ri) invalid trials and equivalent assessments of the effect of validity (pos_sub_validity) and disengagement (pos_sub_disengage) in 'subbed' reaction times.

Finally, the visual field metric (pos_acc_vf, pos_rt_vf, pos_sub_vf) corresponds to the asymmetry in accuracy or reaction time between the left and the right visual fields. It can be calculated by subtracting the accuracy or reaction times for right asterisks from the accuracy or reaction times for left asterisks divided by 2.

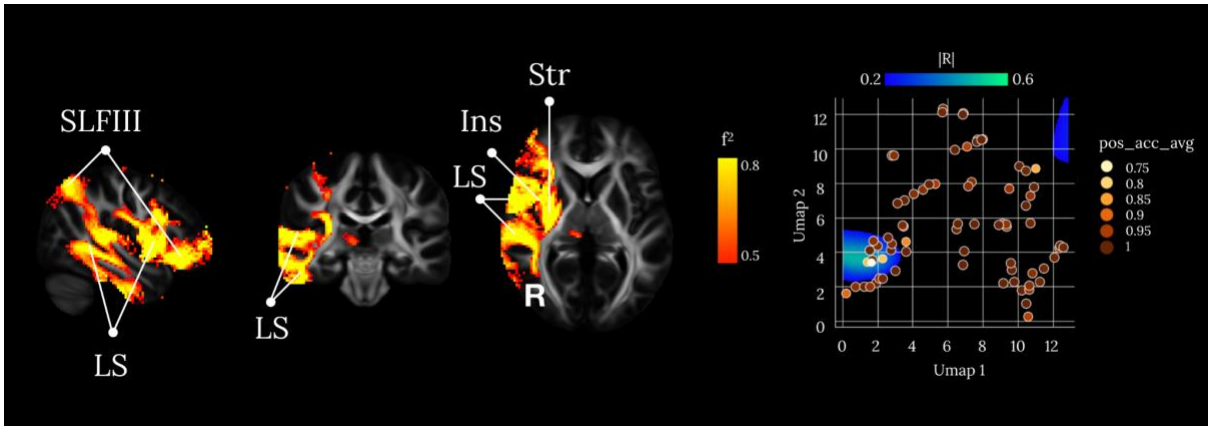

Supplementary Figure 24: brain disconnections and Umap risk territories contributing significantly to the average accuracy (pos_acc_avg) in the *The Posner orienting task*. LS: long segment of the arcuate fasciculus anterior thalamic radiations; Ins: insula; SLFIII: third branch of the superior longitudinal fasciculus; Str: striatum. Maps are freely available at https://neurovault.org/collections/11260/ .

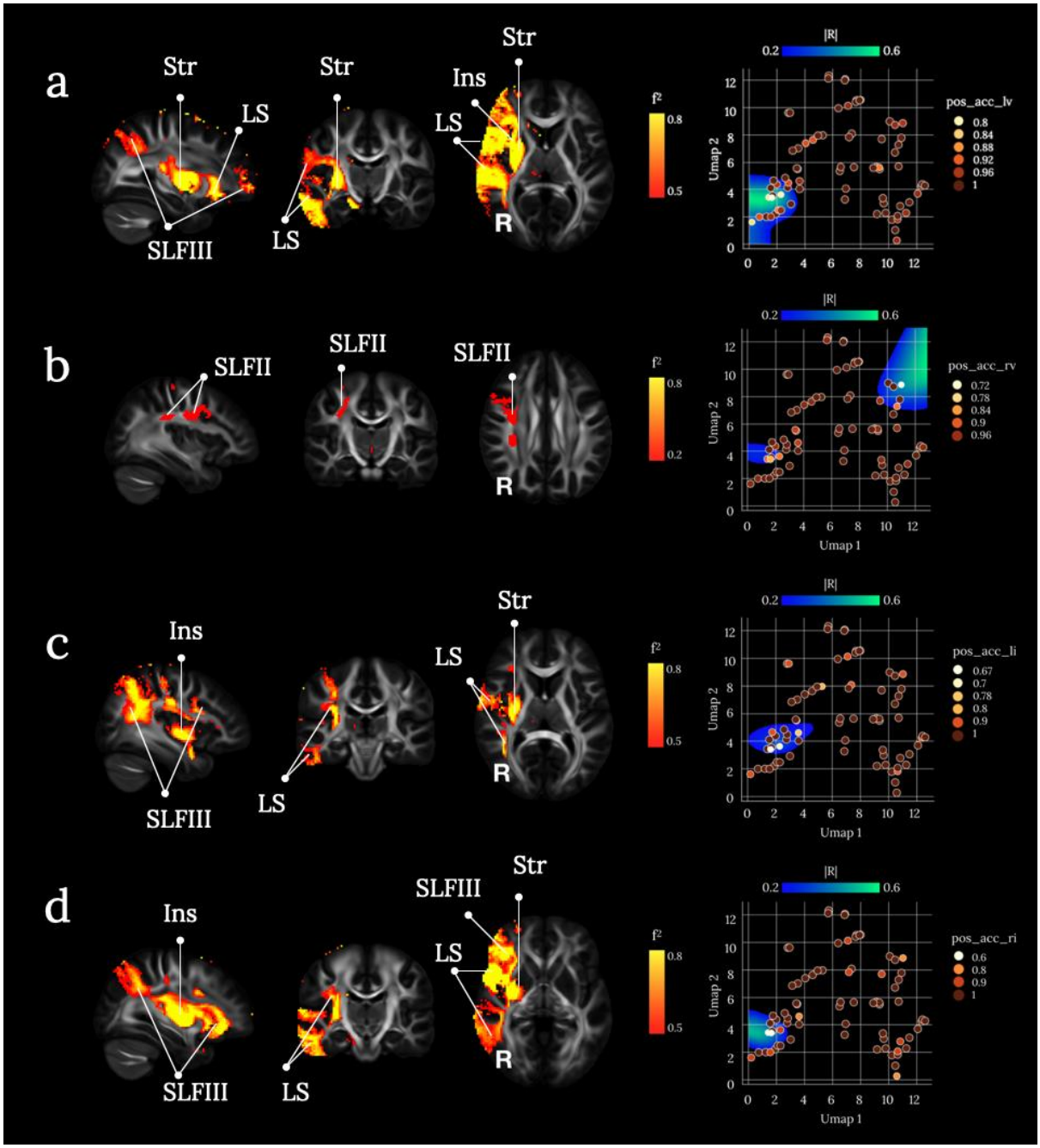

Supplementary Figure 25: brain disconnections and Umap risk territories contributing significantly to the accuracy for the (a) left valid, (b) right valid, (a) left invalid and (b) right invalid asterisks in the *The Posner orienting task*. LS: long segment of the arcuate fasciculus anterior thalamic radiations; Ins: insula; SLF II: second branch of the superior longitudinal fasciculus, SLFIII: third branch of the superior longitudinal fasciculus; Str: striatum. Maps are freely available at https://neurovault.org/collections/11260/ .

The profiles of disconnections associated with the accuracy at the *Posner orienting task* clustered together in comparable areas in the Umap morphospace with medium to large effect size for all conditions except for the percentage of right valid asterisks (see supplementary figure 26a and 26b).
Disconnections leading to reduced accuracy systematically involved the ventral portion of the superior longitudinal fasciculus (mostly the SLF III and the SLF II in some

conditions see Thiebaut de Schotten et al. 2011), the long segment of the arcuate fasciculus, the insula and the striatum in the right hemisphere
The poor results for the right valid target condition might be related to the reduced number of omissions occurring on the cued right hemifield for patients one year after their stroke that limited the variance of the data.
The disconnection of the ventral superior longitudinal fasciculus together with the arcuate fasciculus in the right hemisphere, which connects the core areas of the ventral attention system (Corbetta and Shulman 2002; Parlatini et al. 2017), is in line with previous work reporting that hemispatial neglect and, therefore, the percentage of missed targets would be related to a disconnection of the ventral attention network (Corbetta et al. 2005; Thiebaut de Schotten et al. 2005; Thiebaut de Schotten et al. 2014b). Of importance, the insula is 'at the heart' (Eckert et al. 2009; Menon and Uddin 2010) of the ventral attention system and was significantly disconnected in all conditions, except for the right valid asterisks for the reasons aforementioned.

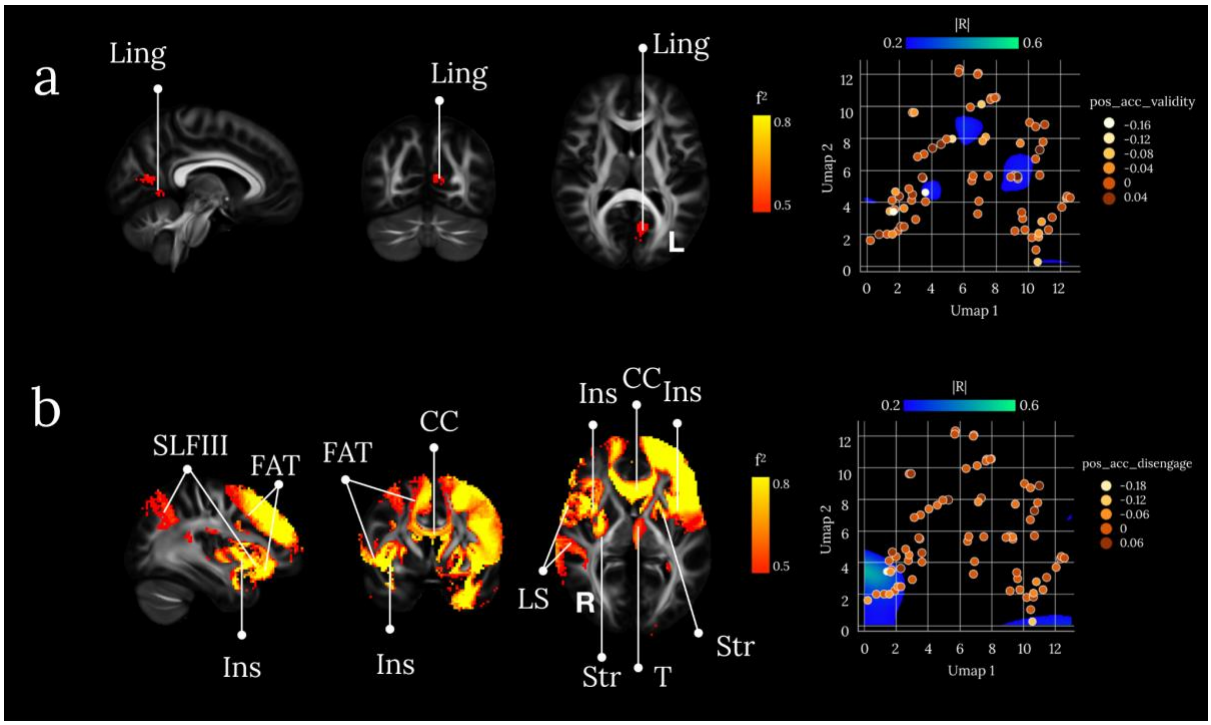

Supplementary Figure 26: brain disconnections and Umap risk territories contributing significantly to accuracy for the (a) validity and (b) disengage conditions in the *Posner orienting task*. Ling: lingual gyrus; Ins: insula; FAT: Frontal Aslant Tract;, SLFIII: third branch of the superior longitudinal fasciculus; Str: striatum, T: Thalamus. Maps are freely available at https://neurovault.org/collections/11260/ .

The profiles of disconnections associated with the percentage of asterisks accurately detected when cued (pos_acc_validity) clustered together in comparable areas in the Umap morphospace with medium to large effect size (see supplementary figure 24 and 25) and were associated with disconnection of the lingual gyrus in the left hemisphere (Supplementary figure 26a). Accuracy for cued asterisks relies partially on dorsal, voluntary orienting of attention (Corbetta and Shulman 2002). While the lingual gyrus is surprising, previous work reported a significant involvement of the visual areas in the

dorsal attention system with decreased activity related to hemispatial neglect and recovery from visual neglect with the re-establishment of this activity (Corbetta et al. 2005). Additionally, the same regions have been reported as damaged after a stroke in the posterior cerebral artery leading again to signs of hemispatial neglect (Bird et al. 2006). Hence, since rehabilitation strategies are mainly focused on the use of the voluntary orienting of attention (Bartolomeo and Chokron 2002) our results suggest that patients may recover with more difficulties from their visual neglect through an early disruption of the dorsal attention network with the disconnection of the lingual gyrus. Future longitudinal analyses exploring the neural bases of visual neglect recovery after a posterior cerebral artery stroke may demonstrate this point further.

The profile of disconnections related to percentage of asterisks accurately detected despite the wrong cue (pos_acc_disengage) clustered together in comparable areas in the Umap morphospace with medium to large effect size (see supplementary figure 26b) and were involved the same network as for the average accuracy including ventral portion of the superior longitudinal fasciculus, the long segment of the arcuate fasciculus, the insula and the striatum

In addition, the anterior portion of the corpus callosum together with the frontal aslant tract and the anterior thalamus were involved.

Pos_acc_disengage is a reorienting of attention that relies on the same structure as the average accuracy condition but also requires an inhibition to perform the reorientation accurately instead of perseverating on the cued target. Simply said, the disengage condition would require additional regions related to inhibition mechanisms compared to the other conditions (i.e., pos_acc_avg, pos_acc_lv, pos_acc_rv, pos_acc_li and pos_acc_ri).

Typically the corpus callosum connectivity between the two hemispheres is critical to the coordination of two hemibodies (Akelaitis 1945; Bogen 1987; Goldstein 1908; Della Sala et al. 1991; Marchetti and Della Sala 1998) through hypothesised inhibitory mechanisms of one hemisphere onto the other (Caplan and Kinsbourne 1981). Accordingly, animal studies exploring the effect of callosal disconnection with frontal lobe damage reveal significant mistakes in the selection paradigm during which monkeys must choose the correct target (Gaffan and Hornak 1997). Similarly split brain patients are less successful than controls are bilateral visual tasks (Luck et al. 1989) comparable to the *Posner orienting task*. Direct electrical stimulation (Kemerdere et al. 2016) abnormal connectivity (Garic et al. 2019) of the frontal aslant tract, or damage to its projections (Aron et al. 2003) have also been associated with deficits in the inhibitory control of behaviour. Finally anterior thalamic lesions in rats (Nelson et al. 2018) and anterior thalamic radiation damage in humans (Koini et al. 2017) abolish inhibitory control.

Hence the circuitry reported for the Pos_acc_disengage condition is concordant with the current literature in the orientation of attention in the inhibitory control.

Since subbed reaction times are just a refinement of raw reaction time and results are mostly similar between the two conditions, we only report below the subbed condition.

However, raw reaction time results are available online (https://neurovault.org/collections/11260/).

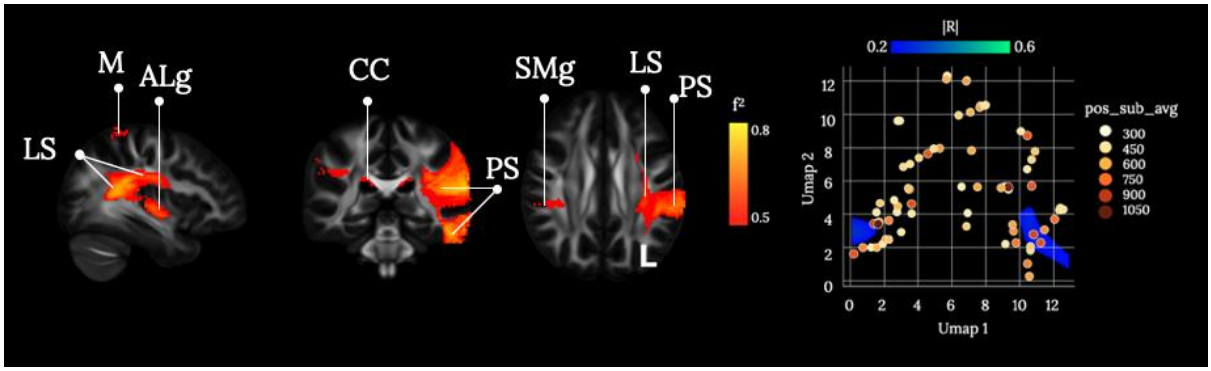

Supplementary Figure 27: brain disconnections and Umap risk territories contributing significantly to 'subbed' average reaction times in the *Posner orienting task*. ALg: insula's anterior long gyrus, CC: Corpus callosum, LS: long segment of the arcuate fasciculus; PS, posterior segment of the arcuate fasciculus, M: Motor Cortex, SMg: supramarginal gyrus. Maps are freely available at https://neurovault.org/collections/11260/ .

The profiles of disconnections related to the 'subbed' average reaction time at the *Posner orienting task* clustered together in comparable areas in the Umap morphospace with medium to large effect size (see supplementary figure 27).
These disconnections involved a circuit composed of the left motor cortex, the long segment and the posterior segment of the arcuate fasciculus in the left hemisphere together with the corpus callosum connections to the right supra marginal gyrus.
While motor disconnections might have an obvious link with the speed of reaction time, the language network represented by the two branches of the arcuate fasciculus reported here might play an important role in the symbol recognition necessary to read (Thiebaut de Schotten et al. 2014a; Huber et al. 2018) and interpret the arrow in the left hemisphere (Karolis et al. 2019). Communication to the right hemisphere via the corpus callosum would be necessary when attention is required to be oriented toward the left.

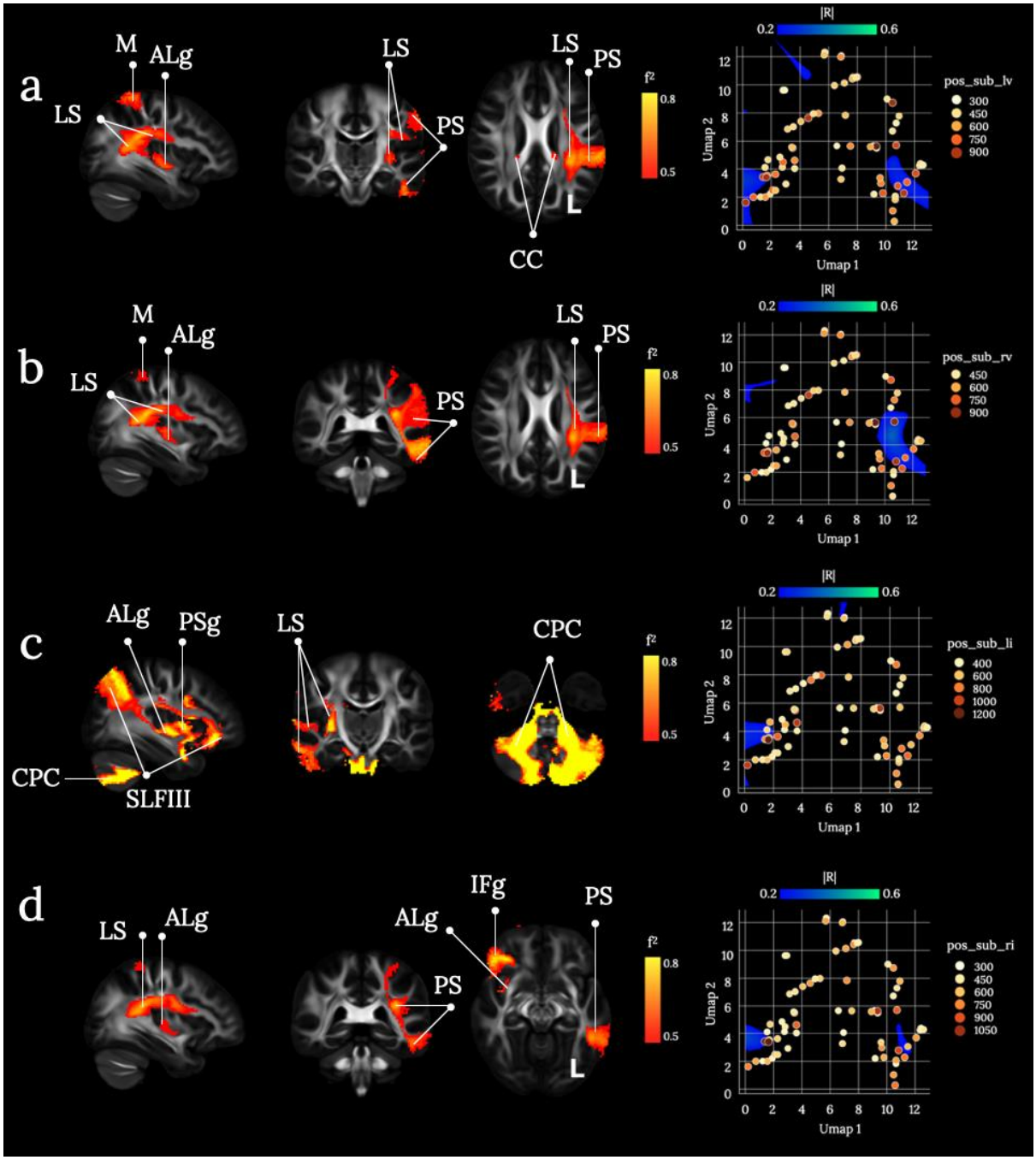

Supplementary Figure 28: brain disconnections and Umap risk territories contributing significantly to 'subbed' reaction times for the (a) left valid, (b) right valid, (a) left invalid and (b) right invalid asterisks in the *The Posner orienting task*. ALg: insula's anterior long gyrus, CC: Corpus callosum, CPC: Cortico-Ponto-Cerebellar tract, LS: long segment of the arcuate fasciculus; PS, posterior segment of the arcuate fasciculus, M: Motor Cortex, SMg: supramarginal gyrus. Maps are freely available at https://neurovault.org/collections/11260/ .

The profiles of disconnections related to the 'subbed' reaction time at the *Posner orienting task* clustered together in comparable areas in the Umap morphospace with medium to large effect size (see supplementary figure 28a and 28b) for all valid conditions. The same network was involved as for the 'subbed' average reaction time with the exception of the missing involvement of the corpus callosum when the valid target appears on the right as predicted above. In that case, when the target appears on the

right most of the processing (interpretation of the target and spatial orientation of the attention) can happen in the left hemisphere compatible with the absence of involvement of the corpus callosum.

For the invalid condition, the reorienting of attention toward the left involved a large network of areas including the cerebellum via the cortico-potocerrbellar tract, the insula, the arcuate and the third branch of the superior longitudinal fasciculus in the right hemisphere. For the reorientation of attention toward the left, the network was comparable to all valid conditions with the exception of the involvement of the right inferior frontal gyrus.

The involvement of the right inferior frontal gyrus in the left and the right invalid conditions is compatible with the inhibitory requirement of the task, activation and deficit of inhibition have been reported respectively in controls functional MRI (Hampshire et al. 2010; Sebastian et al. 2013) and in patients behaviour after a lesion in the right inferior frontal gyrus (Scheffer et al. 2016). However, the involvement of the cerebellum in the reorienting of attention toward the left was atypical of any of the other conditions. While left hemineglect has been reported after a lesion of the cerebellum (Kim et al. 2008; Milano and Heilman 2014), whether cerebellar neglect is more specifically affecting the reorientation of attention toward the left and no other conditions of the *Posner orienting task* awaits for future demonstration. As mentioned previously, the insula is central (Eckert et al. 2009; Menon and Uddin 2010) to the ventral attention system that is activated mainly during the reorienting of attention (Corbetta and Shulman 2002).

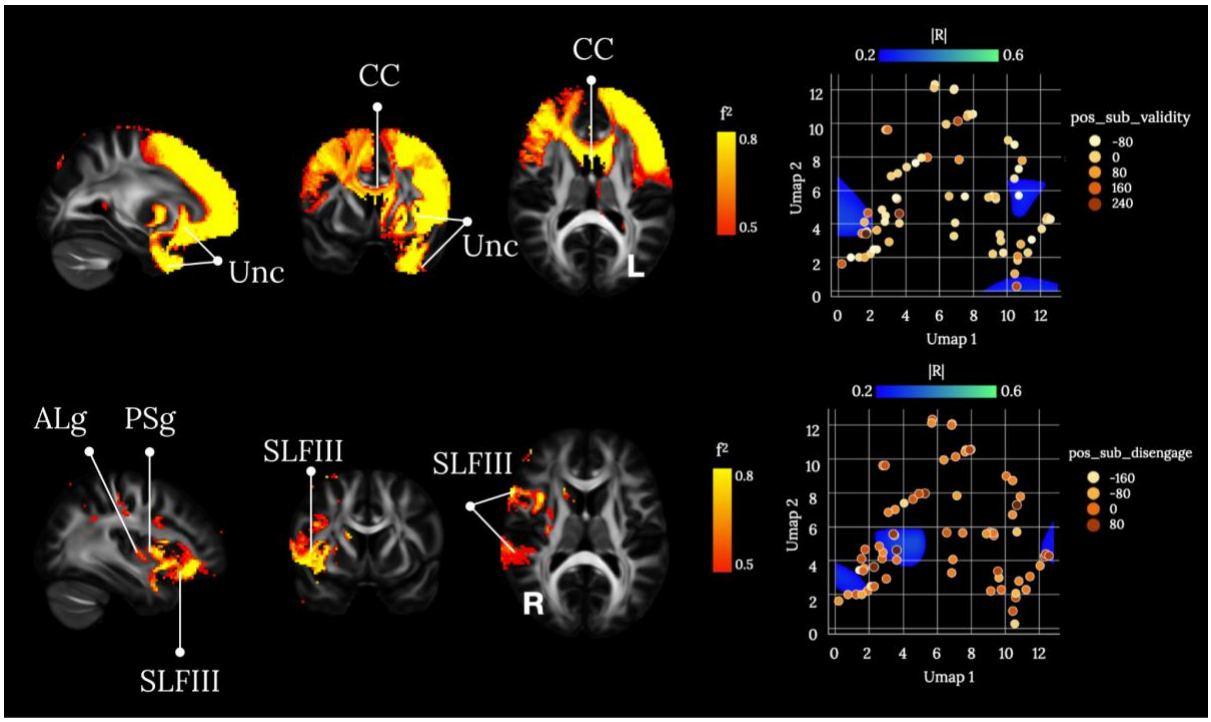

Supplementary Figure 29: brain disconnections and Umap risk territories contributing significantly to 'subbed' average reaction times for the (a) validity and (b) disengage conditions in the *The Posner orienting task*. ALg: insula's anterior long gyrus, PSg: insula's posterior short gyrus, CC: Corpus callosum, SLF III: third branch of the superior longitudinal fasciculus, Unc: uncinate. Maps are freely available at https://neurovault.org/collections/11260/ .

The profiles of disconnections related to the 'subbed' reaction time at the *Posner orienting task* for the validity condition clustered together in comparable areas in the Umap morphospace with medium effect size (see supplementary figure 29a) revealing a large frontal network supported by the corpus callosum and the uncinate fasciculus.
The validity contusion specifically assesses the voluntary orienting of attention with no preference for the side of appearance of the asterisks. The important role of the frontal lobe in the voluntary orientation of attention have previously been demonstrated in patients with brain lesions (Koski et al. 1998) and fits quite elegantly with the pattern of results observed here. The role of the uncinate fasciculus is somewhat less clear with eventual contribution to rule learning required for the optimal achievement of the task (Olson et al. 2015).
In contrast the disconnections related to the disengage condition involved the typical ventral fronto-parietal network supported by the third branch of the superior longitudinal fasciculus in the right hemisphere (Corbetta and Shulman 2002; Parlatini et al. 2017) and including the insula (Eckert et al. 2009; Menon and Uddin 2010).

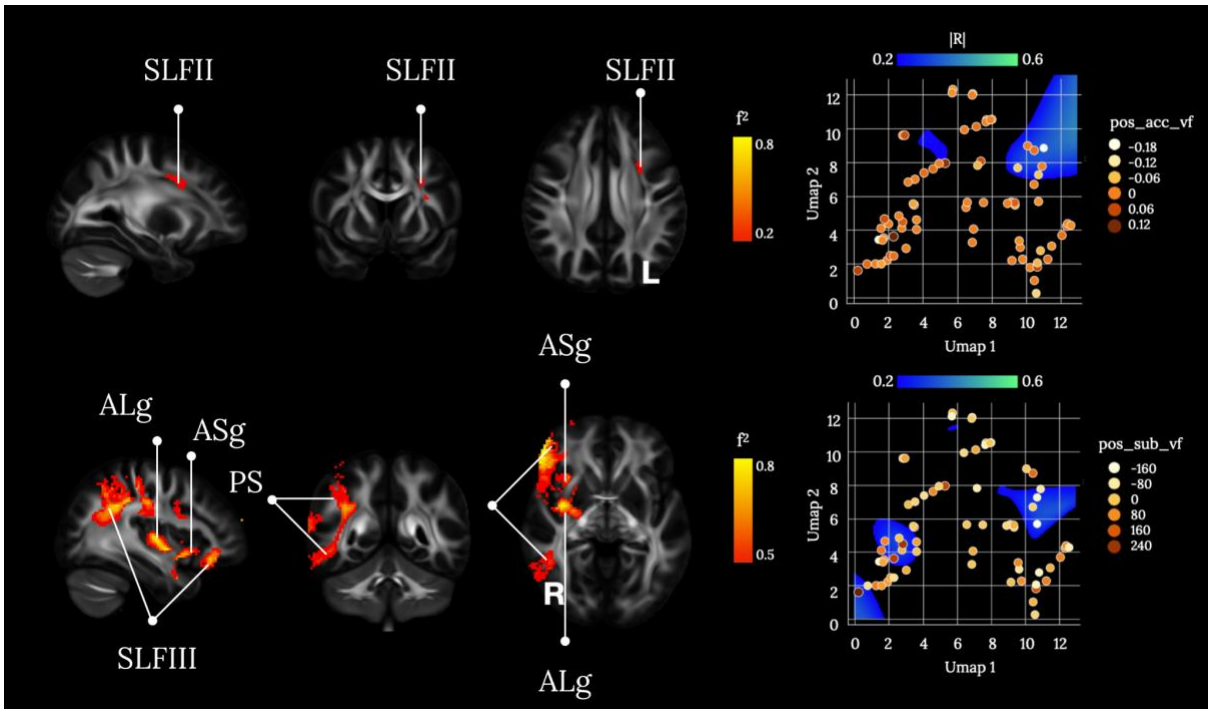

Supplementary Figure 30: brain disconnections and Umap risk territories contributing significantly to asymmetries in the visual fields in terms of (a) accuracy, (b) reaction time in the *The Posner orienting task*. ALg: insula's anterior long gyrus, ASg: insula's anterior short gyrus, PS: arcuate fasciculus' posterior segment, SLF II: second branch of the superior longitudinal fasciculus, SLF III: third branch of the superior longitudinal fasciculus. Maps are freely available at https://neurovault.org/collections/11260/ .

The profiles of disconnections related to the visual field asymmetries at the *Posner orienting task* clustered together in different areas of the Umap morphospace according to whether accuracy (see supplementary figure 30a) or 'subbed' reaction time (see supplementary figure 30b) were measured.
With regard to accuracy the single involvement of a blob located onto the second branch of left superior longitudinal fasciculus appeared to contribute significantly to the asymmetry in the number of asterisks reported in the left and the right visual field. The patient did not report the asterisk when they did not see it.
While the second branch of the superior longitudinal fasciculus has been recently suggested to support conscious processing (Dehaene and Changeux 2011; Parlatini et al. 2017; Mashour et al. 2020) the level to which this process would be preferentially lateralized in the left hemisphere waits for further validation.
in contrast the speed to which target were detected was particularly asymmetrical after a disconnection of the typical ventral fronto-parietal network (Corbetta and Shulman 2002) supported by the SLF III (Parlatini et al. 2017) and involving the insula (Eckert et al. 2009; Menon and Uddin 2010). This result might have been driven by the extra time patients with a lesion in the SLF III might take to process targets requiring their reorientation toward the left.

C.4 Visuospatial memory

Brief visuospatial memory test revised

The brief visuospatial memory test - revised {BVMT-r; \Benedict, 1996 #233} has been used as assessment for visuospatial domain of the memory ability. The test scores are divided in recall memory (immediate/delayed) and additional learning and memory scores (learning, percentage retained, discrimination index, response bias, false alarm).

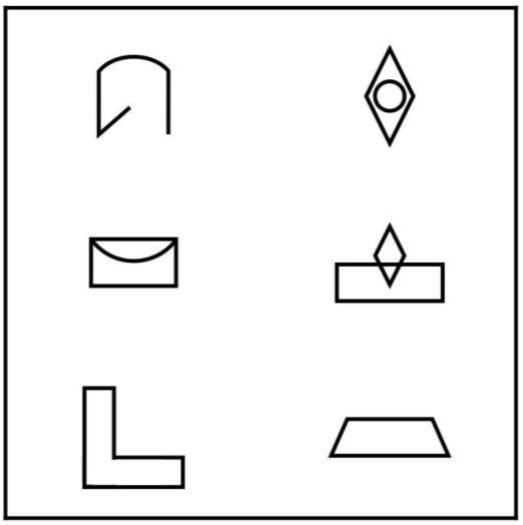

The test material is an 8x11-inch plate containing six geometrical figures presented in a 2x3 matrix (Supplementary Figure 31). The patients are required to observe the figures in three consecutive trials lasting 10s each. The immediate recall task occurs at the end of the first

Supplementary Figure 31. Example of the BVMT stimuli.

trial, when the patients must draw the figures as accurately and fast as they can. The figures are presented again in two following trials (learning trials), at the end of which the patients are encouraged to improve their performance. After a delay of 25m, the delayed recall task is administered, during which the patients are instructed to reproduce the figures matrix by memory. Finally, in the delayed recognition task, the patients are

presented with 12 drawings representing the six matrix figures (target) and six foil figures (nontarget). Patients are required to recognise the six matrix figures, responding “yes” when the target figures are presented and “no” when the non-target figures are shown. For each response in the immediate and delayed recall a 0-1 score is assigned for each drawing according to the drawing position. The type of drawing is also evaluated on a 0-1 scoring scale for each drawing, for a total of 0-36 range score for the immediate recall and 0-18 range for the delayed recall. The immediate and delayed recall scores have been age-normed using the tables provided in the test manual, providing two additional scores, the immediate t and delayed t-scores. Furthermore, scores were calculated for the following variables: 1) Learning, how much the patient has learned by the later trials during the learning phase compared to the first trial (trial 1 - the better of trial 2 or 3); Percent Retained, is the percentage of how much an individual remembers from the later immediate recall trials following the 25-minute delay ((delayed recall score/the better score of trial 2 or 3)*100); 4) Recognition Hits, the total number of correctly identified drawings in the recognition phase (score range: 0-6); 5) Recognition False Alarms, total number of incorrectly identified drawings in the recognition phase (score range: 0-6); 6) Delayed Recognition discrimination index, calculated from proportion of correct recognitions, correct rejections, misses, and false alarms; 7) Recognition Response Bias, how likely the patient is to say “yes“ rather than “no” during the recognition phase (score range: 0-1).

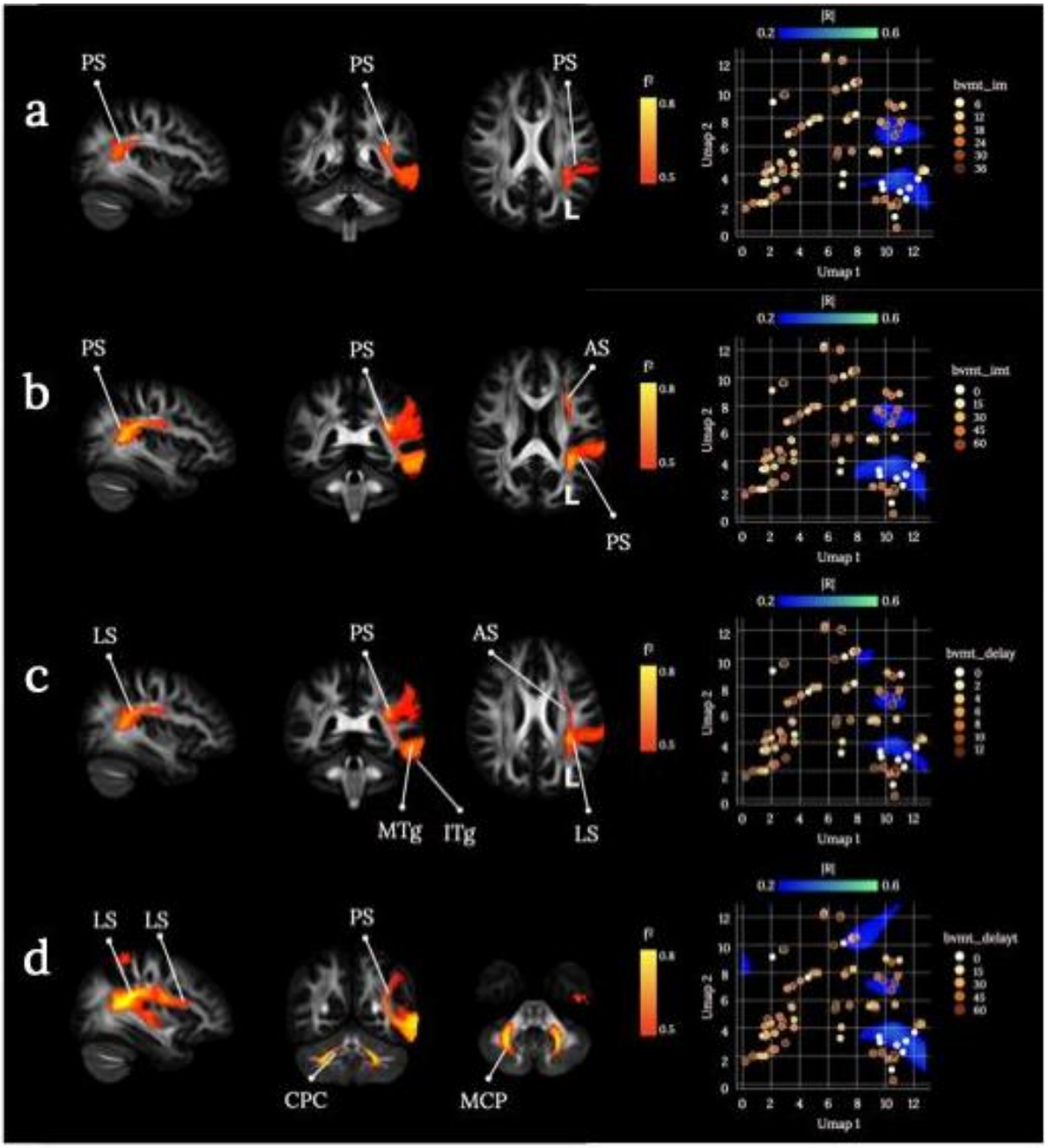

Supplementary Figure 32. Brain disconnections and Umap risk territories contributing significantly to four variables (immediate recall, age-normed immediate recall, immediate delay, age-normed immediate delay) of the *Brief visuospatial memory test revised* (BVTM-R). *(a) Immediate recall* (bvmt-im), (b) *Age-normed immediate recall* (bvmt-imt), (c) *Immediate delay* (bvmt-delay), (d) *Age-normed immediate delay* (bvmt-delayt). AS: anterior segment of the arcuate fasciculus; CPC: cortico-ponto-cerebellar pathway; ITg: inferior temporal gyrus; LS: long segment of the arcuate fasciculus; MCP: middle cerebellar peduncles; MTg: middle temporal gyrus. Maps are freely available at https://neurovault.org/collections/11260/ .

The low scores in immediate recall (raw and t-scores) and delayed recall (raw scores and t-scores) of the BVMT cluster in correspondence of fronts-parietal and parieto-temporal connections of the left hemisphere. The age-normed scores of the delayed recall are predicted also by the disconnection of the cortico-pontine-cerebellar tract. Memory recall has been associated with attentional and integration processes subserved by the

left fronto-parietal structures (Konishi et al. 2000; McDermott et al. 2000; Ciaramelli et al. 2008; Vilberg and Rugg 2008). It has been put forward the hypothesis that different parietal cortices contribute with diverse attentional processes to memory recall. Namely, the dorsal parietal and prefrontal cortices seem to carry out top-down attentional control in the active memory retrieval, while the ventral parietal region subserves the bottom-up attentional processing of spontaneous retrieval (Cabeza et al. 2008). Unfortunately, results of the contribution of the left parietal cortex to memory recall are not consistent (Papagno 2018; for a review).

Nevertheless, visuospatial memory has been prevalently associated with right hemisphere structures (Papagno 2018) and previous studies reported the involvement of different brain structures during the performance of visuospatial memory immediate and delayed recall. For instance, the activation of the right prefrontal cortex has been associated with the performance in the two recall types of the BVTM (Melrose et al. 2020), and the studies on brain damage and neurodegenerative disorders confirmed the role of the medial temporal cortex in memory recall.

However, immediate and delayed recall sub-tasks of the BVMT require object form and object position memory, which rely on visuospatial and mental visual-imagery processes as lesion study revealed (Goldenberg 1992; Moro et al. 2008). A recent meta-analysis (Spagna et al. 2021) put forward the hypothesis that left fronto-parietal and temporal structures participate in the visual mental imagery network by internally driving the attentional control. Thus, our results may reflect the patients' deficit in other cognitive domains required by the BVTM.

Adjusting the delayed recall scores for the age allowed the scores to cluster in correspondence of the cortico-pontine cerebellar tract within the cerebellum. The role of the cerebellum in visual-motor, implicit motor and stimuli-response learning is well established (Ferrari et al. 2018; Thompson and Kim 1996; Kitazawa et al. 1998), as well its participation in conscious memory retrieval (Andreasen et al. 1999; Addis et al. 2016; Dave et al. 2020).

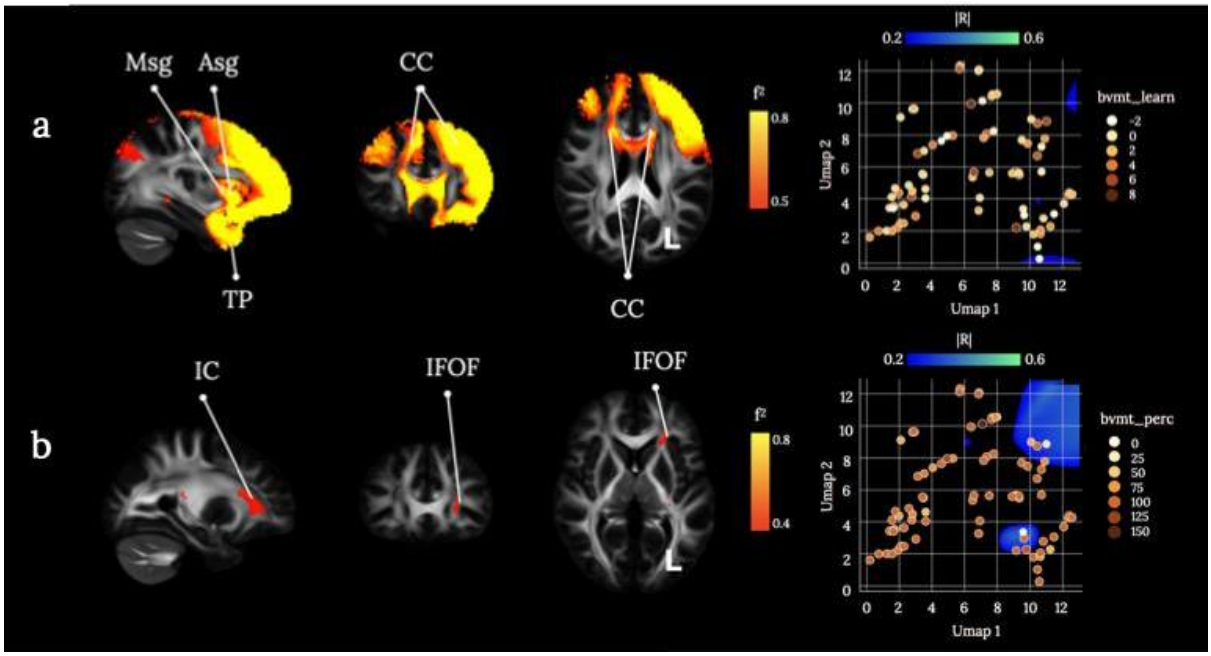

Supplementary Figure 33: Brain disconnections and Umap risk territories contributing significantly to two variables (learning, and percent retained) of the *Brief visuospatial memory test revised* (BVTM-R). *(a) Learning* (bvmt-learn), (b) *percent retained* (bvmt-imt). CC: corpus callosum; Asg: anterior short gyrus of the insula; IC: internal capsule; IFOF: inferior fronto-occipital fasciculus; Msg: middle short gyrus of the insula; TP: temporal pole. Maps are freely available at https://neurovault.org/collections/11260/ .

The low score in the learning variable is predicted mainly by the disconnection of the corpus callosum. Studies on patients with the stenosis of the corpus callosum have revealed the importance of the interhemispheric connection in visual learning {Paul, 2016 #252;Lassonde, 2003 #253}. Specifically, the corpus callosum is associated with visuomotor processing (Berlucchi et al. 1995; Eliassen et al. 2000) and our results confirm that the deficit of visual and motor information integration prevents the performance improvement trial by trial.
The disconnection of fronto-occipital structures via the left Inferior Fronto-occipital Fasciculus predicts low scores of the percent retained scores. The anatomical studies that explored in depth the IFOF structure have identified different components of the tract (Martino et al. 2010; Wu et al. 2016; Rollans and Cummine 2018; Sarubbo et al. 2013). Interestingly, a study explored the contribution of the different components beyond their participation in language-domain processing (Sarubbo et al. 2013). While the anterior and posterior, deep components may be involved in emotion and semantic processing, the middle deep component seems to be dedicated to multi sensor-motor integration. Given that the percent retained score reflects the information retained from previous drawing trials, the disconnection of the IFOF may indicate that sensory-motor integration is the key to the improvement of the drawing performance after a delay.

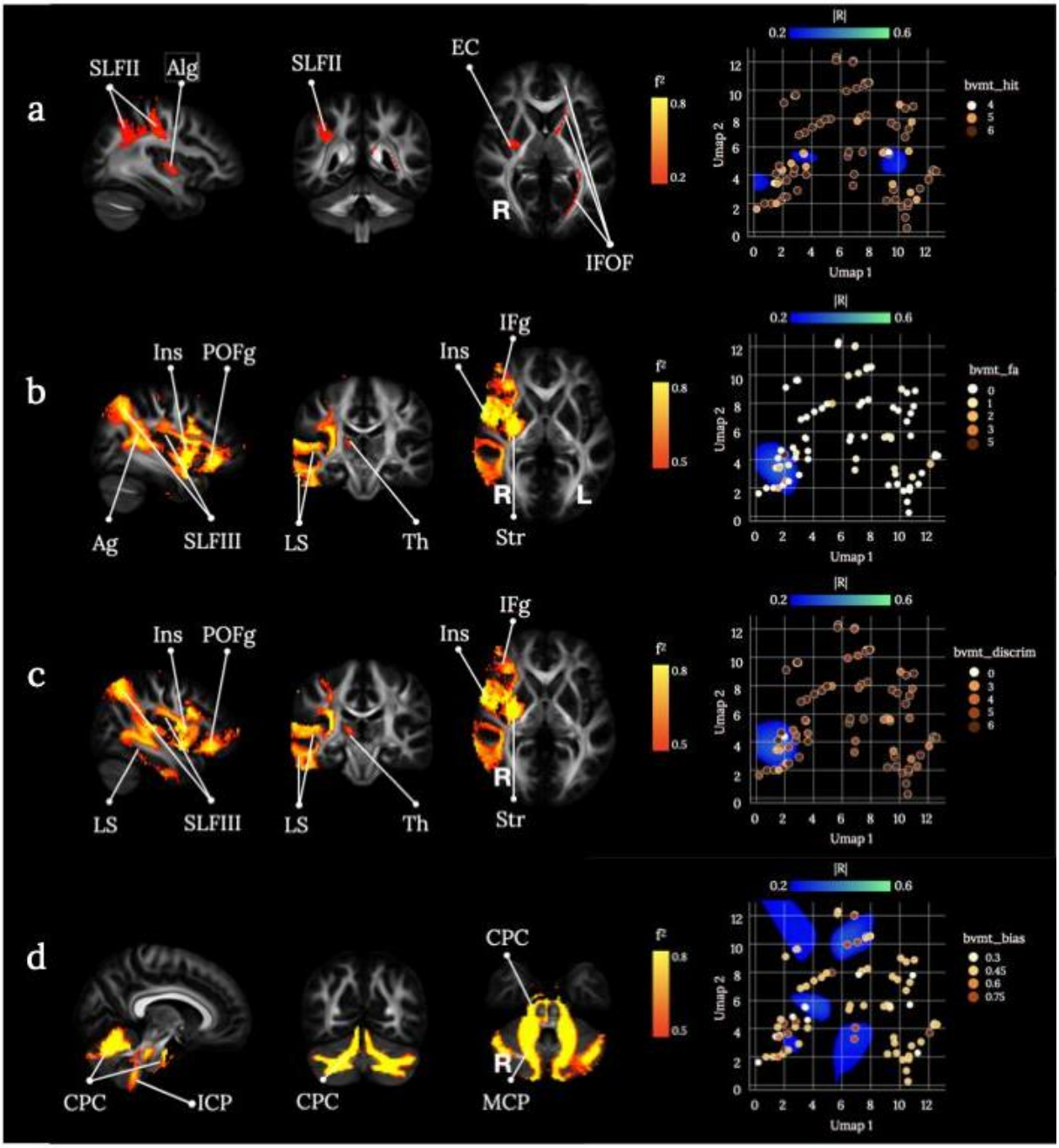

Supplementary Figure 34: Brain disconnections and Umap risk territories contributing significantly to four variables (recognition hits, recognition false alarms, delayed recognition discrimination index, recognition response bias) of the *Brief visuospatial memory test revised* (BVTM-R). *(a) Recognition hits* (bvmt-hit), (b) *recognition false alarms* (bvmt-fa), (c) *delayed recognition discrimination index* (bvmt-discrim), (d) *recognition response bias* (bvmt-bias). ALg: anterior long gyrus of the insula; Ag: angular gyrus; CPC: cortico-ponto-cerebellar pathway; EC: external capsule; ICP: inferior cerebellar peduncles; IFg: inferior frontal gyrus; Ins: insula; IFOF: inferior fronto-occipital fasciculus; LS: long segment of the arcuate fasciculus; MCP: middle cerebellar peduncles; POFg: posterior orbitofrontal gyrus; SLFII: second branch of the superior longitudinal fasciculus; SLFIII: third branch of the superior longitudinal fasciculus; Str: striatum; Th: thalamus. Maps are freely available at https://neurovault.org/collections/11260/ .

A poor performance in the recognition hits score is credited by the disconnection of the angular gyrus and the middle frontal gyrus via the middle, via the second branch of the superior longitudinal fasciculus II, and the fronts-occipital disconnection via the IFOF. The low scores of the false alarm and the delayed recognition discrimination test cluster in correspondence of the disconnection of the supra marginal gyrus and the inferior frontal gyrus, the insula, and the posterior orbitofrontal cortex. The insula and the fronts-parietal network are part of the salience network, which is engaged during the top-down driving of attention toward relevant stimuli (Corbetta et al. 2008) and their activation has been associated with recognition performance (Clemens et al. 2015; Uncapher and Rugg 2009; Festini and Katz 2021). The prefrontal cortex participates in the identification of cues during recognition and exploits the cues to reactivate stored information, then it supports the monitoring, disambiguation and verification of the retrieved information (Simons and Spiers 2003). Further, frontal cortex damage prevents to exert executive control of the recognition process leading to false familiarity attributions (Rapcsak and Edmonds 2011), and the damage of the fronto-striatal pathway with the subsequent deficit in executive control is believed to contribute to memory impairment in Parkinson's disease patients (Gratwicke et al. 2015; for a review). Our results confirm that the integrity of attentional and executive control mechanisms supported by the insular, frontoparietal and striatal connections is crucial to accurately recognise the correct drawings of the BVTM.
The contribution of the fronto-occipital disconnection in the recognition hit scores may suggest that the hits are specifically associated to the visuomotor integration that is needed for the drawing performance improvement described in the percent retained scores section.

The low scores of the recognition Bias correspond to less likelihood that a patient responds "yes" during the recognition phase and are predicted by the disconnections of the cerebellum. It has been proposed that the tendency to less likely identify an item as already presented rather than "new" indicates the need for more cues to use in the memory recognition process (Kantner and Lindsay 2012). Previous studies have identified the contribution to recognition bias of top-down decision making processes driven by the prefrontal cortex (Windmann et al. 2002; Hill and Windmann 2014). The participation of the cerebellum in decision making under uncertainty has been reported as well (Blackwood et al. 2004; Kim et al. 1994). Blackwood and colleagues (2004) proposed that the cerebellum is involved in the building of internal models of external events, given its activation during uncertain tasks demands. These models may support the ability to infer predictions of the uncertainty. One may speculate that the recognition bias score of the BVTM mostly rely on the ability of making predictions during the categorisation of the stimuli as old and new.

C.5 Verbal memory

The Hopkins Verbal Learning Test (HVLT, Brandt 1991) serves as a measure of verbal learning and memory. The HVLT is composed of 12 items, organised into three semantic categories, and presented over three consecutive learning trials. The examiner reads the list aloud at the rate of 1 word every 2 seconds, and the patient is asked to memorise the list. The measure of interest is the patient's free recall. This procedure is repeated two more times. After the learning period, 24 words are read aloud to the patient who needs to verbally indicate if the word was also in the previous 12-item list (12 targets) or not (12 distractors). Whereby the latter are balanced between related distractors, meaning from the same semantic clusters as the target words, or unrelated. The HVLT has three main advantages: a short administration time (~10min), 6 parallel versions allowing for repeated measures for patients who are assessed at frequent intervals, and no ceiling effect on recall in healthy controls. However, while the HVLT appears to adequately assess basic verbal learning capacity, its utility in assessing some of the more complex and qualitative aspects of verbal learning and memory function may be limited (Lacritz and Cullum 1998). We extracted the following scores from the HVLT: the absolute total immediate recall (hvlt_im) with a maximum score of 36 (all 12 words are recalled perfectly across the three trials), learning (hvlt_learn), percentage retained (hvlt_perc), hits (hclt_hit), false-positives related (hvlt_fa1), false-positives unrelated (hvlt_fa2), total false positives (hvlt_fa3), the recognition discremination index (hvlt_discrim), total immediate recall t-scores (hvlt_imt), delayed recall as t-scores (hvlt_delayt), and teh t-score converted discrimination index (hvlt_discrimt). The total immediate recall (hvlt_im) did not survive the first thresholding of R>0.2 and is therefore not included in the further analysis. It is of note though, that immediate recall is a commonly used measure of the test in neuropsychological studies.

Form 1: Four-legged animals, precious stones, human dwellings

Form 1, Part A: Free Recall:

	Trial 1	Trial 2	Trial 3
EMERALD			
HORSE			
TENT			
SAPPHIRE			
HOTEL			

CAVE			
OPAL			
TIGER			
PEARL			
COW			
HUT			
LION			
Number correct recall:			

Form 1, Part B: Recognition

Horse	Ruby*	Cave	Balloon	Coffee	Lion
House*	Opal	Tiger	Boat	Scarf	Pearl
Hut	Emerald	Sapphire	Dog*	Apartment*	Penny
Tent	Mountain	Cat*	Hotel	Cow	Diamond*

NOTE: *An asterix (*) indicates semantically related distractors, while underlined words are the target items from the training list.*

Form 1, Scoring:

Number of true positives (max value is 12): _____

Number of false-positive errors (max value is 12):
Related distractors (max 6):____ Unrelated (max6): ____

Discrimination Index: (Number true-positives) – (Number false-positives) = _____

NOTE from the authors: *While Form 1 was exemplified in detail for the parallel forms, only the items of the parallel forms are listed below.*

Form 2 word list (semantic categories: kitchen utensils, alcoholic beverages, weapons):
Free Recall: Fork, Rum, Pan, Pistol, Sword, Spatula, Bourbon, Vodka, Pot, Cow, Hut, Wine
Recognition:

spoon*	pistol	doll	whiskey*	fork	pot
harmonica	can opener*	sword	pencil	Gun*	vodka
knife*	rum	trout	bomb	pan	gold
wine	lemon	spatula	Bourbon	beer *	rifle

Form 3 word list (semantic categories: musical instruments, fuels, food flavourings):
Free Recall: sugar, trumpet, violin, coal, garlic, kerosine, vanilla, wood, clarinet, flute, cinnamon, gasoline
Recognition:

Pepper*	Garlic	Wood	Drum*	Oil*	Sugar
Harmonica	Salt*	Priest	Chair	Coal	Clarinet
Trumpet	Basement	Cinnamon	Flute	Electricity*	Moon
Kerosine	Vanilla	Gasoline	Sand	Piano*	Violin

Form 4 word list (semantic categories: birds, clothing, carpenter's tools):
Free Recall: canary, shoes, eagle, blouse, nails, crow, bluebird, screwdriver, pants, chisel, skirt, wrench
Recognition:

Bluebird	Shirt*	Chisel	Eagle	Chocolate	Robin*
Chapel	Screwdriver	Crow	Sparrow*	Wrench	Pants
Nails	Socks*	Child	Shoes	Hair	Hammer*
Canary	Apple	Skirt	Saw*	Silver	Blouse

Form 5 word list (semantic categories: occupations/professions, sports, vegetables):
Free Recall: teacher, basketball, lettuce, dentist, tennis, bean, engineer, potato, professor, golf, corn, soccer
Recognition:

Tennis	Football*	Professor	Spinach*	Lawyer*	Submarine

Golf	Dentist	Lettuce	Spider	Water	Bean
Basketball	Doctor*	Corn	Baseball*	Teacher	Snake
Carrot*	Engineer	Glove	Soccer	Potato	tulip

Form 6 word list (semantic categories: fish, parts of a building, weather):
Free Recall: shark, wall, herring, rain, floor, hail, catfish, roof, salmon, storm, ceiling, snow
Recognition:

Hail	Bass*	Snow	Bank	Floor	Mustard
Window*	Ceiling	Canyon	Rain	Ladder	Storm
Herring	Salmon	Tornado*	Trout*	Melon	Roof
Shark	Hurricane*	Elbow	Catfish	Wall	Door*

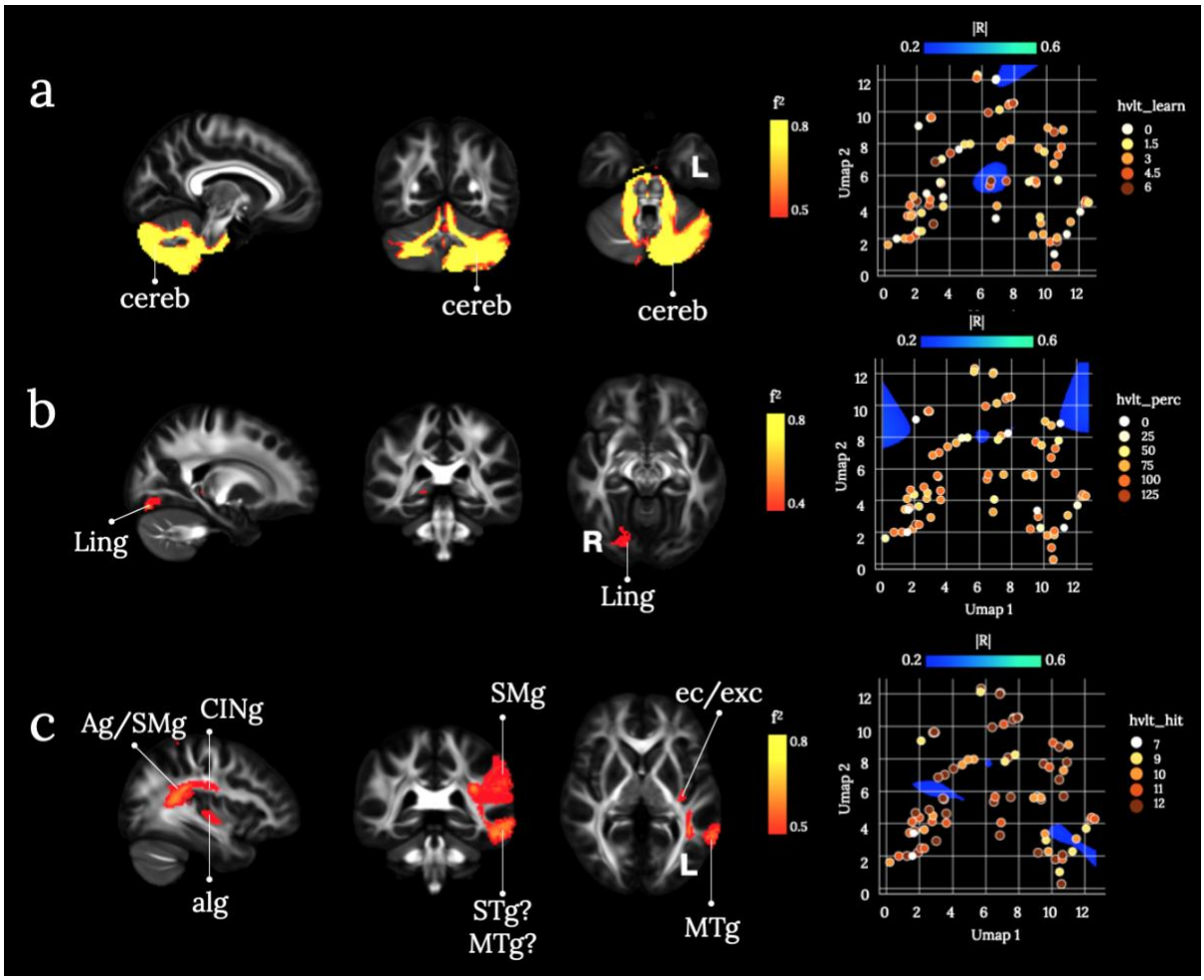

Supplementary Figure 35: Brain disconnections and Umap risk territories contributing significantly to the *The Hopkins Verbal Learning Test* (HVLT) correct responses. (*a*) *learning* (hvlt_learn), (b) percent retained (hvlt_perc), and (c) recognition hits (hvlt_hit).

Ag: angular gyrus; STg: superior temporal gyrus; MTg: middle temporal gyrus; SMg: supramarginal gyrus; alg: anterior long insular gyrus; ec/ecx: external/extreme capsule; cereb: cerebellum; CINg: cingulate gyrus; Ling: lingual gyrus. Maps are freely available at https://neurovault.org/collections/11260/ .

Functional topography and clinical case studies have previously linked the cerebellum to verbal working memory (Marvel and Desmond 2010; Akshoomoff et al. 1992; for a review see Murdoch 2010). In a more recent consensus paper the emerging field of cerebellar neurocognition has been discussed in light of language processing (Mariën et al. 2014). The lingual gyrus is classically associated with reading (e.g. Paulesu et al. 1993) which might indicate a learning strategy whereby the heard words might have been visualised for encoding. Numerous investigations in healthy participants and patient cohorts have demonstrated the importance of the inferior parietal lobe (angular and supramarginal gyri) for verbal working memory by highlighting individual processes such as the phonological loop, sensorimotor integration of speech, representation of phonetic sequences, attentional capture of verbal information, and phonological retrieval (Binder 2015; Herman et al. 2013; López-Barroso et al. 2013; Ravizza et al. 2011; Wise et al. 2001).
A decline in learning and memory has been described for patients with insular tumours (Wu et al. 2011).

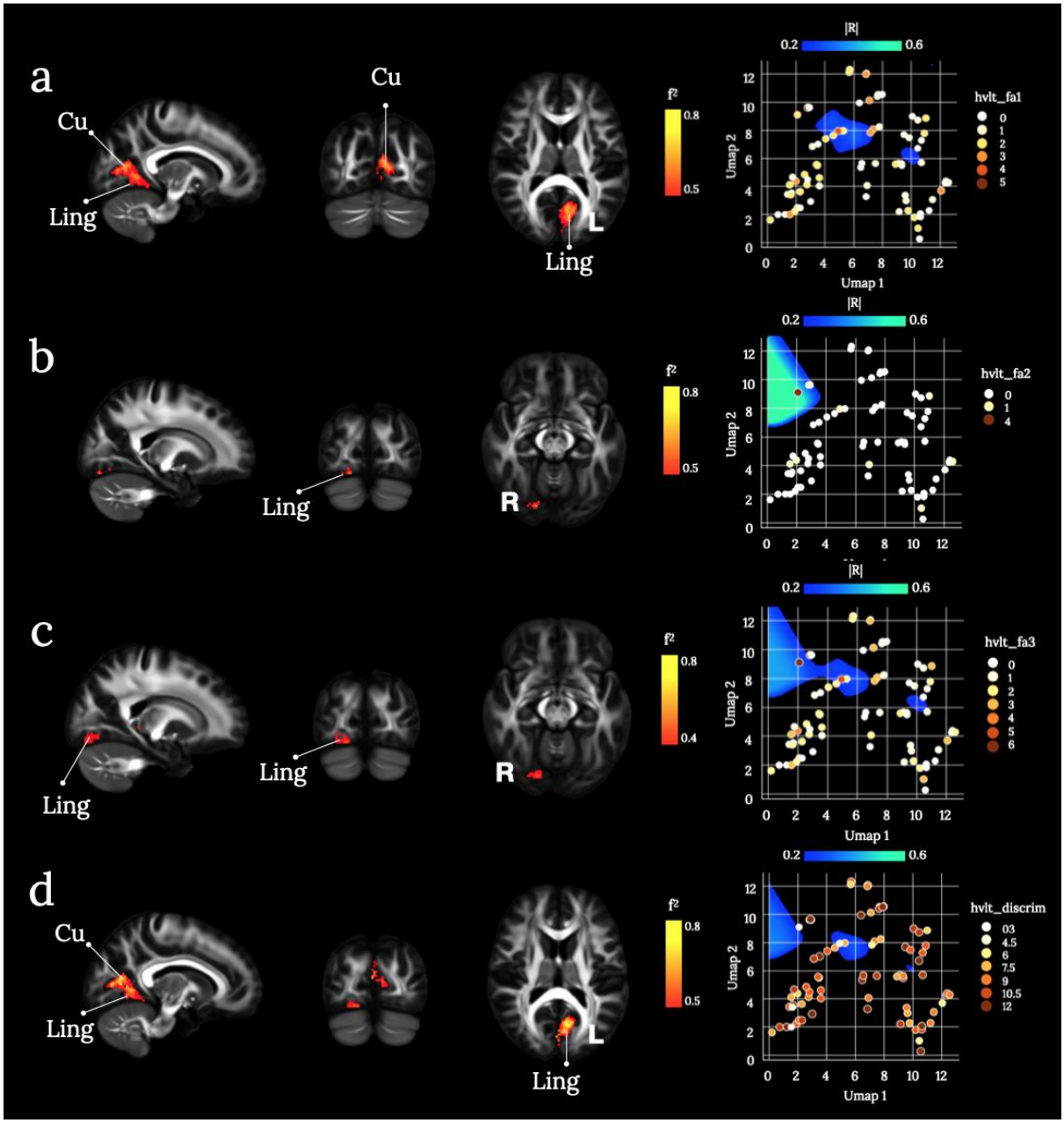

Supplementary Figure 36: Brain disconnections and Umap risk territories contributing significantly to the *The Hopkins Verbal Learning Test* (HVLT) false-positive responses. (*a*) false-positives related (hvlt_fa1), (b) false-positives unrelated (hvlt_fa2), (c) total false positives (hvlt_fa3), and (d) the recognition discremination index (hvlt_discrim). Cu: cuneus; Ling: lingual gyrus. Maps are freely available at https://neurovault.org/collections/11260/ .

According to the composite morphospace results, profiles of disconnections predicting individual false-positive responses and item discremnination were localized in the bilateral lingual gyri and the left cuneus. The lingual gyrus has been implicated in the identification and recognition of words (Mechelli et al. 2000). It has also been linked to visual imagery, which might be an encoding and retrieval strategy during the discremation tasks (Leshikar et al. 2012).

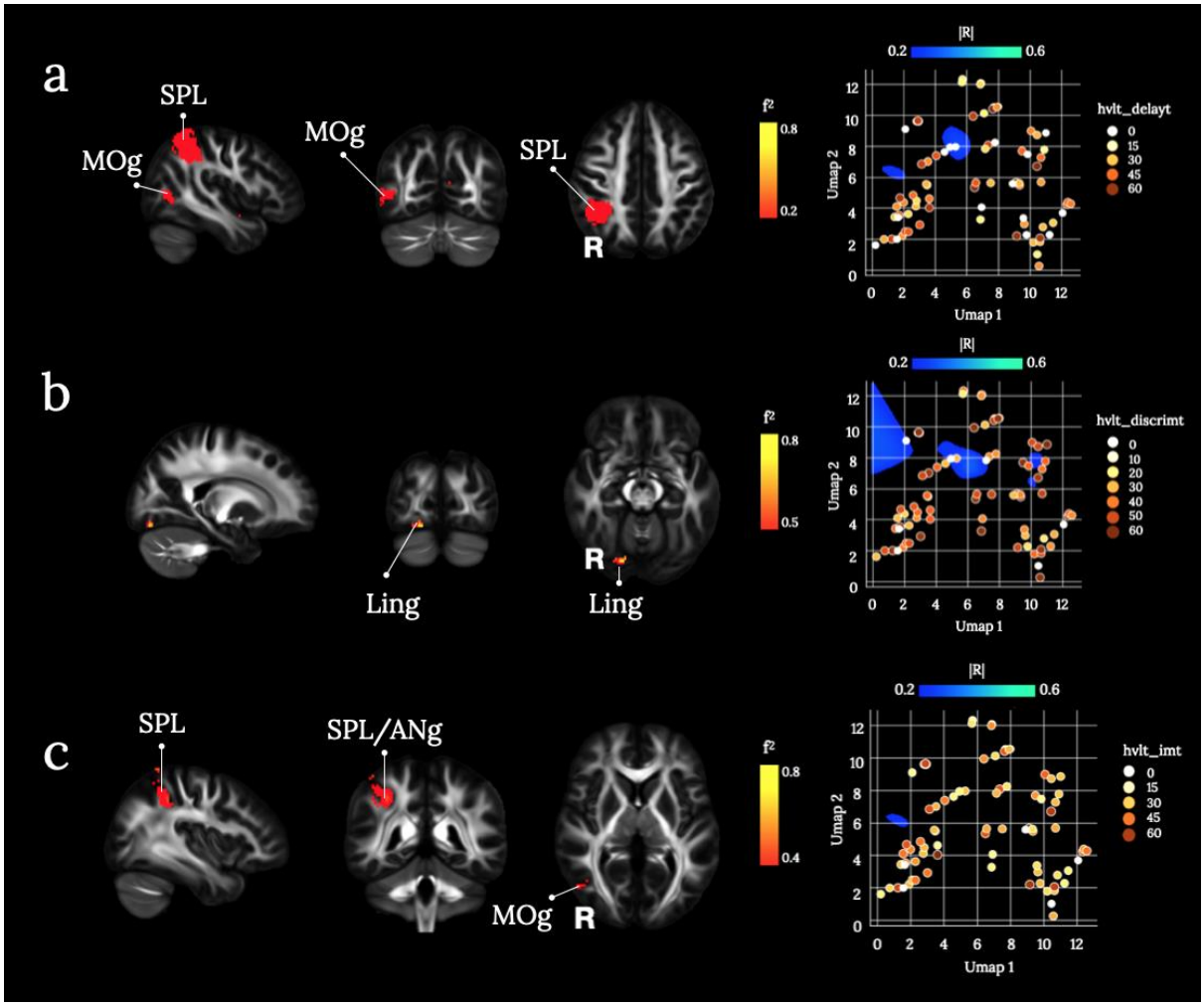

Supplementary Figure 37: Brain disconnections and Umap risk territories contributing significantly to the *The Hopkins Verbal Learning Test* (HVLT) responses after t-score conversion. *(a) delayed recall* (hvlt_delayt), (b) discrimination index (hvlt_discrimt), and (c) total immediate recall (hvlt_imt). ANg: angular gyrus; SPL: superior parietal lobe; Mog: middle occipital gyrus; Cu: cuneus; Ling: lingual gyrus. Maps are freely available at https://neurovault.org/collections/11260/ .

Anatomically, the parietal lobe is at the crossroad between the frontal, occipital, and temporal lobes and highly connected to each lobe. This connectivity pattern results in the parietal lobe being a central hub for multimodal sensory integration. Functional studies have indicated its role in higher cognitive functions that are characteristic of the human species, including semantic and pragmatic aspects of language, episodic retrieval, memory integration, and sustained attention (Catani et al. 2017; Sestieri et al. 2017; Coslett and Schwartz 2018; Husain and Nachev 2007; Singh-Curry and Husain 2009; Seghier 2012). Semantic activations were primarily described for the left hemisphere inferior parietal lobe but have been consistently shown for the right angular gyrus as well (Binder et al. 2009). Given the high semantic load of these word lists, a disconnection of the superior parietal lobe can lead to deficits in the immediate (hvlt_imt) and delayed (hvlt_delayt) recall.

C.6 Pain

Pain is one of the long-term compliance that can manifest after a stroke event. Pain incidence can vary across the stroke survivor population. Lundström et al. (2009) estimated a stroke-related pain incidence of 21% at 1-year after the stroke event (N=140 stroke patients). Langhorne et al. (2000) rated a pain incidence of 34%, and more specifically a shoulder pain of 9 %, in patients up to 30 months after stroke (N=311 stroke patients).

Moreover, pain perception significantly increases in the MRI scanner environment, probably due to higher awareness and alertness, as shown by Ellerbrock et al (2015) in a healthy population.

In our study, pain sensation after the MRI scanning was recorded. A scale ranging between 0-100 was used, and patients had to answer the following question: "*During the scan, how much of the time did you... Feel pain or discomfort*?". A multiple choice of answers was presented:

- all of the time (100%);
- most of the time (80%);
- a good bit of the time (60%);
- some of the time (40%);
- a little of the time (20%);
- none of the time (0%).

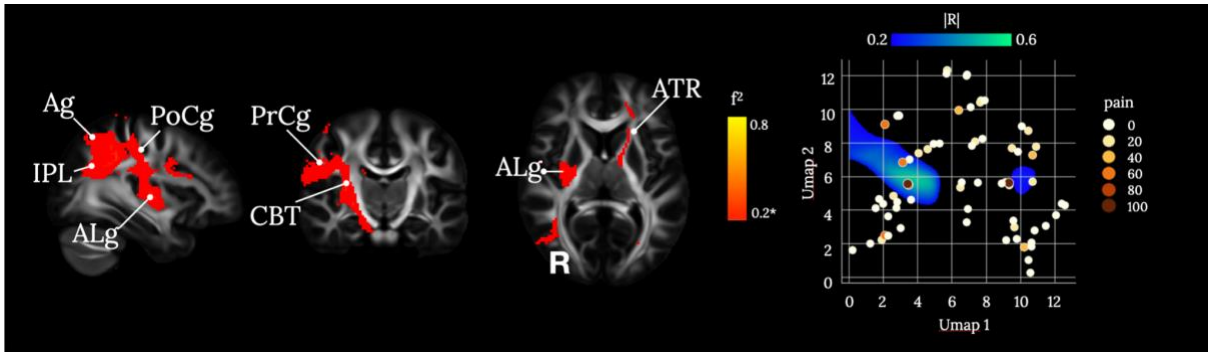

Supplementary figure 38. ALg=Anterior Long insular gyrus; IPL=Inferior parietal lobe; Ag: Angular gyrus; PoCg=PostCentral gyrus; PrCg=PreCentral gyrus; CBT: Cortico Bulbar Tract; ATR=Anterior Thalamic Radiation. * indicate a small effect size (f˙˙˙˙˙˙2<0.5). Maps are freely available at https://neurovault.org/collections/11260/ .

According to the composite morphospace results, profiles of disconnections predicting individual pain perception were localized mainly in the right white matter; including pathways reaching the parietal lobe, posterior insula, post--central gyrus and the lower division of the precentral gyrus. In the left hemisphere, correlations occurred along with the anterior thalamic radiation.

As reviewed by I. Tracey and P.W. Mantyh (2007), brain perception is modulated between the peripheral nervous system and cerebral pain processing. In particular, the nociceptive information ascends to the thalamus in the contralateral spinothalamic tract, medulla, and brainstem. The descending pain modulatory system also includes

projections to the amygdala, hypothalamus, insula, and anterior cingulate cortex. Spinal projections to the brainstem are also extremely important (Tracey and Mantyh 2007).
Our findings are in agreement with the described nociceptive system, highlighting pyramidal connections with the lower portion of the precentral gyrus (cortico bulbar tract fibers), and the postcentral gyrus connected by the spinothalamic tract mainly involved in the somatosensory responses to pain (Basbaum et al. 2009).
In the disconnectome results the right posterior insula and left anterior thalamic radiation were also highlighted.
Our pain related results rechead a low effect size ($f2<0.5$), probably reflecting the brief pain examination conducted. However, the found pain correlates present encouraging results.

C.7 Sickness

The Sickness Impact Profile (SIP) scale is a commonly used scale to assess the quality of life (de Haan et al. 1993). The SIP scale is composed of 136 items divided into 12 subscales, exploring three main aspects: physical, social, and emotional functioning. Van Staten et al. (1997) proposed a shorter and stroke-adapted version of the SIP (SA-SIP) including 30 items subdivided into 8 subscales exploring both physical and psychosocial sickness dimensions. Using the SA-SIP it was possible to explain the 91% of the SIP evaluation variance in stroke patients (N=319, 6-months after stroke onset). This result was replicated in an independent cohort explaining 89% of the sickness profile variance (van Straten et al. 1997). The SA-SIP scale has been also translated in different languages than English (e.g. French, Spanish) for a wider use.

Sip_body

The sip_body constitutes the total score for the sickness of body care and movement.
It has been evaluated with a yes/no answer to the following five questions:

- I make difficult moves with help, for example getting into or out of cars, bathtubs (sip_body1);
- I move my hands or fingers with some limitation or difficulty (sip_body2);
- I get in and out of bed or chairs by grasping something for support or using a cane or walker (sip_body3);
- I have trouble getting shoes, socks, or stockings on (sip_body4);
- I get dressed only with someone's help (sip_body5).

The total sickness of body care and movement score ranges from 0 to 100, and it is calculated as:

sip_body = (sip_body1*84+ sip_body2*64 + sip_body3*82 + sip_body4*57 + sip_body5*88)/3.75

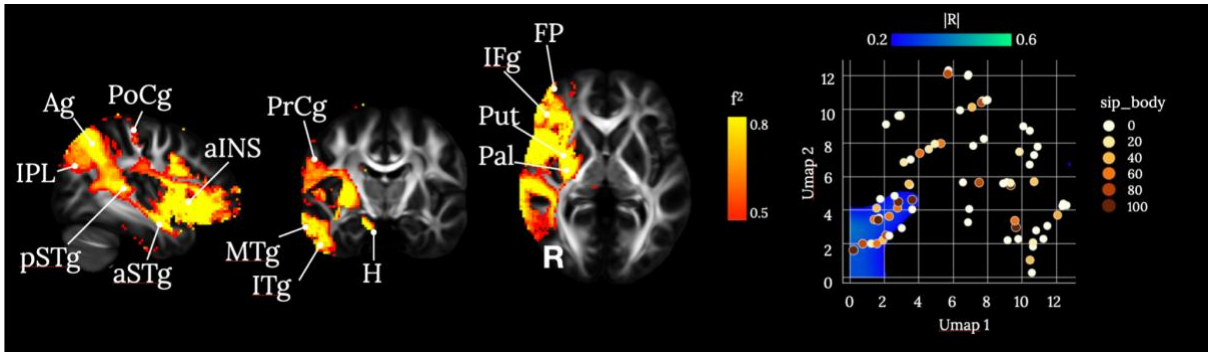

Supplementary figure 39. IPL=Inferior parietal lobe; Ag: Angular gyrus; pSTg=posterior Superior Temporal gyrus; aSTg=anterior Superior Temporal gyrus; PoCg=PostCentral gyrus; aINS=anterior Insula; PrCg=PreCentral gyrus; MTg=Middle Temporal gyrus; ITg=Inferior Temporal gyrus; H=Hippocampus; Put=Putamen; Pal=Pallidum; IFg=Inferior Frontal gyrus; FP=Frontal Pole. Maps are freely available at https://neurovault.org/collections/11260/ .

Sip_mob

The sip_mob constitutes the total score for mobility sickness. It has been evaluated with a yes/no answer to the following three questions:

- I stay home most of the time (sip_mob1);
- I am not going into town (sip_mob2);
- I do not get around in the dark or in unlit places without someone's help (sip_mob3).

The total score for the mobility sickness ranges from 0 to 100, and it is calculated as:

sip_mob = (sip_mob1*66 + sip_mob2*48 + mob3*72)/1.86

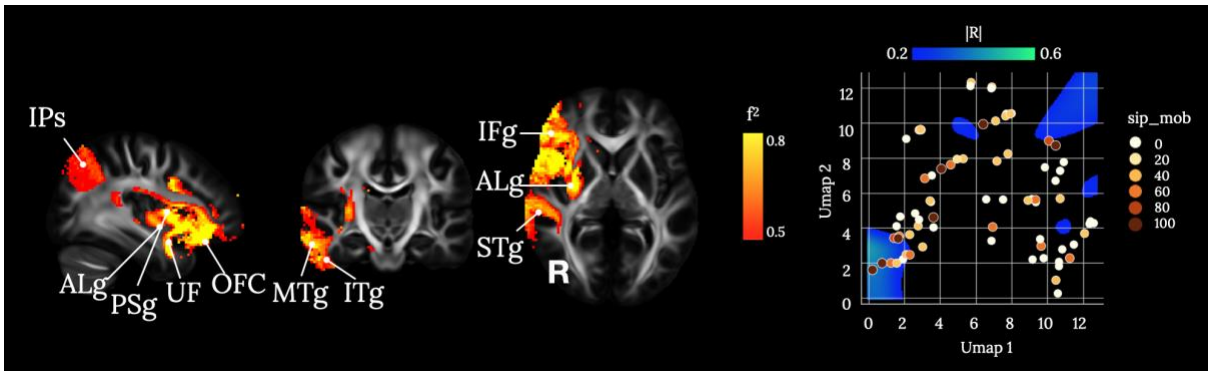

Supplementary figure 40. IPs=IntraParietal sulcus; ALg=Anterior Long insular gyrus; PSg=Posterior Short insular gyrus; UF=Uncinate Fasciculus; OFC=Orbito-Frontal Cortex; MTg=Middle Temporal Gyrus; ITg=Inferior Temporal Gyrus; STg=Superior Temporal Gyrus; IFg=Inferior Frontal gyrus. Maps are freely available at https://neurovault.org/collections/11260/ .

Sip_house

The sip_house constitutes the total score for the household management sickness. It has been evaluated with a yes/no answer to the following four questions:

- I am not doing any of the maintenance or repair work that I would usually do in my home or yard (sip_house1);
- I am not doing any of the shopping that I would usually do (sip_house2);
- I am not doing any of the house cleaning that I would usually do (sip_house3);
- I am not doing any of the clothes washing that I would usually do (sip_house4).

The total score for the household management sickness ranges from 0 to 100, and it is calculated as:

sip_house = (sip_house1*62 + sip_house2*71 + sip_house3*77 + sip_house4*77)/2.87

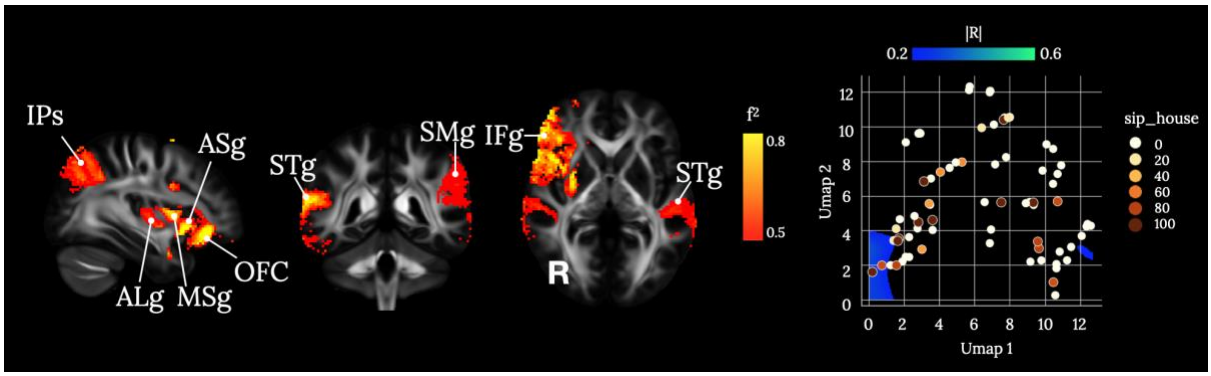

Supplementary figure 41. IPs=Intra-Parietal sulcus; ALg=Anterior Long insular gyrus; MSg=Posterior Short insular gyrus; ASg=Anterior Short insular gyrus; OFC=Orbito-Frontal Cortex; STg=Superior Temporal Gyrus; SMG=Supramarginal gyrus; IFg=Inferior Frontal Gyrus; STg=Superior Temporal Gyrus. Maps are freely available at https://neurovault.org/collections/11260/ .

Sip_amb

The sip_amb constitutes the total score for ambulation sickness evaluated with a yes/no answer to the following three questions:

- I do not walk up or down hills (sip_amb1);
- I get around only by using a walker, crutches, cane, walls, or furniture (sip_amb2);
- I walk more slowly (sip_amb3).

The total sickness of ambulation score ranges from 0 to 100, and it is calcualted as:

sip_amb = (sip_amb1*56 + sip_amb2*79 + sip_amb3*35)/1.7

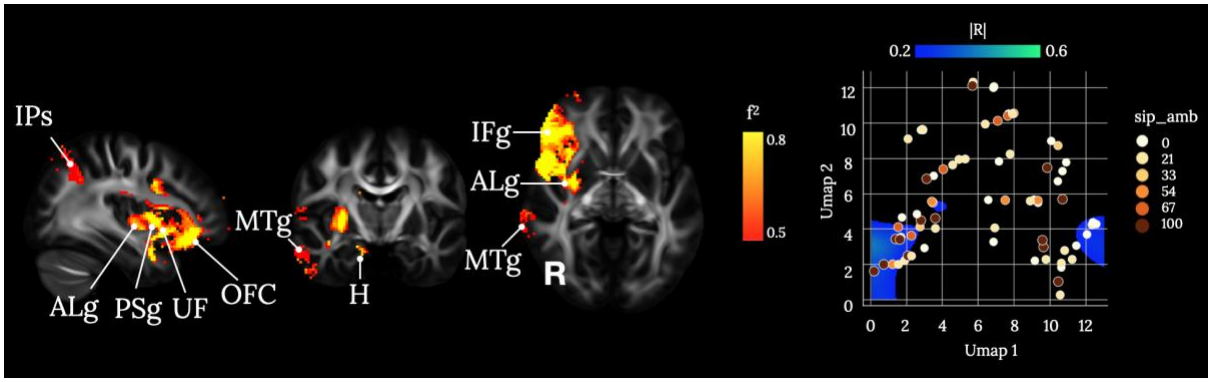

Supplementary figure 42. IPs=Intra-Parietal sulcus; ALg=Anterior Long insular gyrus; PSg=Posterior Short insular gyrus; UF=Uncinate Fasciculus; OFC=Orbito-Frontal Cortex; MTg=Middle Temporal Gyrus; H=Hippocampus; IFg=Inferior Frontal gyrus. Maps are freely available at https://neurovault.org/collections/11260/ .

Sip_physical

The sip_physical is a subtotal scale evaluating the physical sickness dimension. The sip_physical score combines together the sickness scores obtained for body care and movement (sip_body), mobility (sip_mob), household management (sip_house), and ambulation (sip_amb).

The physical sickness score ranges from 0 to 100, and it is calculated as:

sip_physical= (sip_body1*84 + sip_body2*64 + sip_body3*82 + sip_body4*57 + sip_body5*88 + sip_mob1*66 + sip_mob2*48 +sip_mob3*72 + sip_house1*62 + sip_house2*71 + sip_house3*77 + sip_house4*77 +sip_amb1*56 + sip_amb2*79 + sip_amb3*35)/10.18

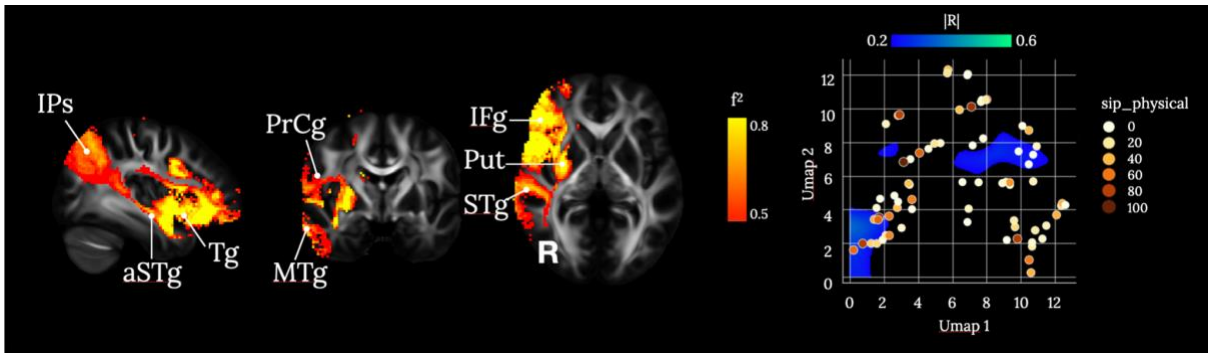

Supplementary figure 43. IPs=Intra-Parietal sulcus; aSTg=anterior Superior Temporal gyrus; Tg=Transverse insular gyrus; MTg=Middle Temporal gyrus; PrCg=PreCentral gyrus; STg=Superior Temporal gyrus; Put=Putamen; IFg=Inferior Frontal gyrus. Maps are freely available at https://neurovault.org/collections/11260/ .

Sip_social

The sip_socail constitutes the total score for the social interaction sickness. It has been evaluated with a yes/no answer to the following five questions:

- I show less interest in other people's problems, for example, don't listen when they tell me about their problems, don't offer to help (sip_social1);
- I often act irritable to those around me, for example, snap at people, give sharp answers, criticize easily (sip_social2);
- I show less affection (sip_social3);
- I am doing fewer social activities with groups of people (sip_social4);
- I talk less to those around me (sip_social5).

The total score of social interaction sickness ranges from 0 to 100, and it is calculated as:

sip_social = (sip_social1*67 + sip_social2*84 + sip_social3*52 + sip_social4*36 + sip_social5*56)/2.95

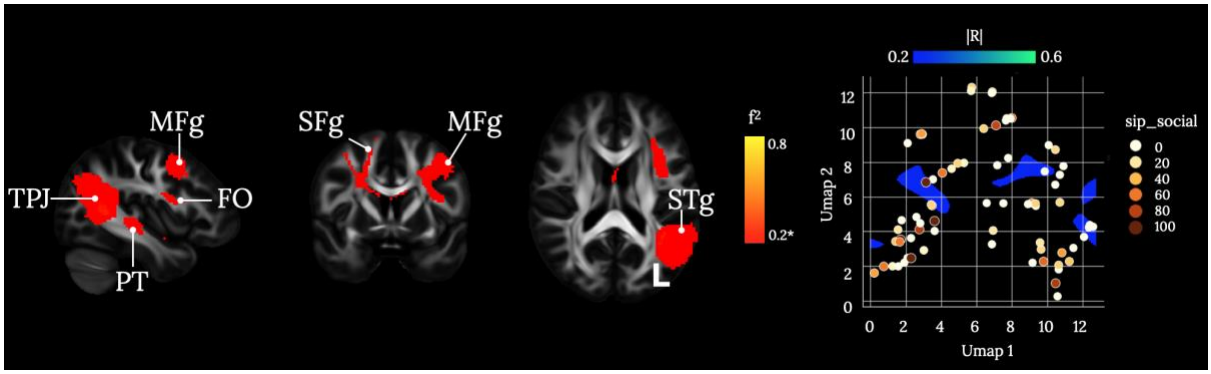

Supplementary figure 44. TPJ=Temporal Parietal Junction; PT=Planum temporale; MFg=Middle Frontal gyrus; FO=Frontal Operculum; SFg=Superior Frontal gyrus; STg=Superior Temporal gyrus. * indicate a small effect size (f‴‴‴‴‴2<0.5). Maps are freely available at https://neurovault.org/collections/11260/ .

Sip_com

The sip_com constitutes the total score for the sickness of communication. It has been evaluated with a yes/no answer to the following three questions:

- I carry on a conversation only when very close to the other person or looking at him (sip_com1);
- I have difficulty speaking, for example, get stuck, stutter, stammer, slur my words (sip_com2);
- I do not speak clearly when I am under stress (sip_com3).

The total communication sickness score ranges from 0 to 100, and it is calculated as:

sip_com = (sip_com1*67 + sip_com2*76 + sip_com3*64)/2.07

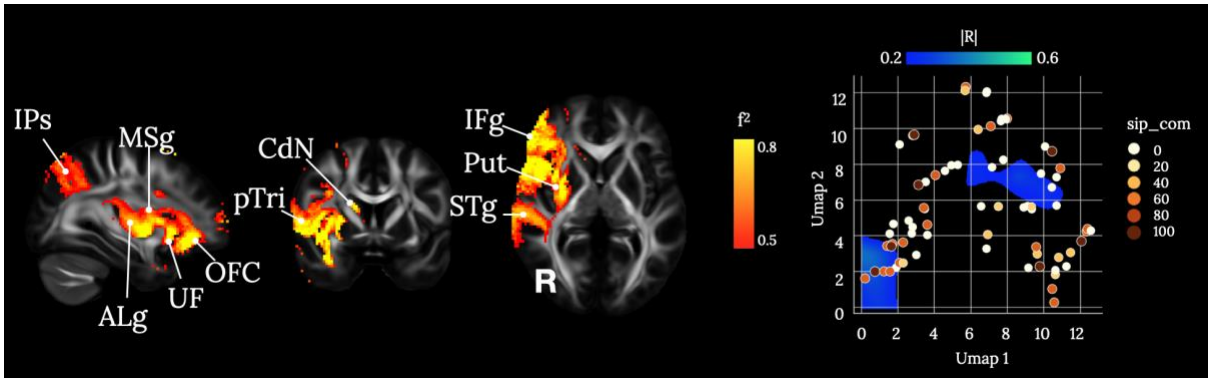

Supplementary figure 45. IPs=Intra-Parietal sulcus; ALg=Anterior Long insular gyrus; MSg=Middle Short insular gyrus; UF=Uncinate Fasciculus; OFC=Orbito Frontal Cortex; pTri=pars Triangularis; CdN=Caudate Nucleus; STg=Superior Temporal gyrus; Put=Putamen; IFg=Inferior Frontal gyrus. Maps are freely available at https://neurovault.org/collections/11260/ .

Sip_emo

The sip_emo constitutes the total score for the sickness of emotional behavior. It is evaluated with a yes/no answer to the following four questions:

- I say how bad or useless I am, for example, that I am a burden on others (sip_emo1);
- I laugh or cry suddenly (sip_emo2);
- I act irritable and impatient with myself, for example, talk badly about myself, swear at myself, blame myself for things that happen (sip_emo3);
- I get sudden frights (sip_emo4).

The total sickness of emotional behavior score ranges from 0 to 100, and it is calculated as:

sip_emo = (sip_emo1*87 + sip_emo2*68 + sip_emo3*78 + sip_emo4*74)/3.07

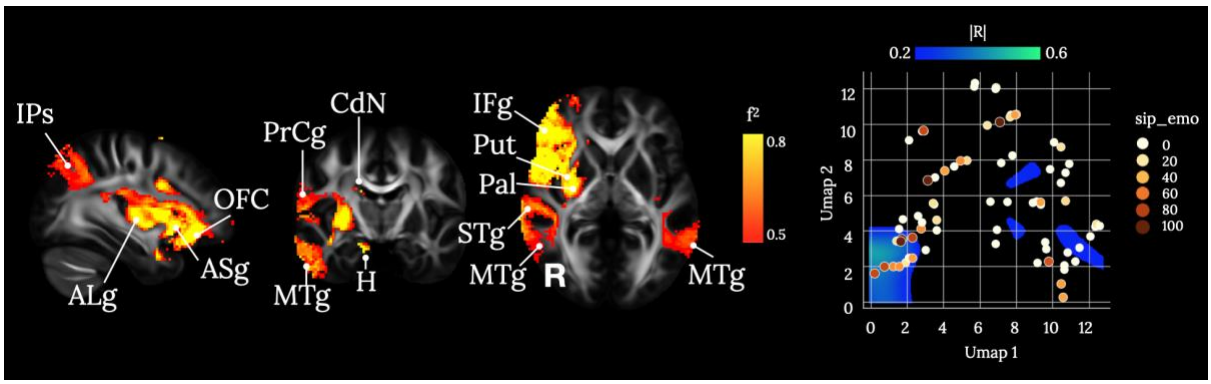

Supplementary figure 46. IPs=Intra-Parietal sulcus; ALg=Anterior Long insular gyrus; ASg=Anterior Short insular gyrus; OFC=Orbito Frontal Cortex; MTg=Middle Temporal gyrus; H=Hippocampus; PrCg=Precentral Central gyrus; CdN=Caudate Nucleus;

STg=Superior Temporal gyrus; Pal=Pallidum; Put=Putamen; IFg=Inferior Frontal gyrus. Maps are freely available at https://neurovault.org/collections/11260/ .

Sip_alert

The sip_alert constitutes the total score for alertness behavior evaluated with a yes/no answer to the following three questions:

- I am confused and start several actions at a time (sip_alert1);
- I make more mistakes than usual (sip_alert2);
- I have difficulty doing activities involving concentration and thinking (sip_alert3).

The total sickness of alertness behaviors ranges from 0 to 100, and it is calcualted as:

sip_alert = (sip_alert1*90 + sip_alert2*64 + sip_alert3*80)/2.34

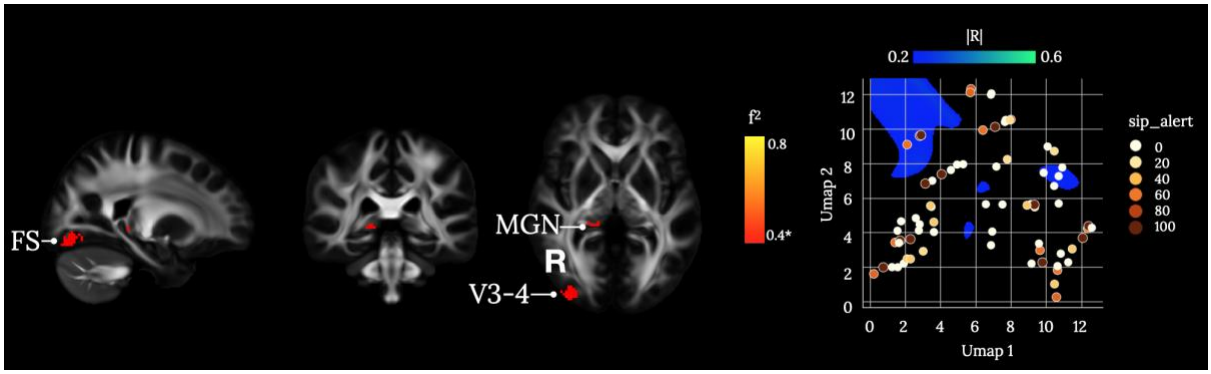

Supplementary Figure 47. FS: Fusiform gyrus, V3-4: Visual cortex 3 and 4, MGN=Middle Geniculate Nucleus. * indicate a small effect size ($f^2<0.5$). Maps are freely available at https://neurovault.org/collections/11260/ .

Sip_psychosoc

The sip_psychosoc is a subtotal scale evaluating the psychosocial sickness dimension. The sip_psychosoc score combines together the different sickness scores obtained for social (sip_social), communication (sip_com), emotional behavior (sip_emo), and alertness behavior (sip_alert).

The psychosocial sickness score ranges from 0 to 100, and it is calculated as:

sip_psychosoc = **(**sip_soc1*67+ sip_soc2*84+ sip_soc3*52+ sip_soc4*36+ sip_soc5*56+ sip_com1*67+ sip_com2*76+ sip_com3*64+ sip_emo1*87+ sip_emo2*68+ sip_emo3*78+ sip_emo4*74+ sip_alert1*90+ sip_alert2*64+ sip_alert3*80) /10.43.

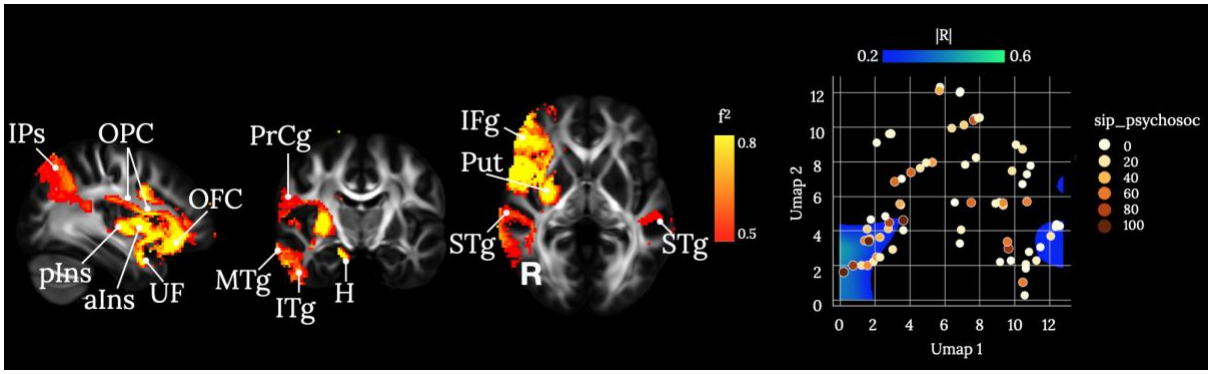

Supplementary figure 48. IPs=Intra-Parietal sulcus; pIns=posterior Insula; aIns=anterior Insula; UF=Uncinate Fasciculus; OPC=Operculum Cortex; OFC=Orbito Frontal Cortex; PrCg=PreCentral gyrus; MTg=Middle Temporal gyrus; ITg=Inferior Temporal gyrus; H=Hippocampus; STg=Superior Temporal gyrus; Put=Putamen; IFg=Inferior Frontal gyrus. Maps are freely available at https://neurovault.org/collections/11260/ .

The disconnectome analyses highlighted the basal ganglia (e.g., putamen, pallidum and caudate body) on the right hemisphere as predictors for most of the sickness scores. In agreement, Van de Port et al. (2004), administering the SA-SIP scale (N=122 stroke patients), found lower scores in total and psychosocial dimensions in subarachnoid haemorrhage and subcortical infarction compared to cortical strokes. The disconnectome analyses did not highlight any infratentorial, internal capsule or thalamic areas. In the paper by Van Straten et al. (1997), in which the SA-SIP scale was originally defined, no differences were found distinguishing infratentorial and supratentorial strokes, whereas lacunar infarctions presented a better overall sickness response compared to cortical and subcortical strokes.

Moreover, in our disconnectome results, the insular gyri presented high-effect size correlations in all the evaluated sickness scores with exception for the social and alertness behaviors. These two sickness scores were the only ones presenting low effect size (<0.5). The insular correlations were strongly lateralized on the right hemisphere. Interestingly, in the study of Harte et al. (2016), investigating patients with a chronic pain condition, fibromyalgia, insular activations in response to visual stimulation were able to discriminate between patients versus healthy participants. In particular, activation in the right anterior insula. Thus, this indicates that a dysregulation of multisensory integration within the right insula can lead to pain conditions, and probably to a higher sickness response.

In the disconnectome results, the right prefrontal cortex was highly correlated with sickness in all the evaluated scores. In the study by Fogel et al. (2011), investigating chronic pain in temporomandibular patients, a decoupling between the prefrontal cortex and the cingulate cortex was measured during cognitive and emotional tasks.

These findings suggest that an unsynchronization between attention and cognition processings can lead to slow behavioral responses, evaluated in several sickness scores (e.g., sip_psychosoc).

Additionally, the uncinate fasciculus, connecting the orbital prefrontal cortex, is strongly involved in social-emotional processing, presenting abnormalities mainly in the right

hemisphere in psychopathy and antisocial personality disorders (Von Der Heide et al. 2013).

The disconnectome results also detect right parietal, temporal and hippocampal regions, and left temporal regions as predictors correlated with sickness. In the study by Shigihara et al. (2013), using magnetoencephalography and mental fatigue conditions, decreased alpha power was measured in the right angular gyrus and increased levels in the left middle and superior temporal gyri, after a 30 minute fatigue inducing 0-back test sessions; whereas after a 2-back session, decreased alpha power was measured in right middle and superior frontal gyrus, and widespread increased levels including the right parahippocampal gyrus, right inferior frontal gyrus and left middle temporal gyrus. These regions were also highlighted from the disconnectome results, and these results indicate that different types of mental fatigue can produce alterations in different brain regions, and with different levels of activity oscillations.

As a limitation, the SA-SIP scale has to be administered with caution to patients presented with a severe stroke, and in case of severe speech and language disorders. In those cases, a proxy respondent, primarily the partner, will answer the questions (van Straten et al. 2000). Thus, the left hemisphere, mainly damaged in case of language impairment, can be underestimated as neuronal correlates of sickness using the SA-SIP scale.

D. White matter atlas of neuropsychological scores

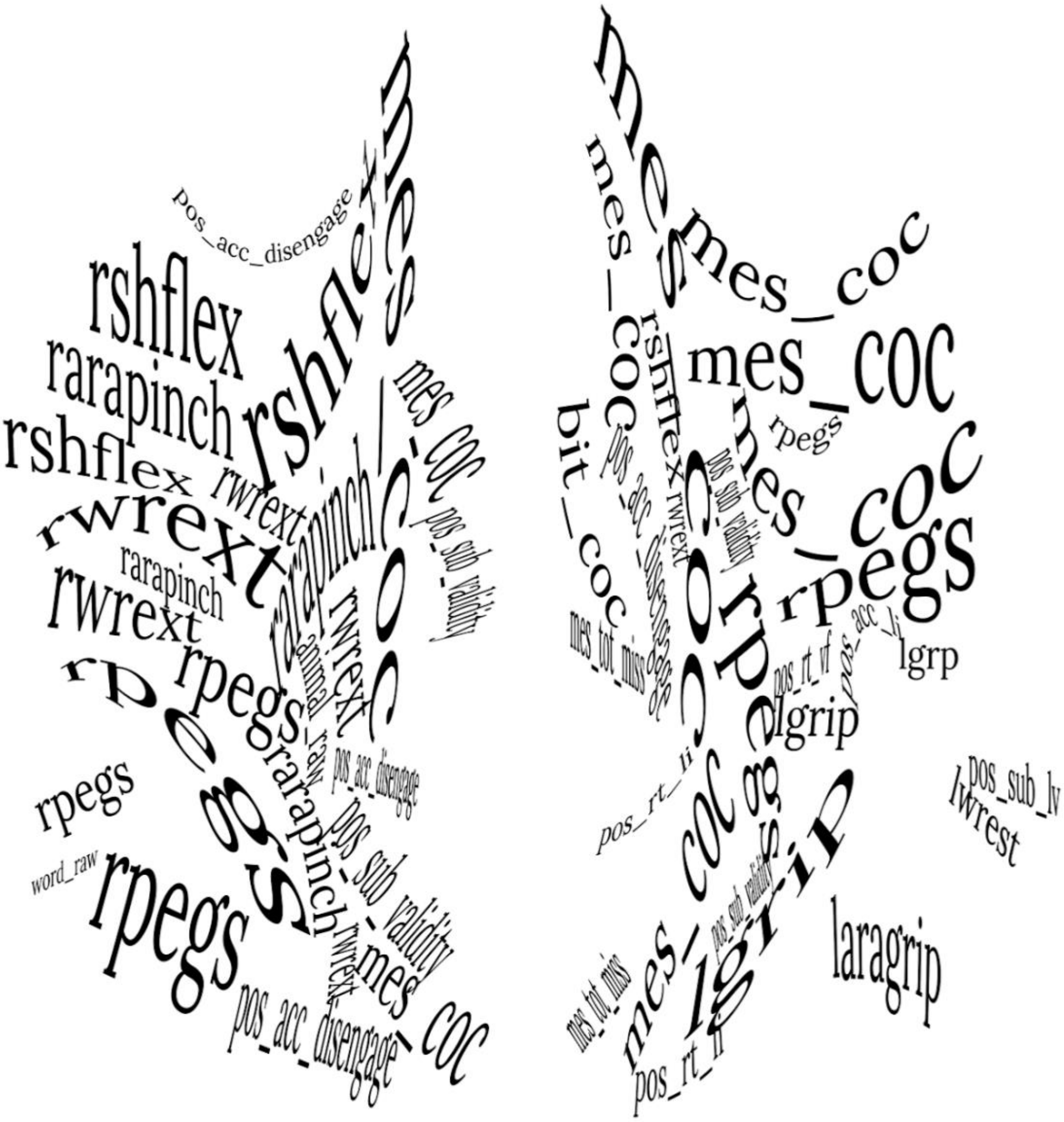

Supplementary Figure 49. z=50 mm (Neurological convention, MNI coordinates).

Supplementary Figure 50. z=40 mm (Neurological convention, MNI coordinates).

Supplementary Figure 51. z=30 mm (Neurological convention, MNI coordinates).

Supplementary Figure 52. z=20 mm (Neurological convention, MNI coordinates).

Supplementary Figure 53. z=10 mm (Neurological convention, MNI coordinates).

Supplementary Figure 54. z=0 mm (Neurological convention, MNI coordinates).

Supplementary Figure 55. z=−10 mm (Neurological convention, MNI coordinates).

Supplementary Figure 56. z=-20 mm (Neurological convention, MNI coordinates).

E. Web application user guide

Before running the online DSD web-application you need to:

1. segment your stroke patient lesion. For this purpose many software can be used, e.g. MRIcron, FSLeyes, mrview, ITKsnap. Lesions can be segmented using T1-weighted MRI contrast or a lesion multi contrast inspection with T2-weighted and FLAIR MRIs.
2. Download and install the BCBlab toolkit following the instructions at http://bcblab.com/BCB/Softwares.html. Run the "Normalisation" command first, and then the "Disconnectome maps".

Subsequently, go to the web-application site http://disconnectomestudio.bcblab.com. Press "select file" and choose the single subject disconnectome, obtained from the BCBlab toolkit computation. Press "upload", and after about one minute the neuropsychological score table shown in the web page will reload to show the calculated 1-year expected scores. Press the "download" button, and an excel file containing the neuropsychological score table will be downloaded to save. .

No files or tables are saved in the web-server. All the computations are run in a temporary directory that is deleted when the output neuropsychological table is ready to be downloaded. Thus, if you want to re-run the analysis, you will have to upload the patient disconnectome file again for a new computation.

F. Supplementary references

Addis DR, Moloney EEJ, Tippett LJ, P. Roberts R, Hach S (2016) Characterizing cerebellar activity during autobiographical memory retrieval: ALE and functional connectivity investigations. Neuropsychologia 90:80-93. doi:https://doi.org/10.1016/j.neuropsychologia.2016.05.025

Akelaitis AJ (1945) Studies of the corpus callosum: IV. Diagonistic dyspraxia in epileptics following partial and complete section of the corpus callosum. Am J Psychiat 101:594–599.

Akshoomoff NA, Courchesne E, Press GA, Iragui V (1992) Contribution of the cerebellum to neuropsychological functioning: Evidence from a case of cerebellar degenerative disorder. Neuropsychologia 30 (4):315-328. doi:https://doi.org/10.1016/0028-3932(92)90105-U

Andreasen NC, O'Leary DS, Paradiso S, Cizadlo T, Arndt S, Watkins GL, Boles Ponto LL, Hichwa RD (1999) The cerebellum plays a role in conscious episodic memory retrieval. Human Brain Mapping 8 (4):226-234. doi:https://doi.org/10.1002/(SICI)1097-0193(1999)8:4<226::AID-HBM6>3.0.CO;2-4

Aron AR, Fletcher PC, Bullmore ET, Sahakian BJ, Robbins TW (2003) Stop-signal inhibition disrupted by damage to right inferior frontal gyrus in humans. Nature Neuroscience 6 (2):115-116. doi:10.1038/nn1003

Baars BJ (2002) The conscious access hypothesis: origins and recent evidence. Trends in Cognitive Sciences 6 (1):47-52. doi:https://doi.org/10.1016/S1364-6613(00)01819-2

Backman C, Gibson SCD, Parsons J (1992) Assessment of Hand Function: The Relationship between Pegboard Dexterity and Applied Dexterity. Canadian Journal of Occupational Therapy 59 (4):208-213. doi:10.1177/000841749205900406

Baier B, Karnath HO (2008) Tight link between our sense of limb ownership and self-awareness of actions. Stroke 39 (2):486-488. doi:10.1161/STROKEAHA.107.495606

Bailey MJ, Riddoch MJ, Crome P (2004) Test–retest stability of three tests for unilateral visual neglect in patients with stroke: Star Cancellation, Line Bisection, and the Baking Tray Task. Neuropsychological Rehabilitation 14 (4):403-419. doi:10.1080/09602010343000282

Baldo JV, Arévalo A, Patterson JP, Dronkers NF (2013) Grey and white matter correlates of picture naming: Evidence from a voxel-based lesion analysis of the Boston Naming Test. Cortex 49 (3):658-667. doi:https://doi.org/10.1016/j.cortex.2012.03.001

Baldo JV, Kacinik N, Ludy C, Paulraj S, Moncrief A, Piai V, Curran B, Turken A, Herron T, Dronkers NF (2018) Voxel-based lesion analysis of brain regions underlying reading and writing. Neuropsychologia 115:51-59. doi:https://doi.org/10.1016/j.neuropsychologia.2018.03.021

Baldo JV, Shimamura AP, Delis DC, Kramer J, Kaplan E (2001) Verbal and design fluency in patients with frontal lobe lesions. Journal of the International Neuropsychological Society 7 (5):586-596. doi:10.1017/S1355617701755063

Barbieri C, De Renzi E (1988) The executive and ideational components of apraxia. Cortex 24 (4):535-543. doi:10.1016/s0010-9452(88)80047-9

Bartolomeo P, Chokron S (2002) Orienting of attention in left unilateral neglect. Neuroscience & Biobehavioral Reviews 26 (2):217-234. doi:https://doi.org/10.1016/S0149-7634(01)00065-3
Bartolomeo P, Thiebaut de Schotten M, Doricchi F (2007) Left Unilateral Neglect as a Disconnection Syndrome. Cerebral Cortex 17 (11):2479-2490. doi:10.1093/cercor/bhl181
Basbaum AI, Bautista DM, Scherrer G, Julius D (2009) Cellular and molecular mechanisms of pain. Cell 139 (2):267-284. doi:10.1016/j.cell.2009.09.028
Bates E, Wilson SM, Saygin AP, Dick F, Sereno MI, Knight RT, Dronkers NF (2003) Voxel-based lesion-symptom mapping. Nat Neurosci 6 (5):448-450. doi:10.1038/nn1050
Begliomini C, Sartori L, Miotto D, Stramare R, Motta R, Castiello U (2015) Exploring manual asymmetries during grasping: a dynamic causal modeling approach. Front Psychol 6:167. doi:10.3389/fpsyg.2015.00167
Benson DF (1979) Aphasia, alexia, agraphia. Churchill Livingstone, New York
Berlucchi G, Aglioti S, Marzi CA, Tassinari G (1995) Corpus callosum and simple visuomotor integration. Neuropsychologia 33 (8):923-936. doi:https://doi.org/10.1016/0028-3932(95)00031-W
Berti A, Bottini G, Gandola M, Pia L, Smania N, Stracciari A, Castiglioni I, Vallar G, Paulesu E (2005) Shared cortical anatomy for motor awareness and motor control. Science 309 (5733):488-491. doi:10.1126/science.1110625
Besharati S, Forkel SJ, Kopelman M, Solms M, Jenkinson PM, Fotopoulou A (2014) The affective modulation of motor awareness in anosognosia for hemiplegia: behavioural and lesion evidence. Cortex 61:127-140. doi:10.1016/j.cortex.2014.08.016
Biesbroek JM, van Zandvoort MJ, Kappelle LJ, Velthuis BK, Biessels GJ, Postma A (2016) Shared and distinct anatomical correlates of semantic and phonemic fluency revealed by lesion-symptom mapping in patients with ischemic stroke. Brain Struct Funct 221 (4):2123-2134. doi:10.1007/s00429-015-1033-8
Binder JR (2015) The Wernicke area. Neurology 85 (24):2170. doi:10.1212/WNL.0000000000002219
Binder JR, Desai RH, Graves WW, Conant LL (2009) Where Is the Semantic System? A Critical Review and Meta-Analysis of 120 Functional Neuroimaging Studies. Cerebral Cortex 19 (12):2767-2796. doi:10.1093/cercor/bhp055
Binkofski F, Buxbaum LJ (2013) Two action systems in the human brain. Brain Lang 127 (2):222-229. doi:10.1016/j.bandl.2012.07.007
Bird CM, Malhotra P, Parton A, Coulthard E, Rushworth MFS, Husain M (2006) Visual neglect after right posterior cerebral artery infarction. Journal of Neurology, Neurosurgery & Psychiatry 77 (9):1008. doi:10.1136/jnnp.2006.094417
Blackwood N, ffytche D, Simmons A, Bentall R, Murray R, Howard R (2004) The cerebellum and decision making under uncertainty. Cognitive Brain Research 20 (1):46-53. doi:https://doi.org/10.1016/j.cogbrainres.2003.12.009
Bogen JE (1987) Physiological consequences of complete or partial commissural section. In: MLJ A (ed) Surgery of the third ventricle. Baltimore, Williams and Wilkins, pp 175–194
Bogousslavsky J, Regli F, Assal G (1986) The syndrome of unilateral tuberothalamic artery territory infarction. Stroke 17 (3):434-441. doi:10.1161/01.str.17.3.434
Bonilha L, Hillis AE, Hickok G, den Ouden DB, Rorden C, Fridriksson J (2017) Temporal lobe networks supporting the comprehension of spoken words. Brain 140 (9):2370-2380. doi:10.1093/brain/awx169
Borich MR, Mang C, Boyd LA (2012) Both projection and commissural pathways are disrupted in individuals with chronic stroke: investigating microstructural white

matter correlates of motor recovery. BMC Neurosci 13:107. doi:10.1186/1471-2202-13-107
Brandt J (1991) The hopkins verbal learning test: Development of a new memory test with six equivalent forms. Clinical Neuropsychologist 5 (2):125-142. doi:10.1080/13854049108403297
Budisavljevic S, Dell'Acqua F, Zanatto D, Begliomini C, Miotto D, Motta R, Castiello U (2017) Asymmetry and Structure of the Fronto-Parietal Networks Underlie Visuomotor Processing in Humans. Cereb Cortex 27 (2):1532-1544. doi:10.1093/cercor/bhv348
Buiatti T, Skrap M, Shallice T (2012) Left- and right-hemisphere forms of phonological alexia. Cognitive Neuropsychology 29 (7-8):531-549. doi:10.1080/02643294.2013.771773
Buxbaum LJ, Shapiro AD, Coslett HB (2014) Critical brain regions for tool-related and imitative actions: a componential analysis. Brain 137 (Pt 7):1971-1985. doi:10.1093/brain/awu111
Cabeza R, Ciaramelli E, Olson IR, Moscovitch M (2008) The parietal cortex and episodic memory: an attentional account. Nature Reviews Neuroscience 9 (8):613-625. doi:10.1038/nrn2459
Cambier J, Elghozi D, Strube E (1980) Lésion du thalamus droit avec syndrome de l'hémisphère mineur. Discussion du concept de négligence thalamique. Rev Neurol 136:105–116
Caplan B, Kinsbourne M (1981) Cerebral lateralization, preferred cognitive mode, and reading ability in normal children. Brain and Language 14 (2):349-370. doi:https://doi.org/10.1016/0093-934X(81)90085-7
Carter AR, Astafiev SV, Lang CE, Connor LT, Rengachary J, Strube MJ, Pope DL, Shulman GL, Corbetta M (2010) Resting interhemispheric functional magnetic resonance imaging connectivity predicts performance after stroke. Ann Neurol 67 (3):365-375. doi:10.1002/ana.21905
Catani M, Dell'Acqua F, Vergani F, Malik F, Hodge H, Roy P, Valabregue R, Thiebaut de Schotten M (2012) Short frontal lobe connections of the human brain. Cortex 48 (2):273-291. doi:https://doi.org/10.1016/j.cortex.2011.12.001
Catani M, Mesulam MM, Jakobsen E, Malik F, Martersteck A, Wieneke C, Thompson CK, Thiebaut de Schotten M, Dell'Acqua F, Weintraub S, Rogalski E (2013) A novel frontal pathway underlies verbal fluency in primary progressive aphasia. Brain 136 (Pt 8):2619-2628. doi:10.1093/brain/awt163
Catani M, Robertsson N, Beyh A, Huynh V, de Santiago Requejo F, Howells H, Barrett RLC, Aiello M, Cavaliere C, Dyrby TB, Krug K, Ptito M, D'Arceuil H, Forkel SJ, Dell'Acqua F (2017) Short parietal lobe connections of the human and monkey brain. Cortex 97:339-357. doi:https://doi.org/10.1016/j.cortex.2017.10.022
Catani M, Thiebaut de Schotten M (2012) Atlas of human brain connections. Oxford University Press, Oxford ; New York
Chung C-S, Caplan LR, Han W, Pessin MS, Lee K-H, Kim J-M (1996) Thalamic haemorrhage. Brain 119 (6):1873-1886. doi:10.1093/brain/119.6.1873
Ciaramelli E, Grady CL, Moscovitch M (2008) Top-down and bottom-up attention to memory: A hypothesis (AtoM) on the role of the posterior parietal cortex in memory retrieval. Neuropsychologia 46 (7):1828-1851. doi:https://doi.org/10.1016/j.neuropsychologia.2008.03.022
Clemens B, Regenbogen C, Koch K, Backes V, Romanczuk-Seiferth N, Pauly K, Shah NJ, Schneider F, Habel U, Kellermann T (2015) Incidental Memory Encoding Assessed with Signal Detection Theory and Functional Magnetic Resonance Imaging (fMRI). Frontiers in Behavioral Neuroscience 9:305

Cloutman LL, Newhart M, Davis CL, Heidler-Gary J, Hillis AE (2011) Neuroanatomical correlates of oral reading in acute left hemispheric stroke. Brain Lang 116 (1):14-21. doi:10.1016/j.bandl.2010.09.002
Corbetta M, Kincade MJ, Lewis C, Snyder AZ, Sapir A (2005) Neural basis and recovery of spatial attention deficits in spatial neglect. Nature Neuroscience 8 (11):1603-1610. doi:10.1038/nn1574
Corbetta M, Patel G, Shulman GL (2008) The Reorienting System of the Human Brain: From Environment to Theory of Mind. Neuron 58 (3):306-324. doi:https://doi.org/10.1016/j.neuron.2008.04.017
Corbetta M, Ramsey L, Callejas A, Baldassarre A, Hacker CD, Siegel JS, Astafiev SV, Rengachary J, Zinn K, Lang CE, Connor LT, Fucetola R, Strube M, Carter AR, Shulman GL (2015) Common behavioral clusters and subcortical anatomy in stroke. Neuron 85 (5):927-941. doi:10.1016/j.neuron.2015.02.027
Corbetta M, Shulman GL (2002) Control of goal-directed and stimulus-driven attention in the brain. Nature Reviews Neuroscience 3 (3):201-215. doi:10.1038/nrn755
Coslett HB, Schwartz MF (2018) Chapter 18 - The parietal lobe and language. In: Vallar G, Coslett HB (eds) Handbook of Clinical Neurology, vol 151. Elsevier, pp 365-375. doi:https://doi.org/10.1016/B978-0-444-63622-5.00018-8
Crinion J, Price CJ (2005) Right anterior superior temporal activation predicts auditory sentence comprehension following aphasic stroke. Brain 128 (12):2858-2871. doi:10.1093/brain/awh659
Dalla Barba G, Brazzarola M, Barbera C, Marangoni S, Causin F, Bartolomeo P, Thiebaut de Schotten M (2018) Different patterns of confabulation in left visuo-spatial neglect. Experimental Brain Research 236 (7):2037-2046. doi:10.1007/s00221-018-5281-8
Damasio AR (1992) Aphasia. N Engl J Med 326 (8):531-539. doi:10.1056/NEJM199202203260806
Davare M, Andres M, Clerget E, Thonnard JL, Olivier E (2007) Temporal dissociation between hand shaping and grip force scaling in the anterior intraparietal area. J Neurosci 27 (15):3974-3980. doi:10.1523/JNEUROSCI.0426-07.2007
Dave S, VanHaerents S, Voss JL (2020) Cerebellar Theta and Beta Noninvasive Stimulation Rhythms Differentially Influence Episodic Memory versus Semantic Prediction. The Journal of Neuroscience 40 (38):7300. doi:10.1523/JNEUROSCI.0595-20.2020
de Haan R, Aaronson N, Limburg M, Hewer RL, van Crevel H (1993) Measuring quality of life in stroke. Stroke 24 (2):320-327. doi:10.1161/01.str.24.2.320
De Renzi E, Faglioni P, Sorgato P (1982) Modality-specific and supramodal mechanisms of apraxia. Brain 105 (Pt 2):301-312. doi:10.1093/brain/105.2.301
De Witte L, Verhoeven J, Engelborghs S, De Deyn PP, Marien P (2008) Crossed aphasia and visuo-spatial neglect following a right thalamic stroke: a case study and review of the literature. Behav Neurol 19 (4):177-194. doi:10.1155/2008/905187
Dehaene S, Changeux J-P (2011) Experimental and Theoretical Approaches to Conscious Processing. Neuron 70 (2):200-227. doi:https://doi.org/10.1016/j.neuron.2011.03.018
Dejerine J (1891) Sur un cas de cécité verbale avec agraphie suivie d'autopsie. Mem Soc Biol 3:197-201
Della Sala S, Marchetti C, Spinnler H (1991) Right-sided anarchic (alien) hand: a longitudinal study. Neuropsychologia 29 (11):1113-1127. doi:10.1016/0028-3932(91)90081-i
Demeurisse G, Demol O, Robaye E (1980) Motor evaluation in vascular hemiplegia. Eur Neurol 19 (6):382-389. doi:10.1159/000115178

Desmurget M, Grafton S (2000) Forward modeling allows feedback control for fast reaching movements. Trends Cogn Sci 4 (11):423-431. doi:10.1016/s1364-6613(00)01537-0
Desmurget M, Sirigu A (2009) A parietal-premotor network for movement intention and motor awareness. Trends Cogn Sci 13 (10):411-419. doi:10.1016/j.tics.2009.08.001
Dreeben-Irimia O (2008) Physical Therapy Clinical Handbook for PTAs. Jones & Bartlett Publishers,
Eckert MA, Menon V, Walczak A, Ahlstrom J, Denslow S, Horwitz A, Dubno JR (2009) At the heart of the ventral attention system: The right anterior insula. Human Brain Mapping 30 (8):2530-2541. doi:https://doi.org/10.1002/hbm.20688
Eliassen JC, Baynes K, Gazzaniga MS (2000) Anterior and posterior callosal contributions to simultaneous bimanual movements of the hands and fingers. Brain 123 (12):2501-2511. doi:10.1093/brain/123.12.2501
Epelbaum S, Pinel P, Gaillard R, Delmaire C, Perrin M, Dupont S, Dehaene S, Cohen L (2008) Pure alexia as a disconnection syndrome: New diffusion imaging evidence for an old concept. Cortex 44 (8):962-974. doi:10.1016/j.cortex.2008.05.003
Ferrari C, Cattaneo Z, Oldrati V, Casiraghi L, Castelli F, D'Angelo E, Vecchi T (2018) TMS Over the Cerebellum Interferes with Short-term Memory of Visual Sequences. Scientific Reports 8 (1):6722. doi:10.1038/s41598-018-25151-y
Fess E, Moran C (1981) American Society of Hand Therapists Clinical Assessment Recommendations.
Festini SB, Katz B (2021) A Frontal Account of False Alarms. Journal of Cognitive Neuroscience 33 (9):1657-1678. doi:10.1162/jocn_a_01683
Forkel SJ, Friedrich P, Thiebaut de Schotten M, Howells H (2021) White matter variability, cognition, and disorders: a systematic review. Brain Structure & Function (in press)
Gaffan D, Hornak J (1997) Visual neglect in the monkey. Representation and disconnection. Brain 120 (9):1647-1657. doi:10.1093/brain/120.9.1647
Gaillard R, Naccache L, Pinel P, Clemenceau Sp, Volle E, Hasboun D, Dupont S, Baulac M, Dehaene S, Adam C, Cohen L (2006) Direct intracranial, FMRI, and lesion evidence for the causal role of left inferotemporal cortex in reading. Neuron 50 (2):191-204. doi:10.1016/j.neuron.2006.03.031
Gajardo-Vidal A, Lorca-Puls DL, Hope TMH, Parker Jones O, Seghier ML, Prejawa S, Crinion JT, Leff AP, Green DW, Price CJ (2018) How right hemisphere damage after stroke can impair speech comprehension. Brain 141 (12):3389-3404. doi:10.1093/brain/awy270
Galloway JC, Koshland GF (2002) General coordination of shoulder, elbow and wrist dynamics during multijoint arm movements. Exp Brain Res 142 (2):163-180. doi:10.1007/s002210100882
Gandola M, Invernizzi P, Sedda A, Ferre ER, Sterzi R, Sberna M, Paulesu E, Bottini G (2012) An anatomical account of somatoparaphrenia. Cortex 48 (9):1165-1178. doi:10.1016/j.cortex.2011.06.012
Garcea FE, Greene C, Grafton ST, Buxbaum LJ (2020) Structural Disconnection of the Tool Use Network after Left Hemisphere Stroke Predicts Limb Apraxia Severity. Cereb Cortex Commun 1 (1):tgaa035. doi:10.1093/texcom/tgaa035
Garic D, Broce I, Graziano P, Mattfeld A, Dick AS (2019) Laterality of the frontal aslant tract (FAT) explains externalizing behaviors through its association with executive function. Developmental Science 22 (2):e12744. doi:https://doi.org/10.1111/desc.12744
Geschwind N (1965) Disconnexion syndromes in animals and man. Brain 88 (3):585-585. doi:10.1093/brain/88.3.585

Glezer LS, Eden G, Jiang X, Luetje M, Napoliello E, Kim J, Riesenhuber M (2016) Uncovering phonological and orthographic selectivity across the reading network using fMRI-RA. Neuroimage 138:248-256. doi:10.1016/j.neuroimage.2016.05.072
Goldenberg G (1992) Loss of visual imagery and loss of visual knowledge—A case study. Neuropsychologia 30 (12):1081-1099. doi:https://doi.org/10.1016/0028-3932(92)90100-Z
Goldenberg G, Spatt J (2009) The neural basis of tool use. Brain 132 (Pt 6):1645-1655. doi:10.1093/brain/awp080
Goldstein K (1908) Zur Lehre von der motorisschen Apraxie. J Psychol Neurol XI:169–187
Goodglass H, Kaplan E (1983) The assessment of aphasia and related disorders (2nd ed.). Liea & Febiger, Philadelphia
Goodglass H, Kaplan E, Barresi B (2000) The Boston Diagnostic Aphasia Examination. Lippincott, Philadelphia
Graff-Radford NR, Damasio H, Yamada T, Eslinger PJ, Damasio AR (1985) Nonhaemorrhagic thalamic infarction: clinical, neuropsychological and electrophysiological findings in four anatomical groups defined by computerized tomography. Brain 108 (2):485-516. doi:10.1093/brain/108.2.485
Gratwicke J, Jahanshahi M, Foltynie T (2015) Parkinson's disease dementia: a neural networks perspective. Brain 138 (6):1454-1476. doi:10.1093/brain/awv104
Greene C, Cieslak M, Volz LJ, Hensel L, Grefkes C, Rose K, Grafton ST (2019) Finding maximally disconnected subnetworks with shortest path tractography. Neuroimage Clin 23:101903. doi:10.1016/j.nicl.2019.101903
Hagoort P (2019) The neurobiology of language beyond single-word processing. Science 366 (6461):55-58. doi:10.1126/science.aax0289
Hampshire A, Chamberlain SR, Monti MM, Duncan J, Owen AM (2010) The role of the right inferior frontal gyrus: inhibition and attentional control. NeuroImage 50 (3):1313-1319. doi:https://doi.org/10.1016/j.neuroimage.2009.12.109
Harte SE, Ichesco E, Hampson JP, Peltier SJ, Schmidt-Wilcke T, Clauw DJ, Harris RE (2016) Pharmacologic attenuation of cross-modal sensory augmentation within the chronic pain insula. Pain 157 (9):1933-1945. doi:10.1097/j.pain.0000000000000593
He BJ, Snyder AZ, Vincent JL, Epstein A, Shulman GL, Corbetta M (2007) Breakdown of Functional Connectivity in Frontoparietal Networks Underlies Behavioral Deficits in Spatial Neglect. Neuron 53 (6):905-918. doi:https://doi.org/10.1016/j.neuron.2007.02.013
Heilman KM, Valenstein E (1998) Frontal lobe neglect in man. Neurology 50 (5):1202. doi:10.1212/WNL.50.5.1202-a
Herman AB, Houde JF, Vinogradov S, Nagarajan SS (2013) Parsing the Phonological Loop: Activation Timing in the Dorsal Speech Stream Determines Accuracy in Speech Reproduction. The Journal of Neuroscience 33 (13):5439. doi:10.1523/JNEUROSCI.1472-12.2013
Hill H, Windmann S (2014) Examining Event-Related Potential (ERP) correlates of decision bias in recognition memory judgments. PLoS One 9 (9):e106411. doi:10.1371/journal.pone.0106411
Hirose G, Kosoegawa H, Saeki M, Kitagawa Y, Oda R, Kanda S, Matsuhira T (1985) The syndrome of posterior thalamic hemorrhage. Neurology 35 (7):998-1002. doi:10.1212/wnl.35.7.998
Hoeren M, Kummerer D, Bormann T, Beume L, Ludwig VM, Vry MS, Mader I, Rijntjes M, Kaller CP, Weiller C (2014) Neural bases of imitation and pantomime in acute stroke patients: distinct streams for praxis. Brain 137 (Pt 10):2796-2810. doi:10.1093/brain/awu203
Howells H, Thiebaut de Schotten M, Dell'Acqua F, Beyh A, Zappala G, Leslie A, Simmons A, Murphy DG, Catani M (2018) Frontoparietal Tracts Linked to Lateralized Hand

Preference and Manual Specialization. Cereb Cortex 28 (7):2482-2494. doi:10.1093/cercor/bhy040
Huber E, Donnelly PM, Rokem A, Yeatman JD (2018) Rapid and widespread white matter plasticity during an intensive reading intervention. Nature Communications 9 (1):2260. doi:10.1038/s41467-018-04627-5
Husain M, Kennard C (1997) Distractor-dependent frontal neglect. Neuropsychologia 35 (6):829-841. doi:https://doi.org/10.1016/S0028-3932(97)00034-1
Husain M, Nachev P (2007) Space and the parietal cortex. Trends in Cognitive Sciences 11 (1):30-36. doi:https://doi.org/10.1016/j.tics.2006.10.011
Husain M, Rorden C (2003) Non-spatially lateralized mechanisms in hemispatial neglect. Nature Reviews Neuroscience 4 (1):26-36. doi:10.1038/nrn1005
Invernizzi P, Gandola M, Romano D, Zapparoli L, Bottini G, Paulesu E (2013) What is mine? Behavioral and anatomical dissociations between somatoparaphrenia and anosognosia for hemiplegia. Behav Neurol 26 (1-2):139-150. doi:10.3233/BEN-2012-110226
Ivanova MV, Akinina YS, Soloukhina OA, Iskra EV, Buivolova OV, Chrabaszcz AV, Stupina EA, Khudyakova MV, Akhutina TV, Dragoy O (2021) The Russian Aphasia Test: The First Comprehensive, Quantitative, Standardized, and Computerized Aphasia Language Battery in Russian. PsyArXiv. doi:doi:10.31234/osf.io/wajdz
Jakobson LS, Servos P, Goodale MA, Lassonde M (1994) Control of proximal and distal components of prehension in callosal agenesis. Brain 117 (Pt 5):1107-1113. doi:10.1093/brain/117.5.1107
Jehkonen M, Ahonen J-P, Dastidar P, Koivisto A-M, Laippala P, Vilkki J (1998) How to detect visual neglect in acute stroke. The Lancet 351 (9104):727-728. doi:https://doi.org/10.1016/S0140-6736(05)78497-X
Jenkinson PM, Papadaki C, Besharati S, Moro V, Gobbetto V, Crucianelli L, Kirsch LP, Avesani R, Ward NS, Fotopoulou A (2020) Welcoming back my arm: affective touch increases body ownership following right-hemisphere stroke. Brain Commun 2 (1):fcaa034. doi:10.1093/braincomms/fcaa034
Jenkinson PM, Preston C, Ellis SJ (2011) Unawareness after stroke: a review and practical guide to understanding, assessing, and managing anosognosia for hemiplegia. J Clin Exp Neuropsychol 33 (10):1079-1093. doi:10.1080/13803395.2011.596822
Jenmalm P, Schmitz C, Forssberg H, Ehrsson HH (2006) Lighter or heavier than predicted: neural correlates of corrective mechanisms during erroneously programmed lifts. J Neurosci 26 (35):9015-9021. doi:10.1523/JNEUROSCI.5045-05.2006
Kantner J, Lindsay DS (2012) Response bias in recognition memory as a cognitive trait. Memory & Cognition 40 (8):1163-1177. doi:10.3758/s13421-012-0226-0
Kaplan E, Goodglass H, Weintraub S (1983) Boston naming test. Lea & Febiger, Philadelphia
Karnath H-O, Ferber S, Himmelbach M (2001) Spatial awareness is a function of the temporal not the posterior parietal lobe. Nature 411 (6840):950-953. doi:10.1038/35082075
Karnath H-O, Rennig J, Johannsen L, Rorden C (2011) The anatomy underlying acute versus chronic spatial neglect: a longitudinal study. Brain 134 (3):903-912. doi:10.1093/brain/awq355
Karnath HO, Baier B, Nagele T (2005) Awareness of the functioning of one's own limbs mediated by the insular cortex? J Neurosci 25 (31):7134-7138. doi:10.1523/JNEUROSCI.1590-05.2005
Karnath HO, Himmelbach M, Rorden C (2002) The subcortical anatomy of human spatial neglect: putamen, caudate nucleus and pulvinar. Brain 125 (2):350-360. doi:10.1093/brain/awf032

Karolis VR, Corbetta M, Thiebaut de Schotten M (2019) The architecture of functional lateralisation and its relationship to callosal connectivity in the human brain. Nature Communications 10 (1):1417. doi:10.1038/s41467-019-09344-1
Karussis D, Leker RR, Abramsky O (2000) Cognitive dysfunction following thalamic stroke: a study of 16 cases and review of the literature. Journal of the Neurological Sciences 172 (1):25-29. doi:https://doi.org/10.1016/S0022-510X(99)00267-1
Keith RA, Granger CV, Hamilton BB, Sherwin FS (1987) The functional independence measure: a new tool for rehabilitation. Adv Clin Rehabil 1:6-18
Kellor M, Frost J, Silberberg N, Iversen I, Cummings R (1971) Hand strength and dexterity. Am J Occup Ther 25 (2):77-83
Kemerdere R, de Champfleur NM, Deverdun J, Cochereau J, Moritz-Gasser S, Herbet G, Duffau H (2016) Role of the left frontal aslant tract in stuttering: a brain stimulation and tractographic study. Journal of Neurology 263 (1):157-167. doi:10.1007/s00415-015-7949-3
Kim EJ, Choi KD, Han MK, Lee BH, Seo SW, Moon SY, Heilman KM, Na DL (2008) Hemispatial neglect in cerebellar stroke. Journal of the Neurological Sciences 275 (1):133-138. doi:https://doi.org/10.1016/j.jns.2008.08.012
Kim SG, Uğurbil K, Strick PL (1994) Activation of a Cerebellar Output Nucleus During Cognitive Processing. Science 265 (5174):949-951. doi:10.1126/science.8052851
Kitazawa S, Kimura T, Yin P-B (1998) Cerebellar complex spikes encode both destinations and errors in arm movements. Nature 392 (6675):494-497. doi:10.1038/33141
Knopman DS, Selnes OA, Niccum N, Rubens AB (1984) Recovery of naming in aphasia: relationship to fluency, comprehension and CT findings. Neurology 34 (11):1461-1470. doi:10.1212/wnl.34.11.1461
Koini M, Rombouts SARB, Veer IM, Van Buchem MA, Huijbregts SCJ (2017) White matter microstructure of patients with neurofibromatosis type 1 and its relation to inhibitory control. Brain Imaging and Behavior 11 (6):1731-1740. doi:10.1007/s11682-016-9641-3
Konishi S, Wheeler ME, Donaldson DI, Buckner RL (2000) Neural Correlates of Episodic Retrieval Success. NeuroImage 12 (3):276-286. doi:https://doi.org/10.1006/nimg.2000.0614
Koski LM, Paus T, Petrides M (1998) Directed attention after unilateral frontal excisions in humans. Neuropsychologia 36 (12):1363-1371. doi:https://doi.org/10.1016/S0028-3932(98)00018-9
Kranczioch C, Debener S, Schwarzbach J, Goebel R, Engel AK (2005) Neural correlates of conscious perception in the attentional blink. Neuroimage 24 (3):704-714. doi:10.1016/j.neuroimage.2004.09.024
Kravitz DJ, Saleem KS, Baker CI, Mishkin M (2011) A new neural framework for visuospatial processing. Nature Reviews Neuroscience 12 (4):217-230. doi:10.1038/nrn3008
Kreisler A, Godefroy O, Delmaire C, Debachy B, Leclercq M, Pruvo JP, Leys D (2000) The anatomy of aphasia revisited. Neurology 54 (5):1117-1123. doi:10.1212/wnl.54.5.1117
Kumral E, Kocaer T, Ertubey NO, Kumral K (1995) Thalamic hemorrhage. A prospective study of 100 patients. Stroke 26 (6):964-970. doi:10.1161/01.str.26.6.964
Lacritz LH, Cullum CM (1998) The Hopkins Verbal Learning Test and CVLT: A preliminary comparison. Archives of Clinical Neuropsychology 13:623–628
Lansing AE, Ivnik RJ, Cullum CM, Randolph C (1999) An empirically derived short form of the Boston naming test. Archives of clinical neuropsychology : the official journal of the National Academy of Neuropsychologists 14 (6):481-487
Leibovitch FS, Black SE, Caldwell CB, Ebert PL, Ehrlich LE, Szalai JP (1998) Brain-behavior correlations in hemispatial neglect using CT and SPECT: the Sunnybrook Stroke Study. Neurology 50 (4):901-908. doi:10.1212/wnl.50.4.901

Leshikar ED, Duarte A, Hertzog C (2012) Task-selective memory effects for successfully implemented encoding strategies. PLoS One 7 (5):e38160. doi:10.1371/journal.pone.0038160
Li Y, Wu P, Liang F, Huang W (2015) The microstructural status of the corpus callosum is associated with the degree of motor function and neurological deficit in stroke patients. PLoS One 10 (4):e0122615. doi:10.1371/journal.pone.0122615
Liu W, Whitall J, Kepple TM (2013) Multi-joint coordination of functional arm reaching: induced position analysis. J Appl Biomech 29 (2):235-240. doi:10.1123/jab.29.2.235
López-Barroso D, Catani M, Ripollés P, Dell, Acqua F, Rodríguez-Fornells A, de Diego-Balaguer R (2013) Word learning is mediated by the left arcuate fasciculus. Proceedings of the National Academy of Sciences 110 (32):13168. doi:10.1073/pnas.1301696110
Luck SJ, Hillyard SA, Mangun GR, Gazzaniga MS (1989) Independent hemispheric attentional systems mediate visual search in split-brain patients. Nature 342 (6249):543-545. doi:10.1038/342543a0
Lunven M, Thiebaut De Schotten M, Bourlon C, Duret C, Migliaccio R, Rode G, Bartolomeo P (2015) White matter lesional predictors of chronic visual neglect: a longitudinal study. Brain 138 (3):746-760. doi:10.1093/brain/awu389
Lyle RC (1981) A performance test for assessment of upper limb function in physical rehabilitation treatment and research. Int J Rehabil Res 4 (4):483-492. doi:10.1097/00004356-198112000-00001
Mack WJ, Freed DM, Williams BW, Henderson VW (1992) Boston Naming Test: shortened versions for use in Alzheimer's disease. J Gerontol 47 (3):P154-158. doi:10.1093/geronj/47.3.p154
Manes F, Paradiso S, Springer JA, Lamberty G, Robinson RG (1999) Neglect after right insular cortex infarction. Stroke 30 (5):946-948. doi:10.1161/01.str.30.5.946
Mani S, Mutha PK, Przybyla A, Haaland KY, Good DC, Sainburg RL (2013) Contralesional motor deficits after unilateral stroke reflect hemisphere-specific control mechanisms. Brain 136 (Pt 4):1288-1303. doi:10.1093/brain/aws283
Marchetti C, Della Sala S (1998) Disentangling the alien and anarchic hand. . Cognitive Neuropsychiatry 3:191–207
Mariën P, Ackermann H, Adamaszek M, Barwood CHS, Beaton A, Desmond J, De Witte E, Fawcett AJ, Hertrich I, Küper M, Leggio M, Marvel C, Molinari M, Murdoch BE, Nicolson RI, Schmahmann JD, Stoodley CJ, Thürling M, Timmann D, Wouters E, Ziegler W (2014) Consensus Paper: Language and the Cerebellum: an Ongoing Enigma. The Cerebellum 13 (3):386-410. doi:10.1007/s12311-013-0540-5
Martino J, Brogna C, Robles SG, Vergani F, Duffau H (2010) Anatomic dissection of the inferior fronto-occipital fasciculus revisited in the lights of brain stimulation data. Cortex 46 (5):691-699. doi:https://doi.org/10.1016/j.cortex.2009.07.015
Marvel CL, Desmond JE (2010) Functional Topography of the Cerebellum in Verbal Working Memory. Neuropsychology Review 20 (3):271-279. doi:10.1007/s11065-010-9137-7
Mashour GA, Roelfsema P, Changeux J-P, Dehaene S (2020) Conscious Processing and the Global Neuronal Workspace Hypothesis. Neuron 105 (5):776-798. doi:https://doi.org/10.1016/j.neuron.2020.01.026
Mathiowetz V, Volland G, Kashman N, Weber K (1985) Adult norms for the Box and Block Test of manual dexterity. Am J Occup Ther 39 (6):386-391. doi:10.5014/ajot.39.6.386
McDermott KB, Jones TC, Petersen SE, Lageman SK, Roediger HL, III (2000) Retrieval Success is Accompanied by Enhanced Activation in Anterior Prefrontal Cortex During Recognition Memory: An Event-Related fMRI Study. Journal of Cognitive Neuroscience 12 (6):965-976. doi:10.1162/08989290051137503

Mechelli A, Humphreys GW, Mayall K, Olson A, Price CJ (2000) Differential effects of word length and visual contrast in the fusiform and lingual gyri during reading. Proc Biol Sci 267 (1455):1909-1913. doi:10.1098/rspb.2000.1229
Meier EL, Sheppard SM, Goldberg EB, Head CR, Ubellacker DM, Walker A, Hillis AE (2020) Naming errors and dysfunctional tissue metrics predict language recovery after acute left hemisphere stroke. Neuropsychologia 148:107651-107651. doi:10.1016/j.neuropsychologia.2020.107651
Melrose RJ, Zahniser E, Wilkins SS, Veliz J, Hasratian AS, Sultzer DL, Jimenez AM (2020) Prefrontal working memory activity predicts episodic memory performance: A neuroimaging study. Behavioural Brain Research 379:112307. doi:https://doi.org/10.1016/j.bbr.2019.112307
Menon V, Uddin LQ (2010) Saliency, switching, attention and control: a network model of insula function. Brain Structure and Function 214 (5):655-667. doi:10.1007/s00429-010-0262-0
Mesulam MM (1985) Principle of Behavioural Neurology: Tests of Directed Attention and Memory (Contemporary Neurology Series). F.A. Davis Company,
Mesulam MM, Thompson CK, Weintraub S, Rogalski EJ (2015) The Wernicke conundrum and the anatomy of language comprehension in primary progressive aphasia. Brain 138 (Pt 8):2423-2437. doi:10.1093/brain/awv154
Miall RC, Christensen LO, Cain O, Stanley J (2007) Disruption of state estimation in the human lateral cerebellum. PLoS Biol 5 (11):e316. doi:10.1371/journal.pbio.0050316
Milano NJ, Heilman KM (2014) Cerebellar Allocentric and Action-Intentional Spatial Neglect. Cognitive and Behavioral Neurology 27 (3)
Moro V, Berlucchi G, Lerch J, Tomaiuolo F, Aglioti SM (2008) Selective deficit of mental visual imagery with intact primary visual cortex and visual perception. Cortex 44 (2):109-118. doi:https://doi.org/10.1016/j.cortex.2006.06.004
Moro V, Pacella V, Scandola M, Besharati S, Rossato E, Jenkinson P, Fotopoulou A (2021) A fronto-insular-parietal network for the sense of body ownership. Research Square. doi:10.21203/rs.3.rs-428666/v1
Mort DJ, Malhotra P, Mannan SK, Rorden C, Pambakian A, Kennard C, Husain M (2003) The anatomy of visual neglect. Brain 126 (9):1986-1997. doi:10.1093/brain/awg200
Murdoch BE (2010) The cerebellum and language: Historical perspective and review. Cortex 46 (7):858-868. doi:https://doi.org/10.1016/j.cortex.2009.07.018
Mutha PK, Haaland KY, Sainburg RL (2012) The effects of brain lateralization on motor control and adaptation. J Mot Behav 44 (6):455-469. doi:10.1080/00222895.2012.747482
Naeser MA, Helm-Estabrooks N, Haas G, Auerbach S, Srinivasan M (1987) Relationship between lesion extent in 'Wernicke's area' on computed tomographic scan and predicting recovery of comprehension in Wernicke's aphasia. Arch Neurol 44 (1):73-82. doi:10.1001/archneur.1987.00520130057018
Nelson AJD, Powell AL, Kinnavane L, Aggleton JP (2018) Anterior thalamic nuclei, but not retrosplenial cortex, lesions abolish latent inhibition in rats. Behav Neurosci 132 (5):378-387. doi:10.1037/bne0000265
Nicholas LE, Brookshire RH, Maclennan DL, Schumacher JG, Porrazzo SA (1989) Revised administration and scoring procedures for the Boston Naming test and norms for non-brain-damaged adults. Aphasiology 3 (6):569-580. doi:10.1080/02687038908249023
Nowak DA, Hermsdorfer J, Topka H (2003) Deficits of predictive grip force control during object manipulation in acute stroke. J Neurol 250 (7):850-860. doi:10.1007/s00415-003-1095-z

Olson IR, Heide RJVD, Alm KH, Vyas G (2015) Development of the uncinate fasciculus: Implications for theory and developmental disorders. Developmental Cognitive Neuroscience 14:50-61. doi:https://doi.org/10.1016/j.dcn.2015.06.003
Oxford Grice K, Vogel KA, Le V, Mitchell A, Muniz S, Vollmer MA (2003) Adult norms for a commercially available Nine Hole Peg Test for finger dexterity. Am J Occup Ther 57 (5):570-573. doi:10.5014/ajot.57.5.570
Pacella V, Foulon C, Jenkinson PM, Scandola M, Bertagnoli S, Avesani R, Fotopoulou A, Moro V, Thiebaut de Schotten M (2019) Anosognosia for hemiplegia as a tripartite disconnection syndrome. Elife 8. doi:10.7554/eLife.46075
Papagno C (2018) Chapter 19 - Memory deficits. In: Vallar G, Coslett HB (eds) Handbook of Clinical Neurology, vol 151. Elsevier, pp 377-393. doi:https://doi.org/10.1016/B978-0-444-63622-5.00019-X
Parlatini V, Radua J, Dell'Acqua F, Leslie A, Simmons A, Murphy DG, Catani M, Thiebaut de Schotten M (2017) Functional segregation and integration within fronto-parietal networks. NeuroImage 146:367-375. doi:https://doi.org/10.1016/j.neuroimage.2016.08.031
Paulesu E, Frith CD, Frackowiak RSJ (1993) The neural correlates of the verbal component of working memory. Nature 362 (6418):342-345. doi:10.1038/362342a0
Pazzaglia M, Smania N, Corato E, Aglioti SM (2008) Neural underpinnings of gesture discrimination in patients with limb apraxia. J Neurosci 28 (12):3030-3041. doi:10.1523/JNEUROSCI.5748-07.2008
Qiu M, Darling WG, Morecraft RJ, Ni CC, Rajendra J, Butler AJ (2011) White matter integrity is a stronger predictor of motor function than BOLD response in patients with stroke. Neurorehabil Neural Repair 25 (3):275-284. doi:10.1177/1545968310389183
Rafal RD, Posner MI (1987) Deficits in human visual spatial attention following thalamic lesions. Proceedings of the National Academy of Sciences 84 (20):7349. doi:10.1073/pnas.84.20.7349
Rapcsak SZ, Edmonds EC (2011) The Executive Control of Face Memory. Behavioural Neurology 24:692460. doi:10.3233/BEN-2011-0339
Ravizza SM, Hazeltine E, Ruiz S, Zhu DC (2011) Left TPJ activity in verbal working memory: Implications for storage- and sensory-specific models of short term memory. NeuroImage 55 (4):1836-1846. doi:https://doi.org/10.1016/j.neuroimage.2010.12.021
Robson H, Zahn R, Keidel JL, Binney RJ, Sage K, Lambon Ralph MA (2014) The anterior temporal lobes support residual comprehension in Wernicke's aphasia. Brain 137 (3):931-943. doi:10.1093/brain/awt373
Rojkova K, Volle E, Urbanski M, Humbert F, Dell'Acqua F, Thiebaut de Schotten M (2016) Atlasing the frontal lobe connections and their variability due to age and education: a spherical deconvolution tractography study. Brain Structure and Function 221 (3):1751-1766. doi:10.1007/s00429-015-1001-3
Rollans C, Cummine J (2018) One tract, two tract, old tract, new tract: A pilot study of the structural and functional differentiation of the inferior fronto-occipital fasciculus. Journal of Neurolinguistics 46:122-137. doi:https://doi.org/10.1016/j.jneuroling.2017.12.009
Romano D, Maravita A (2019) The dynamic nature of the sense of ownership after brain injury. Clues from asomatognosia and somatoparaphrenia. Neuropsychologia 132:107119. doi:10.1016/j.neuropsychologia.2019.107119
Rorden C, Karnath H-O (2010) A simple measure of neglect severity. Neuropsychologia 48 (9):2758-2763. doi:https://doi.org/10.1016/j.neuropsychologia.2010.04.018
Sarubbo S, De Benedictis A, Maldonado IL, Basso G, Duffau H (2013) Frontal terminations for the inferior fronto-occipital fascicle: anatomical dissection, DTI study and

functional considerations on a multi-component bundle. Brain Struct Funct 218 (1):21-37. doi:10.1007/s00429-011-0372-3
Scandola M, Gobbetto V, Bertagnoli S, Bulgarelli C, Canzano L, Aglioti SM, Moro V (2021) Gesture errors in left and right hemisphere damaged patients: A behavioural and anatomical study. Neuropsychologia 162:108027. doi:10.1016/j.neuropsychologia.2021.108027
Schaechter JD, Fricker ZP, Perdue KL, Helmer KG, Vangel MG, Greve DN, Makris N (2009) Microstructural status of ipsilesional and contralesional corticospinal tract correlates with motor skill in chronic stroke patients. Hum Brain Mapp 30 (11):3461-3474. doi:10.1002/hbm.20770
Schaefer SY, Haaland KY, Sainburg RL (2009a) Dissociation of initial trajectory and final position errors during visuomotor adaptation following unilateral stroke. Brain Res 1298:78-91. doi:10.1016/j.brainres.2009.08.063
Schaefer SY, Haaland KY, Sainburg RL (2009b) Hemispheric specialization and functional impact of ipsilesional deficits in movement coordination and accuracy. Neuropsychologia 47 (13):2953-2966. doi:10.1016/j.neuropsychologia.2009.06.025
Scheffer M, Kroeff C, Steigleder BG, Klein LA, Grassi-Oliveira R, de Almeida RMM (2016) Right frontal stroke: extra-frontal lesions, executive functioning and impulsive behaviour. Psicologia: Reflexão e Crítica 29 (1):28. doi:10.1186/s41155-016-0018-8
Schmitz C, Jenmalm P, Ehrsson HH, Forssberg H (2005) Brain activity during predictable and unpredictable weight changes when lifting objects. J Neurophysiol 93 (3):1498-1509. doi:10.1152/jn.00230.2004
Sebastian A, Pohl MF, Klöppel S, Feige B, Lange T, Stahl C, Voss A, Klauer KC, Lieb K, Tüscher O (2013) Disentangling common and specific neural subprocesses of response inhibition. NeuroImage 64:601-615. doi:https://doi.org/10.1016/j.neuroimage.2012.09.020
Seghier ML (2012) The Angular Gyrus: Multiple Functions and Multiple Subdivisions. The Neuroscientist 19 (1):43-61. doi:10.1177/1073858412440596
Serrien DJ, Ivry RB, Swinnen SP (2006) Dynamics of hemispheric specialization and integration in the context of motor control. Nat Rev Neurosci 7 (2):160-166. doi:10.1038/nrn1849
Sestieri C, Shulman GL, Corbetta M (2017) The contribution of the human posterior parietal cortex to episodic memory. Nature Reviews Neuroscience 18 (3):183-192. doi:10.1038/nrn.2017.6
Shigihara Y, Tanaka M, Ishii A, Kanai E, Funakura M, Watanabe Y (2013) Two types of mental fatigue affect spontaneous oscillatory brain activities in different ways. Behav Brain Funct 9:2. doi:10.1186/1744-9081-9-2
Simons JS, Spiers HJ (2003) Prefrontal and medial temporal lobe interactions in long-term memory. Nature Reviews Neuroscience 4 (8):637-648. doi:10.1038/nrn1178
Singh-Curry V, Husain M (2009) The functional role of the inferior parietal lobe in the dorsal and ventral stream dichotomy. Neuropsychologia 47 (6):1434-1448. doi:https://doi.org/10.1016/j.neuropsychologia.2008.11.033
Sirigu A, Daprati E, Ciancia S, Giraux P, Nighoghossian N, Posada A, Haggard P (2004) Altered awareness of voluntary action after damage to the parietal cortex. Nat Neurosci 7 (1):80-84. doi:10.1038/nn1160
Spagna A, Hajhajate D, Liu J, Bartolomeo P (2021) Visual mental imagery engages the left fusiform gyrus, but not the early visual cortex: A meta-analysis of neuroimaging evidence. Neuroscience & Biobehavioral Reviews 122:201-217. doi:https://doi.org/10.1016/j.neubiorev.2020.12.029
Stewart JC, Dewanjee P, Tran G, Quinlan EB, Dodakian L, McKenzie A, See J, Cramer SC (2017) Role of corpus callosum integrity in arm function differs based on motor severity after stroke. Neuroimage Clin 14:641-647. doi:10.1016/j.nicl.2017.02.023

Stinear CM, Barber PA, Smale PR, Coxon JP, Fleming MK, Byblow WD (2007) Functional potential in chronic stroke patients depends on corticospinal tract integrity. Brain 130 (Pt 1):170-180. doi:10.1093/brain/awl333

Tarhan LY, Watson CE, Buxbaum LJ (2015) Shared and Distinct Neuroanatomic Regions Critical for Tool-related Action Production and Recognition: Evidence from 131 Left-hemisphere Stroke Patients. J Cogn Neurosci 27 (12):2491-2511. doi:10.1162/jocn_a_00876

Thiebaut de Schotten M, Cohen L, Amemiya E, Braga LW, Dehaene S (2014a) Learning to read improves the structure of the arcuate fasciculus. Cereb Cortex 24 (4):989-995. doi:10.1093/cercor/bhs383

Thiebaut de Schotten M, Dell'Acqua F, Forkel SJ, Simmons A, Vergani F, Murphy DGM, Catani M (2011) A lateralized brain network for visuospatial attention. Nature Neuroscience 14 (10):1245-1246. doi:10.1038/nn.2905

Thiebaut de Schotten M, Tomaiuolo F, Aiello M, Merola S, Silvetti M, Lecce F, Bartolomeo P, Doricchi F (2014b) Damage to White Matter Pathways in Subacute and Chronic Spatial Neglect: A Group Study and 2 Single-Case Studies with Complete Virtual "In Vivo" Tractography Dissection. Cerebral Cortex 24 (3):691-706. doi:10.1093/cercor/bhs351

Thiebaut de Schotten M, Urbanski M, Duffau H, Volle E, Lévy R, Dubois B, Bartolomeo P (2005) Direct Evidence for a Parietal-Frontal Pathway Subserving Spatial Awareness in Humans. Science 309 (5744):2226-2228. doi:10.1126/science.1116251

Thompson RF, Kim JJ (1996) Memory systems in the brain and localization of a memory. Proceedings of the National Academy of Sciences 93 (24):13438. doi:10.1073/pnas.93.24.13438

Tomatsu S, Ishikawa T, Tsunoda Y, Lee J, Hoffman DS, Kakei S (2016) Information processing in the hemisphere of the cerebellar cortex for control of wrist movement. J Neurophysiol 115 (1):255-270. doi:10.1152/jn.00530.2015

Tombaugh TN, Kozak J, Rees L (1999) Normative Data Stratified by Age and Education for Two Measures of Verbal Fluency: FAS and Animal Naming. Archives of Clinical Neuropsychology 14 (2):167-177. doi:https://doi.org/10.1016/S0887-6177(97)00095-4

Tracey I, Mantyh PW (2007) The cerebral signature for pain perception and its modulation. Neuron 55 (3):377-391. doi:10.1016/j.neuron.2007.07.012

Treisman AM, Gelade G (1980) A feature-integration theory of attention. Cognitive Psychology 12 (1):97-136. doi:https://doi.org/10.1016/0010-0285(80)90005-5

Uncapher MR, Rugg MD (2009) Selecting for Memory? The Influence of Selective Attention on the Mnemonic Binding of Contextual Information. The Journal of Neuroscience 29 (25):8270. doi:10.1523/JNEUROSCI.1043-09.2009

Ungerleider L, Mishkin M (1982) Two cortical visual systems. In Analysis of visual behavior. MIT Press,

Vallar G, Perani D (1986) The anatomy of unilateral neglect after right-hemisphere stroke lesions. A clinical/CT-scan correlation study in man. Neuropsychologia 24 (5):609-622. doi:https://doi.org/10.1016/0028-3932(86)90001-1

Van de Port IG, Ketelaar M, Schepers VP, Van den Bos GA, Lindeman E (2004) Monitoring the functional health status of stroke patients: the value of the Stroke-Adapted Sickness Impact Profile-30. Disabil Rehabil 26 (11):635-640. doi:10.1080/09638280410001672481

van Straten A, de Haan RJ, Limburg M, Schuling J, Bossuyt PM, van den Bos GA (1997) A stroke-adapted 30-item version of the Sickness Impact Profile to assess quality of life (SA-SIP30). Stroke 28 (11):2155-2161. doi:10.1161/01.str.28.11.2155

van Straten A, de Haan RJ, Limburg M, van den Bos GA (2000) Clinical meaning of the Stroke-Adapted Sickness Impact Profile-30 and the Sickness Impact Profile-136. Stroke 31 (11):2610-2615. doi:10.1161/01.str.31.11.2610

Vanbellingen T, Kersten B, Van Hemelrijk B, Van de Winckel A, Bertschi M, Muri R, De Weerdt W, Bohlhalter S (2010) Comprehensive assessment of gesture production: a new test of upper limb apraxia (TULIA). Eur J Neurol 17 (1):59-66. doi:10.1111/j.1468-1331.2009.02741.x

Vilberg KL, Rugg MD (2008) Memory retrieval and the parietal cortex: A review of evidence from a dual-process perspective. Neuropsychologia 46 (7):1787-1799. doi:https://doi.org/10.1016/j.neuropsychologia.2008.01.004

Villardita C, Cultrera S, Cupone V, Mejìa R (1985) Neuropsychological test performances and normal aging. Archives of Gerontology and Geriatrics 4 (4):311-319. doi:https://doi.org/10.1016/0167-4943(85)90038-X

Von Der Heide RJ, Skipper LM, Klobusicky E, Olson IR (2013) Dissecting the uncinate fasciculus: disorders, controversies and a hypothesis. Brain 136 (Pt 6):1692-1707. doi:10.1093/brain/awt094

Wade DT, Wood VA, Heller A, Maggs J, Langton Hewer R (1987) Walking after stroke. Measurement and recovery over the first 3 months. Scand J Rehabil Med 19 (1):25-30

Watson RT, Heilman KM (1979) Thalamic neglect. Neurology 29 (5):690-694. doi:10.1212/wnl.29.5.690

Watson RT, Valenstein E, Heilman KM (1981) Thalamic Neglect: Possible Role of the Medial Thalamus and Nucleus Reticularis in Behavior. Archives of Neurology 38 (8):501-506. doi:10.1001/archneur.1981.00510080063009

Waxman SG, Ricaurte GA, Tucker SB (1986) Thalamic hemorrhage with neglect and memory disorder. Journal of the Neurological Sciences 75 (1):105-112. doi:https://doi.org/10.1016/0022-510X(86)90053-5

Weiss PH, Ubben SD, Kaesberg S, Kalbe E, Kessler J, Liebig T, Fink GR (2016) Where language meets meaningful action: a combined behavior and lesion analysis of aphasia and apraxia. Brain Struct Funct 221 (1):563-576. doi:10.1007/s00429-014-0925-3

Weissman DH, Roberts KC, Visscher KM, Woldorff MG (2006) The neural bases of momentary lapses in attention. Nature Neuroscience 9 (7):971-978. doi:10.1038/nn1727

Whiteside DM, Kealey T, Semla M, Luu H, Rice L, Basso MR, Roper B (2016) Verbal Fluency: Language or Executive Function Measure? Appl Neuropsychol Adult 23 (1):29-34. doi:10.1080/23279095.2015.1004574

Wilson B, Cockburn JF, Halligan P (1987) Development of a behavioral test of visuospatial neglect. Arch Phys Med Rehabil 68 (2):98-102

Windmann S, Urbach TP, Kutas M (2002) Cognitive and Neural Mechanisms of Decision Biases in Recognition Memory. Cerebral Cortex 12 (8):808-817. doi:10.1093/cercor/12.8.808

Wise RJS, Scott SK, Blank SC, Mummery CJ, Murphy K, Warburton EA (2001) Separate neural subsystems within `Wernicke's area'. Brain 124 (1):83-95. doi:10.1093/brain/124.1.83

Woollams AM, Halai A, Lambon Ralph MA (2018) Mapping the intersection of language and reading: the neural bases of the primary systems hypothesis. Brain Structure and Function 223 (8):3769-3786. doi:10.1007/s00429-018-1716-z

Wu AS, Witgert ME, Lang FF, Xiao L, Bekele BN, Meyers CA, Ferson D, Wefel JS (2011) Neurocognitive function before and after surgery for insular gliomas. J Neurosurg 115 (6):1115-1125. doi:10.3171/2011.8.JNS11488

Wu Y, Sun D, Wang Y, Wang Y (2016) Subcomponents and Connectivity of the Inferior Fronto-Occipital Fasciculus Revealed by Diffusion Spectrum Imaging Fiber Tracking. Frontiers in Neuroanatomy 10:88

Xu T, Jha A, Nachev P (2018) The dimensionalities of lesion-deficit mapping. Neuropsychologia 115:134-141. doi:10.1016/j.neuropsychologia.2017.09.007